AD-A167 813 FULL-SCALE CRASH TEST (T-41) OF THE YAH-63 ATTACK HELICOPTER(U) ARMY AVIATION SYSTEMS COMMAND ST LOUIS MO K F SMITH APR 86 USAAVSCOM-TR-86-D-2 1/2

UNCLASSIFIED F/G 1/3 NL

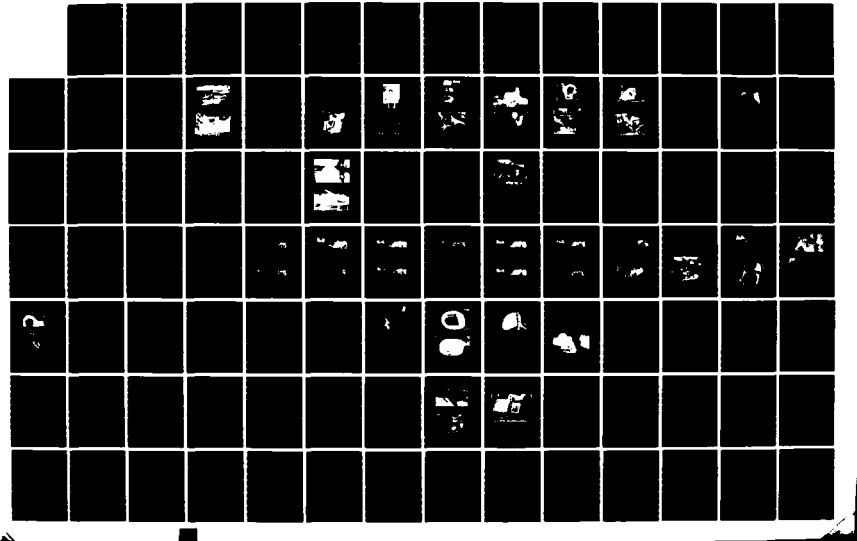

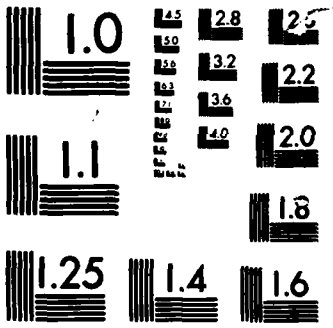

MICROCOPY CHART

12

USAAVSCOM TR-86-D-2

US ARMY
AVIATION
SYSTEMS COMMAND

FULL-SCALE CRASH TEST (T-41) OF THE YAH-63 ATTACK HELICOPTER

Kent F. Smith

April 1986

AVIATION APPLIED TECHNOLOGY DIRECTORATE
US ARMY AVIATION RESEARCH AND TECHNOLOGY ACTIVITY (AVSCOM)
Fort Eustis, VA. 23604-5577

AVSCOM — PROVIDING LEADERS THE DECISIVE EDGE

DISCLAIMERS

The findings in this report are not to be construed as an official Department of the Army position unless so designated by other authorized documents.

When Government drawings, specifications, or other data are used for any purpose other than in connection with a definitely related Government procurement operation, the United States Government thereby incurs no responsibility nor any obligation whatsoever; and the fact that the Government may have formulated, furnished, or in any way supplied the said drawings, specifications, or other data is not to be regarded by implication or otherwise as in any manner licensing the holder or any other person or corporation, or conveying any rights or permission, to manufacture, use, or sell any patented invention that may in any way be related thereto.

Trade names cited in this report do not constitute an official endorsement or approval of the use of such commercial hardware or software.

DISPOSITION INSTRUCTIONS

Destroy this report by any method which precludes reconstruction of the document. Do not return it to the originator.

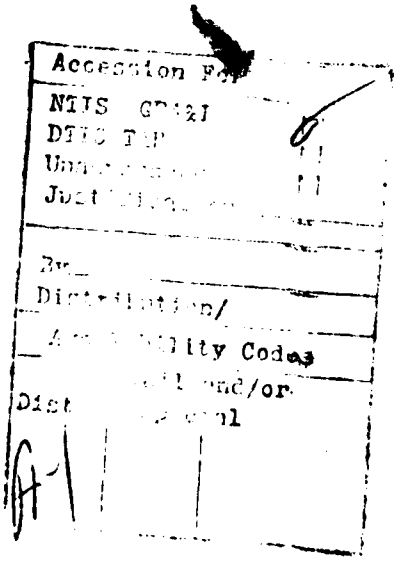

Unclassified
SECURITY CLASSIFICATION OF THIS PAGE

REPORT DOCUMENTATION PAGE

1a. REPORT SECURITY CLASSIFICATION Unclassified	1b. RESTRICTIVE MARKINGS
2a. SECURITY CLASSIFICATION AUTHORITY	3. DISTRIBUTION / AVAILABILITY OF REPORT Approved for public release; distribution is unlimited.
2b. DECLASSIFICATION / DOWNGRADING SCHEDULE	
4. PERFORMING ORGANIZATION REPORT NUMBER(S) USAAVSCOM TR 86-D-2	5. MONITORING ORGANIZATION REPORT NUMBER(S)
6a. NAME OF PERFORMING ORGANIZATION Aviation Applied Technology Directorate 6b. OFFICE SYMBOL (If applicable)	7a. NAME OF MONITORING ORGANIZATION
6c. ADDRESS (City, State, and ZIP Code) U.S. Army Aviation Research and Technology Activity (AVSCOM) Fort Eustis, Virginia 23604-5577	7b. ADDRESS (City, State, and ZIP Code)
8a. NAME OF FUNDING / SPONSORING ORGANIZATION 8b. OFFICE SYMBOL (If applicable)	9. PROCUREMENT INSTRUMENT IDENTIFICATION NUMBER
8c. ADDRESS (City, State, and ZIP Code)	10. SOURCE OF FUNDING NUMBERS PROGRAM ELEMENT NO. / PROJECT NO. / TASK NO. HT 81-01 / WORK UNIT ACCESSION NO.

11. TITLE (Include Security Classification)
Full-Scale Crash Test (T-41) of the YAH-63 Attack Helicopter (Emergency locator Transmitters)

12. PERSONAL AUTHOR(S)
Kent F. Smith

13a. TYPE OF REPORT	13b. TIME COVERED FROM ____ TO ____	14. DATE OF REPORT (Year, Month, Day)	15. PAGE COUNT
		April 1986	94

16. SUPPLEMENTARY NOTATION
(Inflatable Body and Head Restraint System)

17. COSATI CODES		
FIELD	GROUP	SUB-GROUP

18. SUBJECT TERMS (Continue on reverse if necessary and identify by block number)
Helicopter, Crash Test, IBAHRS, ELT, Crashworthiness, Crash Impact, Crash Safety, Crash, Impact Dynamics, Energy Absorption,

19. ABSTRACT (Continue on reverse if necessary and identify by block number)
T-41 was jointly conducted by the Aviation Applied Technology Directorate and the NASA-Langley Research Center. The purpose of the effort was to assess the effectiveness of the structural crashworthiness features designed into the YAH-63 during a severe but potentially survivable accident and to evaluate the performance of several developmental crashworthy systems in a real-world helicopter crash environment. Because this was the first crash test of an attack helicopter and the first of a helicopter having designed-in crashworthiness, T-41 offers unique data for predicting the crash impact behavior of future helicopters. Keywords:

20. DISTRIBUTION / AVAILABILITY OF ABSTRACT	21. ABSTRACT SECURITY CLASSIFICATION
☒ UNCLASSIFIED/UNLIMITED ☐ SAME AS RPT. ☐ DTIC USERS	Unclassified
22a. NAME OF RESPONSIBLE INDIVIDUAL Kent F. Smith	22b. TELEPHONE (Include Area Code) (804) 878-5875/2103 / 22c. OFFICE SYMBOL SAVRT-TY-ASV

DD FORM 1473, 84 MAR 83 APR edition may be used until exhausted. All other editions are obsolete.

SECURITY CLASSIFICATION OF THIS PAGE
Unclassified

PREFACE

The Project Engineer for the full-scale crash test described herein was Mr. Kent F. Smith, Aviation Applied Technology Directorate, U.S. Army Aviation Research and Technology Activity (AVSCOM), Fort Eustis, Virginia. Special gratitude is expressed for the assistance of Dr. Robert G. Thomson (deceased), Chief of the NASA-Langley Research Center (LRC) Impact Dynamics Research Facility, for his attention and help given during the planning phase of T-41 and for his valuable assistance in expediting test preparation at LRC.

The following individuals and organizations were responsible for and provided support to the various on-board experiments:

- Mr. Jim McElhenny, Naval Air Development Center, Inflatable Body and Head Restraint System (IBAHRS)
- MAJ William Stuck, U.S. Army Aviation Systems Command, Integrated Helmet and Display Sight System (IHADSS)
- Mr. Don White, Hamilton Standard Division of United Technologies Corporation, Brassboard Flight Data Recorder (FDR)
- Mr. Daniel Watters, Naval Air Test Center, Flight Incident Recorder/Crash Position Locator (FIR/CPL)
- Mr. Huey Carden, NASA-Langley Research Center, Emergency Locator Transmitters (ELT)

The author extends his gratitude to the following individuals for their contributions to the T-41 test effort:

Mr. Claude Castle, NASA-LRC (retired)
Mr. Leon Domzalski, Naval Air Development Center
Mr. Jim Cronkhite, Bell Helicopter Textron, Inc.
Mr. Tom Haas, Bell Helicopter Textron, Inc.
Mr. George Perry, Bell Helicopter Textron, Inc.
Mr. Paul Triplett, Aviation Applied Technology Directorate
Mr. Ron Bott, Aviation Applied Technology Directorate
Mr. Richard Bywaters, Aviation Applied Technology Directorate (retired)

The author is also indebted to the following organizations for the support specified:

NASA-Langley Research Center for facility support, conducting the test, instrumentation support, data recording and reduction, high-speed photography, and test specimen disposal.

U.S. Army Transportation School Aviation Maintenance Training Department, Fort Eustis, Virginia, for conducting multiple weight and balance checks.

TABLE OF CONTENTS

LIST OF FIGURES

LIST OF FIGURES - Continued

LIST OF FIGURES - Continued

LIST OF FIGURES - Continued

LIST OF TABLES

INTRODUCTION

The modern U.S. Army attack helicopter is often designed around conflicting requirements. Light weight and agility needed to survive at low altitudes in rugged, confined terrain is partially compromised by the weight of avionics and ordnance required to perform the mission. In recent years, the U.S. Army has increasingly recognized the value of crashworthiness inherent in the basic helicopter design as being a worthwhile weight and performance trade-off in minimizing the personnel and equipment losses. These savings accrue during training activity as well as on the battlefield. Crashworthiness is also a positive morale factor and improves the combat effectiveness of the fleet.

The U.S. Army Aviation Systems Command's Aviation Applied Technology Directorate (AATD) has conducted 41 full-scale crash tests of both rotary- and fixed-wing aircraft in the last 20 years. The most recent AATD full-scale crash test, T-41, is discussed in this report with respect to the performance of certain energy attenuating features designed to enhance crew survival and minimize material losses.

T-41 was jointly conducted on 8 July 1981 by the Aviation Applied Technology Directorate and the NASA-Langley Research Center to assess the effectiveness of the structural crashworthiness features designed into the YAH-63 during a severe but potentially survivable accident and to evaluate the performance of several developmental crashworthy systems in a real-world helicopter crash environment. Because this was the first crash test of an attack helicopter and the first of a helicopter having designed-in crashworthiness, T-41 offers unique data for predicting the crash impact behavior of future helicopters.

TEST SPECIMEN

GENERAL

The test aircraft, the Bell Helicopter Textron (BHT) YAH-63 (designated BHT model 409 prototype, tail number 74-22246), was one of three BHT prototypes built to participate in the fly-off competition for the advanced attack helicopter (AAH). Crashworthiness features were a design requirement, as the then-current revision of the Army's Crash Survival Design Guide (Reference 1) was to be used as a guide. During the YAH-63 design period, the Army's crashworthiness military standard, MIL-STD-1290(AV) (Reference 2), had not yet been published.

AATD obtained the YAH-63 aircraft (Figure 1) as residual hardware within the overall AAH effort. It is a twin-engine attack helicopter whose primary mission is to destroy enemy tanks. Two crewmen, a pilot and copilot/gunner (CPG), are seated in tandem under a greenhouse canopy. The CPG occupies the front cockpit while the pilot is aft. The aircraft is powered by two General Electric T-700 turboshaft engines developing approximately 1500 shaft horsepower each at sea level. The aircraft is 51.9 feet long, 17.2 feet wide, and 13.2 feet high. Test gross weight was 13,768 pounds with the longitudinal center of gravity located 2.8 inches forward of the main rotor mast centerline at fuselage station (FS) 297.2.

The airframe was received minus the engines and much of the avionics equipment normally located in the forward electronics bays. Dummy engines were designed to duplicate the weight, center of gravity (CG), and pitch and yaw moments of inertia of actual T-700 engines. These were mounted on the airframe's existing engine mounts (Figure 2). All canopy glass, access panels, and non-load-bearing cowling over critical areas such as transmission and engine bays were removed for unimpeded viewing of the dynamic behavior of the crewmen, high mass items, and main structure. The two-bladed main rotor, normally 50.0 feet in span, was cut down to one-third span (16.67 feet) for this test. This was done to more accurately simulate inertia loads borne by the transmission mounts during an actual crash. In actual crashes, the main rotor is normally turning, creating lift, and thus cancelling a good portion of rotor blade inertial effects on the transmission structural mounts. Another consideration was the desire for data consistency, in that the same one-third main rotor span was used in a preceding AATD crash test (T-40) in 1976 of a CH-47 helicopter (Reference 3). Finally, a surplus 30mm nose gun turret assembly was located and mounted in its design location at FS 122.

CRASHWORTHY LANDING GEAR

The YAH-63 landing gear is a crashworthy design of tricyle configuration. The nose gear is hung from parallel trailing arms, as shown in Figure 3, with a single shock strut to absorb energy and mounted to the main aircraft structure in the vicinity of FS 195. Each main gear is mounted on a shock strut attached to the inboard stub wing which is joined to the main fuselage structure at FS 320. A drag link consisting of a rigid aluminum I-beam completes the main gear geometry (see Figure 4). All shock struts are of conventional air/oil design equipped with a velocity-dependent pressure relief

orifice as shown in Figure 5. The separator piston is free floating within the strut and separates the air side from the oil side. For ordinary landing conditions involving sink speeds up to approximately 20 ft/sec, the strut functions normally as shown by the upper right curve of Figure 5. For crash impact conditions, characterized by high shock strut closure velocities, sufficient pressure is developed in the upper chambers--above the metering orifices--to actuate the blow-off valves located atop the crash orifice. As a result, hydraulic fluid is vented to atmosphere through restrictive orifices absorbing crash energy. The lower right curve represents the strut loading characteristics in the crash condition. Restrictive orifices are sized to obtain a total landing gear energy absorption capacity equivalent to a 20-ft/sec impact. All three struts were disassembled and serviced prior to the test to ensure that specification oil quantities and air pressures existed. MIL-H-83282A fire-resistant hydraulic fluid (450°F flash point) was used in servicing each strut to minimize the postcrash fire hazard.

CREW STATIONS

Copilot/Gunner (Forward) Cockpit

The YAH-63 forward CPG cockpit was modified in a manner so as to more closely represent that of an AH-64 Apache copilot/gunner (forward) cockpit. Figure 6 shows the test configuration for this crew station. The standard YAH-63 crew seat was removed and replaced with a production AH-64 crashworthy crew seat (Figure 7). The seat is bulkhead mounted and armored with boron carbide tile bonded to laminated Kevlar and has a total weight of 136.6 pounds, including cushions and restraint system. The armored bucket is designed to stroke up to 12.3 inches in the vertical direction to absorb crash impact loads using two inversion tube energy attenuators. The fixed-load attenuators are sized for a 14.5 G stroking load based on the weight of an equipped 50th percentile Army aviator. The bucket is supported by roller bearings engaging steel guide tubes to restrict its stroking to the vertical direction only. This is very important in limiting the aviator's forward/lateral strike envelope within the cramped confines of the AH-64 cockpit. This seat was designed to meet the requirements of the Army's crashworthy crew seat specification, MIL-S-58095(AV) (Reference 4).

The restraint system installed in this crew location was a prototype of the jointly developed Army/Navy inflatable body and head restraint system (IBAHRS). This system is illustrated in Figure 8. An airframe-mounted crash sensor is used to identify a crash condition and to trigger separate sodium azide gas generators sewn into the base of each shoulder strap. The gas generators inflate the two automotive-type airbags within 30 milliseconds to tighten the restraint, improve the decelerative load distribution over the upper torso, and substantially reduce the occupant's strike envelope. The crash sensor is programmed to identify an actual crash condition as opposed to merely a hard landing or flight maneuver or gust load. The sensor is normally floor-mounted, but due to the absence of main floor structure in the YAH-63, the sensor box was mounted overhead in the forward electronics bay at FS 215. Figure 9 is a photo of the sensor installation prior to the test. Reference 5 provides a complete description of the IBAHRS. The IBAHRS was installed and supported technically by personnel from the Naval Air Development Center.

The AH-64 incorporates a weapon's sighting device termed an optical relay tube (ORT) in the forward cockpit. Figure 10 is a photo of the actual AH-64 installation. The close proximity of the ORT to the CPG places it within the potential head and upper torso strike envelope of this crewman. A dummy ORT, constructed of lightweight styrofoam, was fabricated and sized to the overall ORT dimensions. It was mounted in the forward YAH-63 cockpit at the same relative distance from the seat reference point as found in the AH-64. The intent of the dummy ORT was twofold: (1) to determine whether or not the CPG restrained with an IBAHRS would contact the ORT in a 95th percentile potentially survivable crash, and (2) if contact was made, to establish, through high-speed photography, the approximate relative striking velocity. The test installation of the dummy ORT is shown in Figure 6.

A prototype helmet was worn by the CPG test dummy so that this crewman would be fully representative of an AH-64 CPG. The integrated helmet and display sight system (IHADSS) is a helmet recontoured in front to readily accept the ORT padded eyepiece during "heads down" use by the CPG. The helmet incorporates an electronic monocle attached to either the left or right side (CPG's preference) called the helmet display unit (HDU). This HDU is essentially a 1-inch cathode-ray tube that will project imagery to a combining glass in front of the crewman's eyes. The symbology displayed consists of such information as airspeed, height above ground, aircraft heading, and weapons tracking and sighting data. The IHADSS, complete with HDU, weighs approximately 3.6 pounds. The IHADSS is shown in Figure 11.

Test dummies selected for both crewman locations were identical 50th percentile General Motors Hybrid II anthropomorphic dummies weighing 171 pounds each without clothing or helmets. To better reveal dummy movements, they were dressed only in flight helmets, light-colored underwear and flight boots.

Pilot (Aft) Cockpit

The standard crew seat manufactured for the YAH-63 was retained and used for the pilot's crew seat in T-41. The installation at this crew station is shown in Figure 12. The bulkhead-mounted crashworthy crew seat design has the capability of a maximum 12-inch vertical stroke at a constant 14.5 G based on a 50th percentile aviator. This crew seat uses two inverted tube energy attenuators operating in compression during the stroking process. As such, they are alignment-critical devices for proper functioning. This is in contrast to the inverted tube attenuators used in the production AH-64 crew seat, which operate in tension and are self-aligning during stroking. The standard YAH-63 crew seat was an early 1970's design with known deficiencies, but was tested in T-41 for comparison only.

BRASSBOARD FLIGHT DATA RECORDER (FDR)

Since 1976, the Aviation Applied Technology Directorate has pursued the exploratory development of a solid-state digital flight and crash data recorder with no moving parts. Using the data compression principle and a solid-state memory, a version of the device has been ground tested as well as flight tested aboard a BLACK HAWK helicopter. In its final form it will be hardened and fireproofed to withstand severe crash environments. Retrieval of

the recorder after a crash will enable accident investigators to re-create up to 36 flight and impact parameters over the last 30 minutes, typically, of the flight. It is also capable of recording data up to 5 seconds at a higher sampling rate after the initial impact pulse. As a crash-hardened model was not available at the time of T-41, a ground-mounted brassboard version was tested for its recording accuracy of two accelerometer readings. Actual recorder accelerometers were co-located on the CPG bulkhead side-by-side with the standard test accelerometers mounted at that location. Sensor signals were fed by umbilical cable to the brassboard FDR located in the data recording trailer. The two parameters measured were longitudinal and vertical acceleration of the CPG bulkhead. Additional information regarding the development and preliminary testing of the FDR is available in Reference 6. The brassboard FDR was supported technically by personnel from Hamilton Standard Division of United Technologies Corporation.

FLIGHT INCIDENT RECORDER/CRASH POSITION LOCATOR (FIR/CPL)

The U.S. Navy is currently developing a crash survivable and floatable flight incident recorder with a combined locator beacon function. It uses a solid-state memory module encased in an energy absorbent and buoyant "donut" airfoil (Figure 13) designed to use a pyrotechnic squib release mechanism to eject away from the aircraft on impact. When ejected, the unit immediately begins to transmit on the 243 MHz emergency frequency. The memory module contains approximately 750,000 bits of nonvolatile metal nitride oxide semiconductor/block organized random access memory (MNOS/BORAM). The unit tested in T-41 was externally mounted to the starboard side of the tail boom at FS 523. For this particular test, the FIR/CPL was triggered to deploy by frangible, normally closed switches mounted on the tail skid, which is on the lower horizontal tail at FS 680 (Figure 14), and by a similar switch mounted on the fuselage belly at FS 347. The memory module for T-41 contained prerecorded digital data with the intent to look at data retention on a posttest basis. The emergency radio beacon was set to transmit on 243.5 MHz (offset from the 243 MHz emergency frequency), and a Naval aircraft was scheduled to orbit the vicinity at 10,000 feet during the test and attempt to receive the signal. The installed FIR/CPL is shown in Figure 15. Naval Air Test Center personnel were responsible for the FIR/CPL experiment with technical support supplied by Leigh Instruments, Ltd., personnel.

EMERGENCY LOCATOR TRANSMITTERS (ELTs)

ELTs, required on most general aviation aircraft since 1974, are small, lightweight radio transmitters with a self-contained power supply designed to activate in the event of a crash and to transmit a characteristic signal for search and rescue homing. Unfortunately, these units are experiencing reliability problems with both false alarms (over 95 percent of all signals are false) and failure to activate after an actual crash. Redesign of ELT switching devices to eliminate these problems has been an ongoing effort by NASA-LRC. Three complete ELTs as well as a bank of 16 switches of various designs were installed on the left inboard fuselage structure at FS 204. In addition to strict accelerometer-type switches, experimental types sensing velocity change as well as peak accelerations were a part of this experiment. A self-contained on-board instrumentation system developed by NASA-LRC monitored performance of the switches throughout the crash sequence. Figure 16 shows a typical ELT test installation.

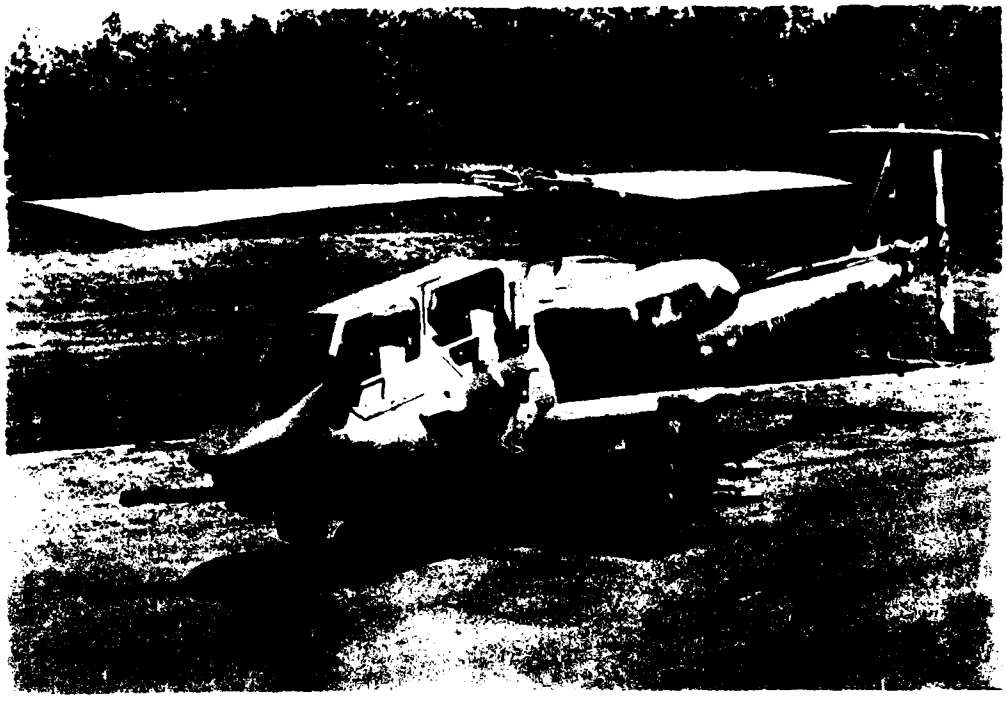

Figure 1. YAH-63 attack helicopter.

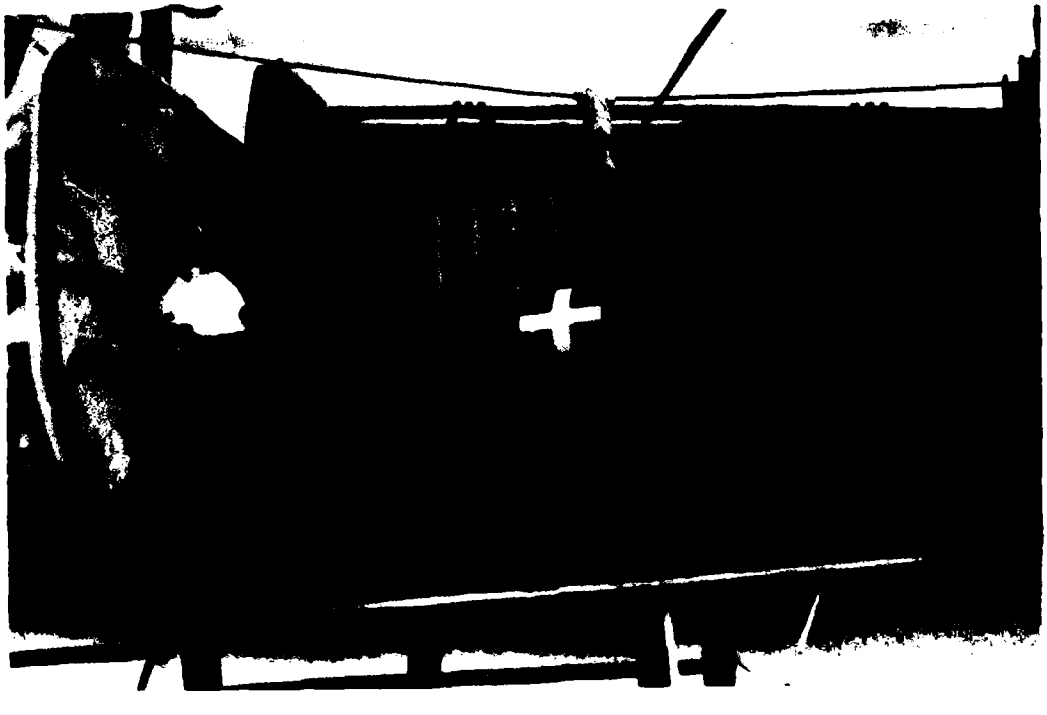

Figure 2. T-700 dummy engine mass mounted to YAH-63 airframe.

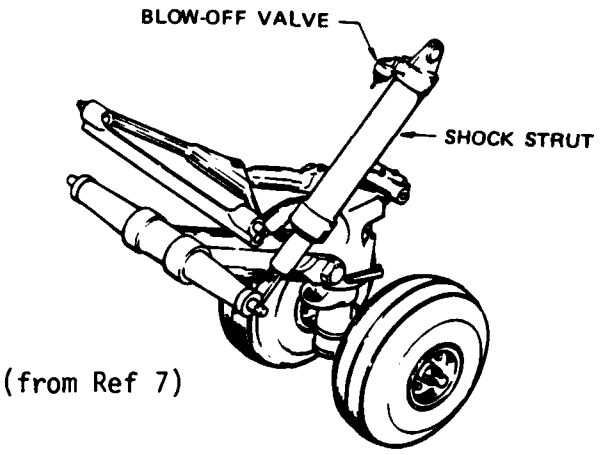

Figure 3. YAH-63 nose gear configuration.

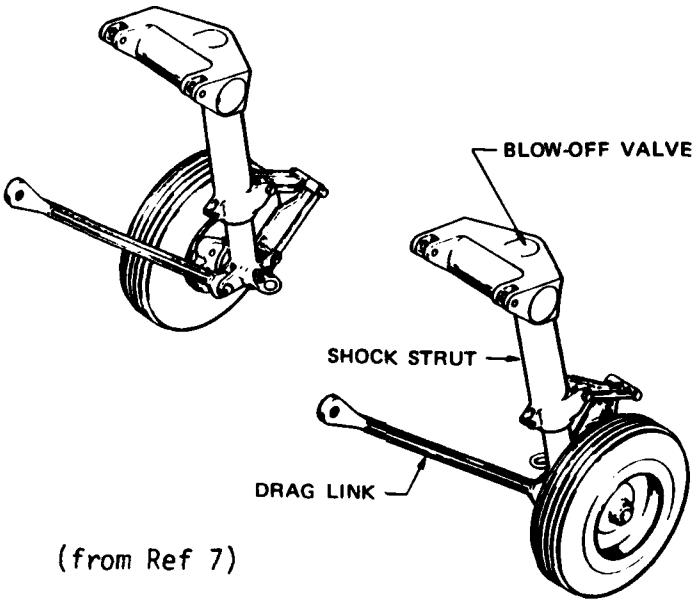

Figure 4. YAH-63 main gear configuration.

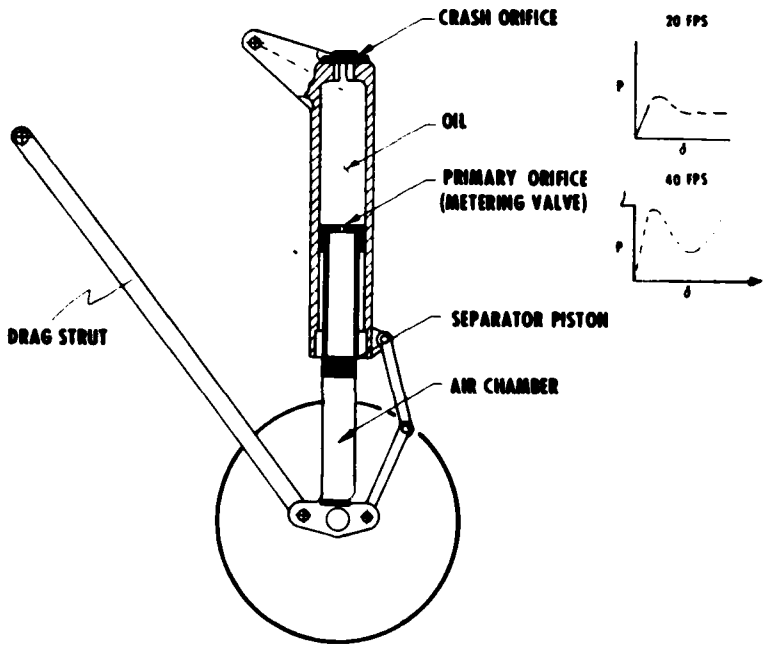

Figure 5. YAH-63 main landing gear - functional sketch.

Figure 6. T-41 test installation at CPG crew station.

Figure 7. AH-64 production crashworthy crew seat.

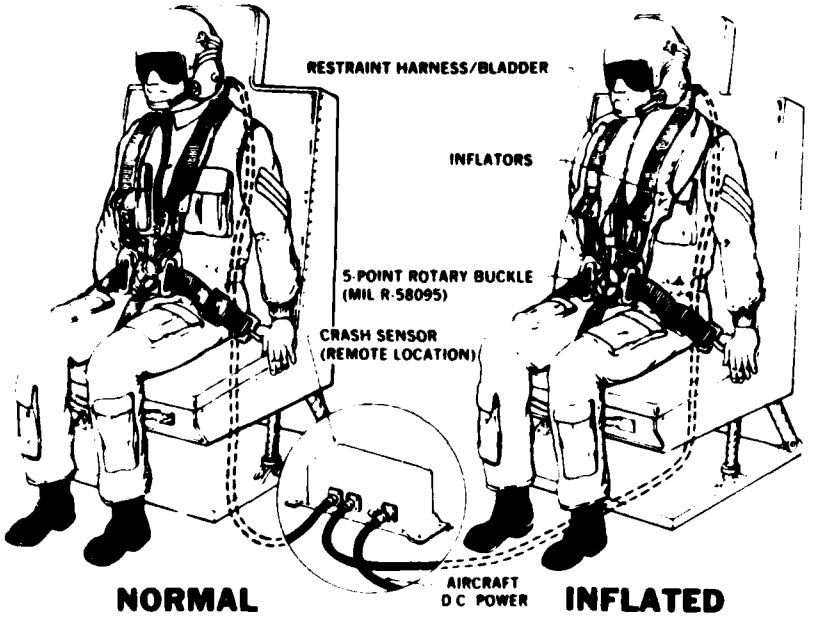

Figure 8. Inflatable body and head restraint system.

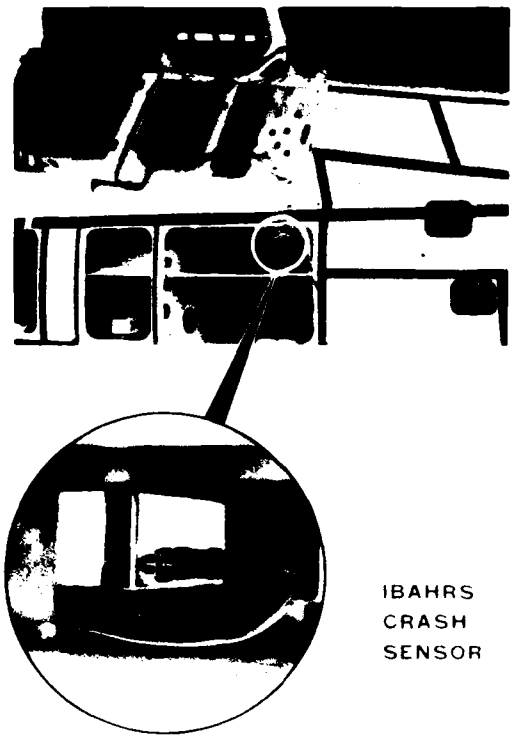

Figure 9. IBAHRS crash sensor location on T-41.

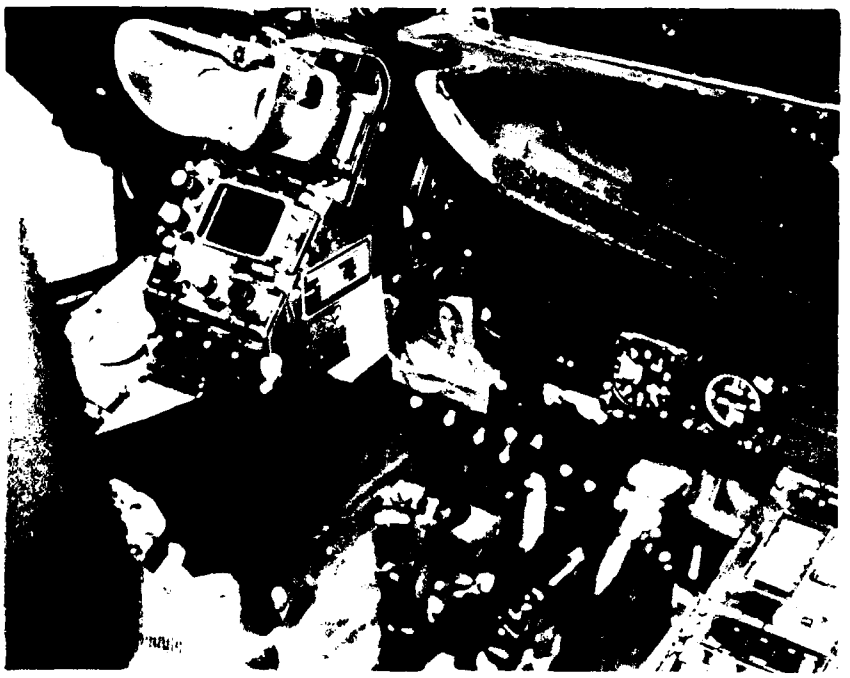

Figure 10. AH-64 CPG cockpit showing optical relay tube.

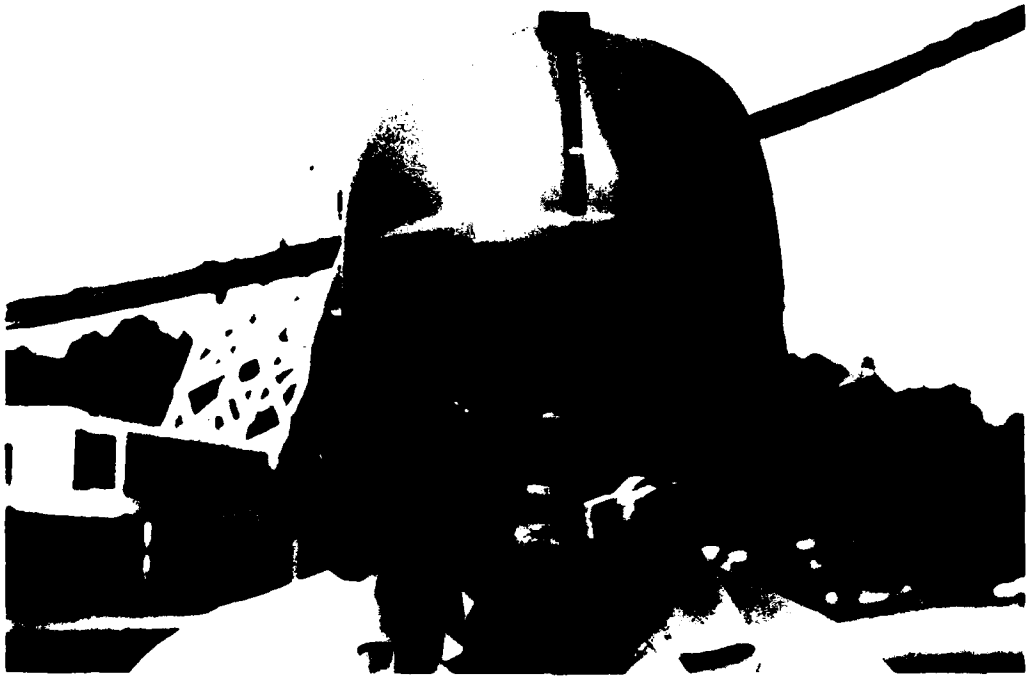

Figure 11. Integrated helmet and display sight system.

Figure 12. T-41 pilot (aft) cockpit test installation.

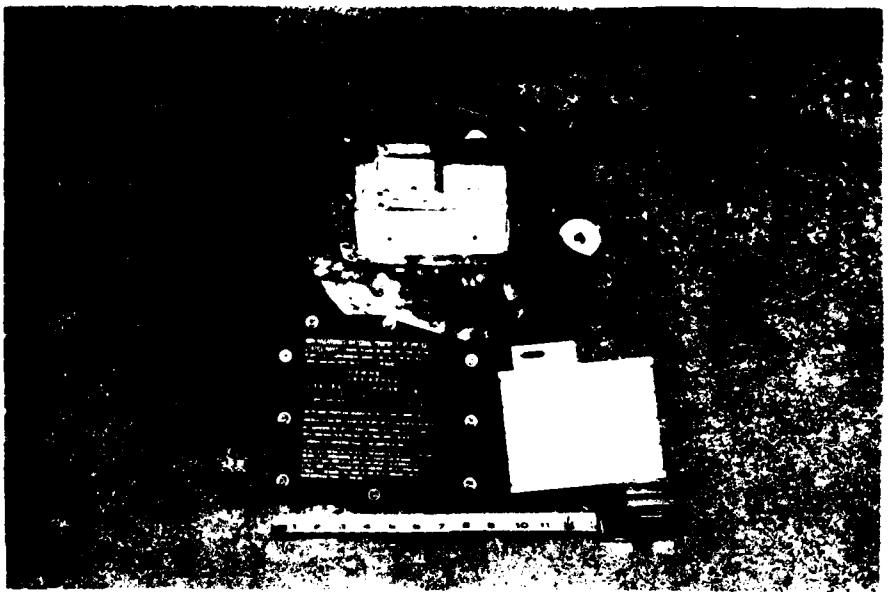

Figure 13. Disassembled flight incident recorder/crash position locator, showing solid-state memory module.

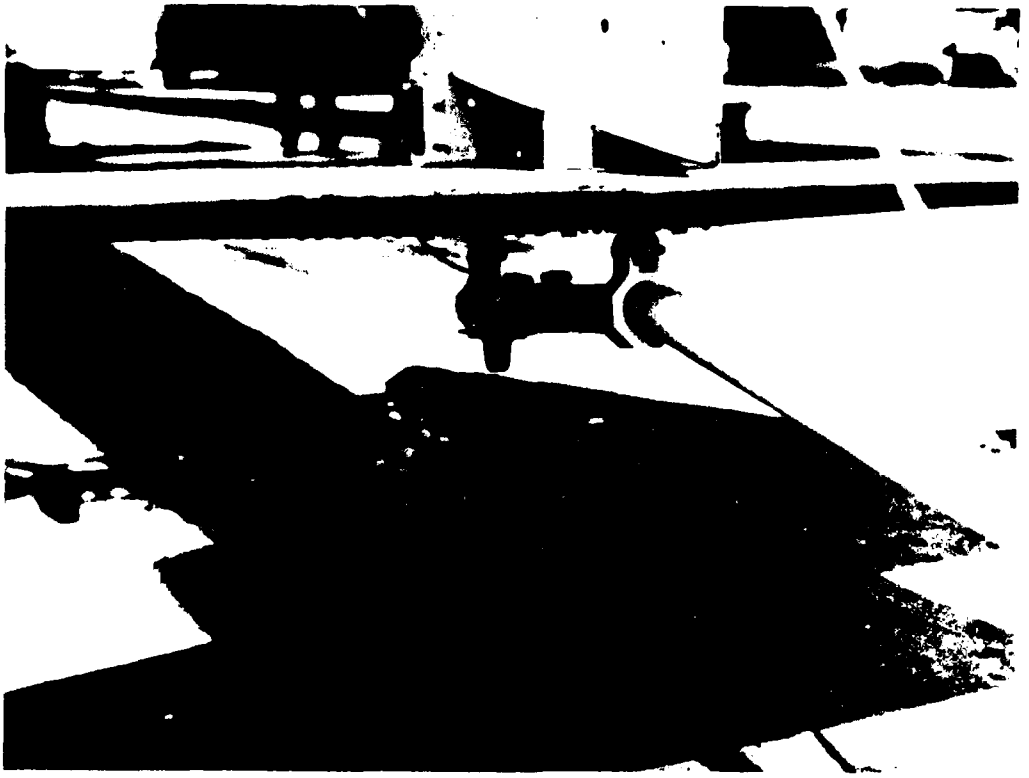

Figure 14. Tail-skid-mounted frangible trigger switch for deploying FIR/CPL.

Figure 15. FIR/CPL installed on YAH-63 starboard tail boom.

Figure 16. Typical NASA-Langley Research Center emergency locator transmitter (ELT) installation.

TEST FACILITY

The YAH-63 crash test, T-41, was performed at the NASA-LRC Impact Dynamics Research Facility shown in Figure 17. The facility, originally constructed as a lunar lander training facility for the Apollo space program, consists of a 220-foot-high by 400-foot-long gantry and associated office, shop, and control areas. The gantry is supported by three sets of inclined legs spread 267 feet apart at ground level and 67 feet apart at the 218-foot level. A movable bridge spans the gantry at the 218-foot level with the ability to traverse the length of the gantry. Along the center line of the gantry, at ground level, is a reinforced concrete strip 400 feet long, 30 feet wide, and 8 inches thick, which is used as an impact surface.

The apparatus necessary to conduct the T-41 crash test is illustrated in Figure 18. Swing-cable pivot-point platforms, located at the west end of the gantry, support the winches, sheaves, and pulley systems that control the length of the swing cables. A pullback platform, attached to the underside of the moveable bridge, supports the winch, sheave, and pully system that controls the length of the pullback cable. Swing and pullback cables are attached to a specially designed lifting harness, which supports the helicopter from ground lift-off to release position during testing (Figure 19). This harness is attached to special mounting bolts on steel support plates sandwiched to the stub wing mounting lugs and then to the swing and pullback cables. The harness system cable lengths were designed and assembled with the swing and pullback cables so that the helicopter would approach the impact conditions outlined in the Test Procedure section.

Each harness cable attached to the pullback cable was equipped with pyrotechnic cable cutters. The harness points attached to the swing cables were connected to the helicopter mounting bolts by pyrotechnic release nuts. Pyrotechnic nuts, releasing all suspension cables, are fired by a lanyard system attached at the tail boom and adjusted to activate the firing circuit at the desired descent height during the swing. Therefore, except for the data umbilical cables, the helicopter impacts the ground in free flight. The lanyard system consists of a contact switch activated by pulling a pin.

Figure 17. NASA-Langley Research Center Impact Dynamics Research Facility.

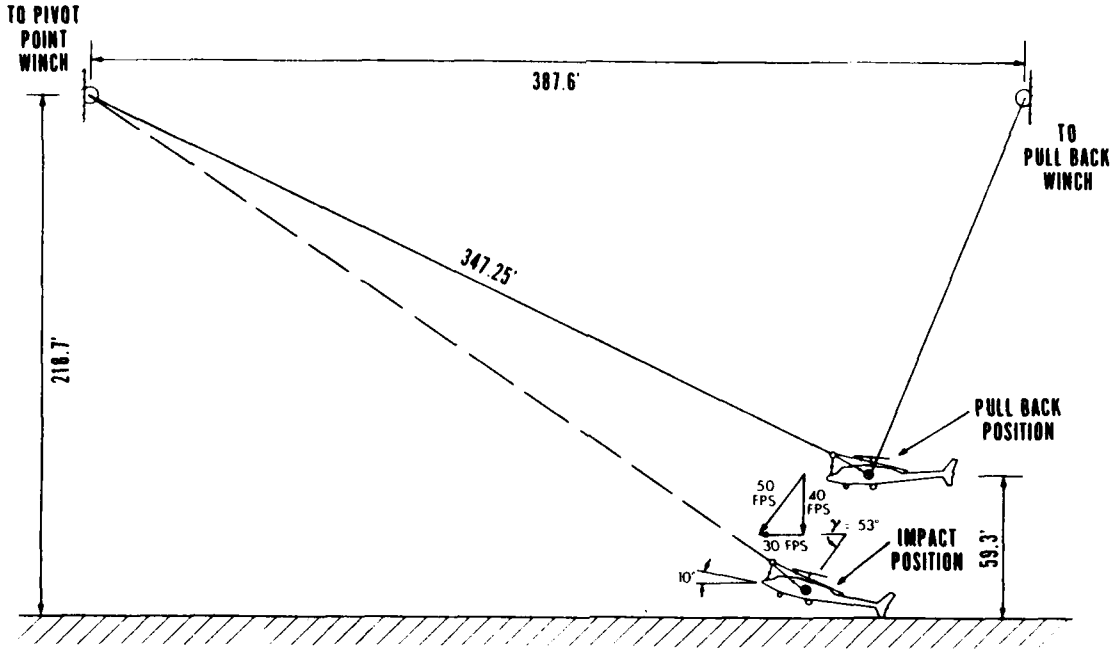

Figure 18. T-41 swing/pullback cable geometry.

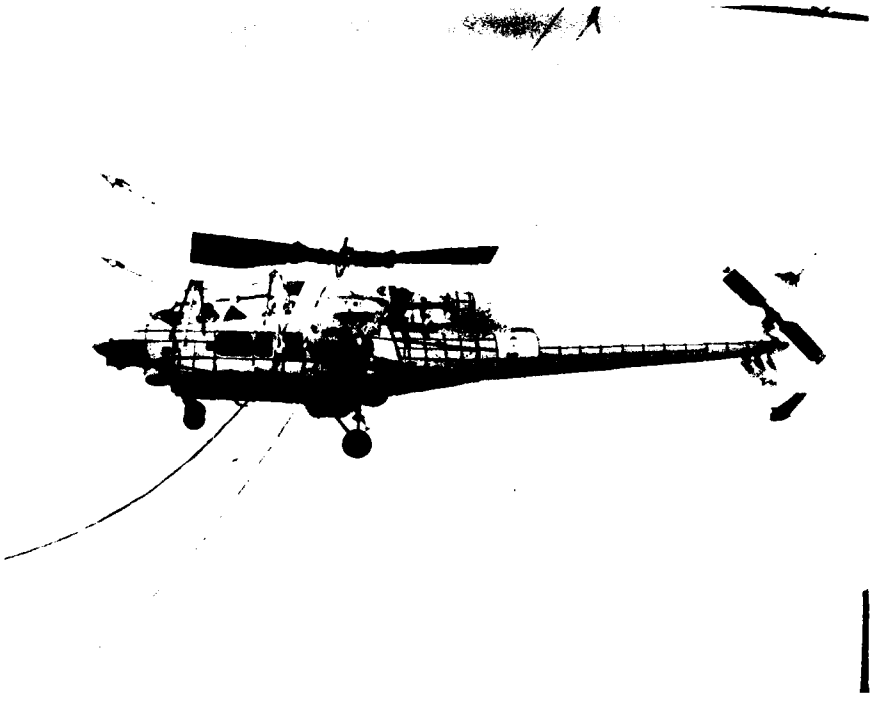

Figure 19. YAH-63 in pullback position.

TEST PROCEDURE

WEIGHT AND BALANCE

The basic YAH-63 test specimen was received at AATD unassembled and without engines. The aircraft was reassembled and instrumented in preparation for the crash test. Unsuccessful attempts were made to locate unserviceable T-700 engines; thus, dummy engine masses, made of 5-1/2-inch solid bar stock, were fabricated to approximate T-700 weight, CG, and pitch/yaw moments of inertia. The dummy masses were then mounted by rigid flanges to the three-point engine mounts at each location. Engine masses were 487 pounds each and their pitch/yaw moment of inertia was 80,588 lb-in^2.

The YAH-63 primary mission loading conditions of 15,984 pounds gross weight and FS 295.5 CG location were selected as a baseline reference. Included in this gross weight were the following items:

Item	Weight (lb)
TOW missile launchers (2)	212
TOW missiles (8)	328
Missile tubes (8)	104
Launcher fairing (2)	40
Ejectable ammunition tray	221
Ammunition (30mm)	728
Total	1633

Because of their crushable mass, locating these jettisonable items beneath the stub wings as stores or in the lower fuselage crush area would provide some extra energy attenuation during a crash. However, the decision was made to delete the weight of these components, since the pilot would most likely elect to "punch off" these potentially hazardous items if he had sufficient warning of an inevitable crash. As mentioned in the test specimen description, the original 50.0-foot main rotor blade was reduced in span by two-thirds in an attempt to account for rotor lift effects. The combined weight of the two removed blade sections was 583 pounds. The final test weight calculation was:

Primary mission gross weight	-	15,984 lb
Less: jettisonable items	-	-1,633 lb
two-thirds main rotor	-	-583 lb
Test weight:		13,768 lb

Longitudinal CG location for T-41 was the same as that of the primary mission, FS 295.5, corrected for the removal of jettisonable stores, ammo tray and ammo, and the outer two-thirds of the main rotor blades. This test CG position became FS 297.2, or 2.8 inches forward of the main rotor mast centerline. Figure 20 shows how the primary mission and test conditions fit into the aircraft CG envelope.

The primary mission called for 232 gallons of JP-4 fuel, or 1505 pounds. This fuel weight was approximated for T-41 by filling the tanks with 1517 pounds (182 gallons) of colored water, since safety regulations prohibit crash testing with fuel at NASA-LRC. Total fuel capacity was 364.3 gallons, or 2368 pounds. Thus, for T-41, fuel tanks were 64 percent full by weight and 50 percent full by volume.

After all test instrumentation and experiments had been outfitted, the aircraft was lifted at its three hardpoints with load cells installed for weight measurement. Two hardpoints were located at the left and right stub wing root structure at FS 277.89 and an aft hardpoint was on the fuselage centerline at FS 347.10. The process of adding water to the fuel tanks was then begun. The YAH-63 has forward and aft fuselage crashworthy fuel tanks located beneath the transmission between FS 278 and FS 342. The aft tank was filled with 859 pounds of water (colored red) and the forward tank with 658 pounds (colored green). Gross weight at this point was 13,111 pounds, or 657 pounds shy of the test gross weight target of 13,768 pounds. Lead ballast was added over the nose gun turret (379 pounds at FS 120.2) and to a shelf inside the tail boom (278 pounds at FS 417) to simultaneously yield the target gross weight and CG conditions. Table 1 is a complete weight and balance breakdown of the principal items on board.

SWING CABLE RIGGING

The YAH-63 was lifted by a network of cables attached to the left and right main stub wing box structure through a specially fabricated pair of steel lift plates. Main lift points were located at the longitudinal CG (FS 297.2). Figure 21 shows the right-hand lift plate placement prior to installation of the stub wing. Two swing cables and two pullback cables powered by winches lifted the aircraft. Two pair of positioning cables--one pair to the nose and one pair to the tail rotor drive shaft--were then adjusted in length to achieve the planned 10-degree nose-up impact attitude as shown in Figure 22. The swing cables were locked in this position, and the aircraft was raised by the pullback cables until the CG of the test specimen was at the desired height of 59.3 feet. This height was calculated to provide a flight path that would result in the planned impact conditions given in Table 2.

The planned crash conditions for T-41 were selected because they would produce deformation of the primary airframe structure and provide a stringent test of crashworthy features at the upper limits for which they were designed. The 50-ft/sec resultant velocity vector represents the 95th percentile potentially survivable accident as defined by MIL-STD-1290AV.

ELECTRONIC INSTRUMENTATION

Seventy-nine electronic sensors were used to record data during the test. These consisted of 50 accelerometers, 12 strain gages, 7 pressure transducers, 6 deflection sensors, and 4 tensiometers (load cells). Figure 23 shows the general location of each type of instrument. Sensors were installed during the month preceding the test. Appendix A provides a detailed description of the instrumentation used in this test, how it was installed and calibrated, and the recording procedures used.

PHOTOGRAPHIC INSTRUMENTATION

Color motion picture coverage was provided by both ground-mounted and on-board high-speed cameras. Ground- and gantry-mounted coverage was by ten D. B. Milliken cameras operating at 400 frames per second (fps) plus a pair of panning cameras (a D. B. Milliken at 400 fps and an Arriflex at 24 fps) viewing the left side of the aircraft. On-board cameras consisted of one D. B. Milliken profiling the pilot (rear) crew station operating at 372 fps and two D. B. Millikens (186 and 372 fps, respectively) profiling the copilot/gunner (front) crew station. On-board cameras were scheduled to operate at 200 and 400 fps, but due to unavoidable drain to the on-board batteries, cameras slowed to the quoted speeds. For proper viewing of the potential strike envelope for each crewmember, it was necessary to locate the cameras at a distance of approximately 44 inches from the outer skin of the aircraft's left side. Special mounting brackets designed and fabricated to withstand 75 G vertically were installed as camera support. Figure 24 shows the on-board camera installation.

Four 70mm Hulcher still sequence cameras were located to view the left, right, nose, and tail of the aircraft. These cameras provided high resolution still photographs of the crash sequence at 50-millisecond intervals. The tripod-mounted cameras were triggered electronically to begin sequence shooting during the preimpact swing. Figure 25 is a schematic showing all camera locations.

TABLE 1. WEIGHT AND BALANCE SUMMARY

Item	Weight (lb)	Longitudinal Station (in.)	Moment (in.-lb)
Basic YAH-63	9409	305.5614	2,875,027
Dummy T-700 engines (2)	974	358.0000	348,692
CPG crew seat (AH-64)	137	182.4000	24,989
CPG dummy and helmet	175	173.0000	30,275
CPG cameras (2)	20	177.0000	3,540
Pilot crew seat (YAH-63)	149	242.2000	36,088
Pilot dummy and helmet	175	234.0000	40,950
Pilot camera (1)	10	244.0000	2,440
Camera mounts (2)	120	210.0000	25,200
Stub wing lift plates (2)	175	294.0000	51,450
Batteries (2)	60	232.0000	13,920
IBAHRS J-box	35	193.0000	6,755
Navy FIR/CPL	14	494.0000	6,916
Nose gun turret	185	122.2000	22,607
Fuel (water) - fwd tank	658	293.2500	192,959
Fuel (water) - aft tank	859	324.1400	278,436
Tail ballast (removed)	-44	679.0000	-29,876
Nose ballast	379	120.2000	45,556
Tail boom ballast	278	417.0000	115,926
Totals at test	13,768	297.2000	4,091,850

TABLE 2. T-41 CRASH TEST PLANNED IMPACT PARAMETERS

Pitch angle, deg	+10
Yaw angle, deg	0
Roll angle, deg	0
Flight path angle, deg	-53.1
Vertical velocity, ft/sec	40
Horizontal velocity, ft/sec	30
Resultant velocity, ft/sec	50

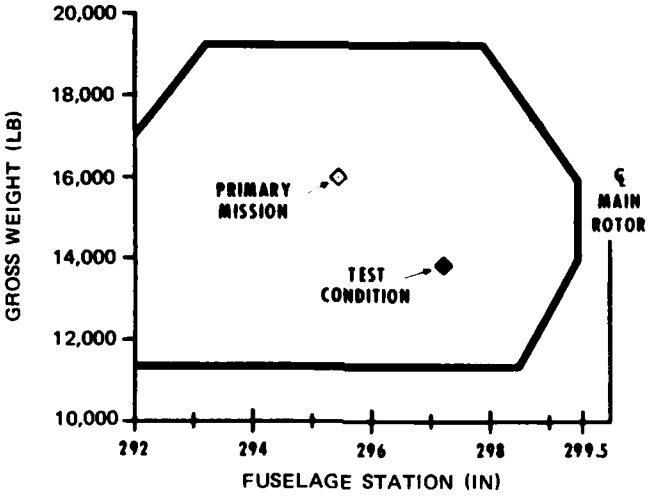

Figure 20. YAH-63 center-of-gravity envelope.

Figure 21. Starboard stub wing lift plate installed.

Figure 22. YAH-63 in preimpact attitude

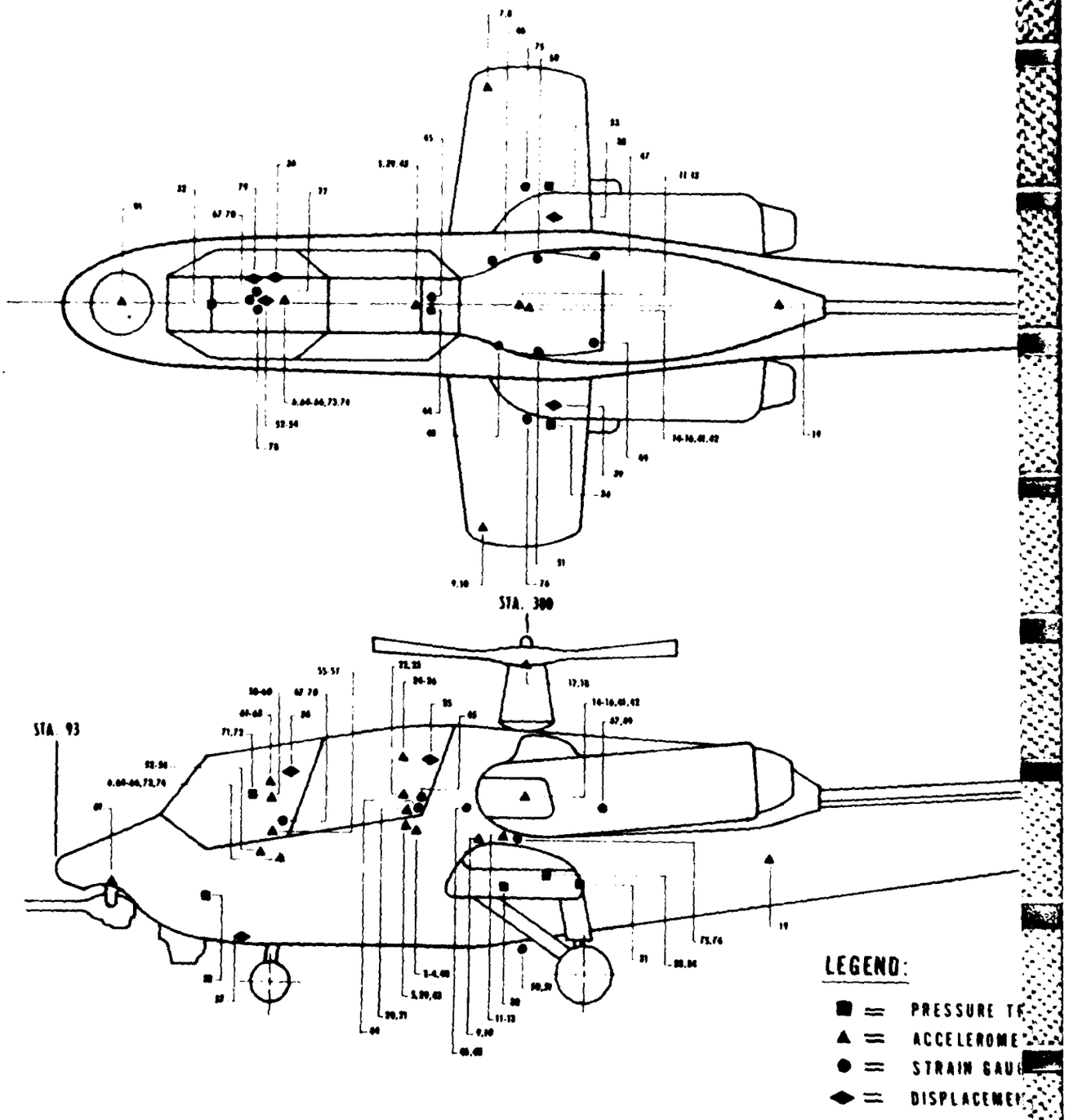

Figure 23. T-41 sensor locations.

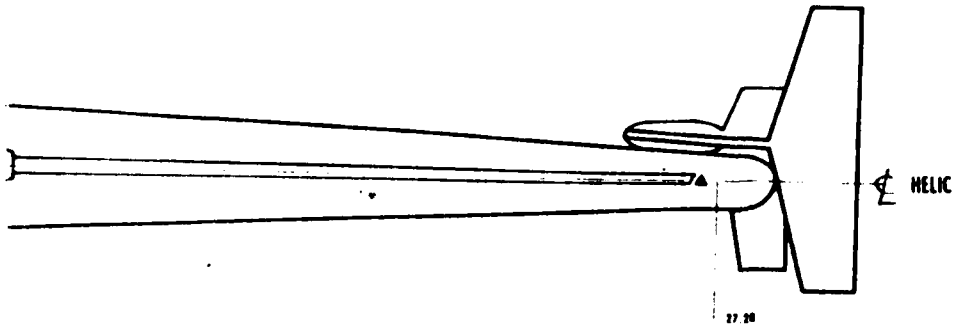

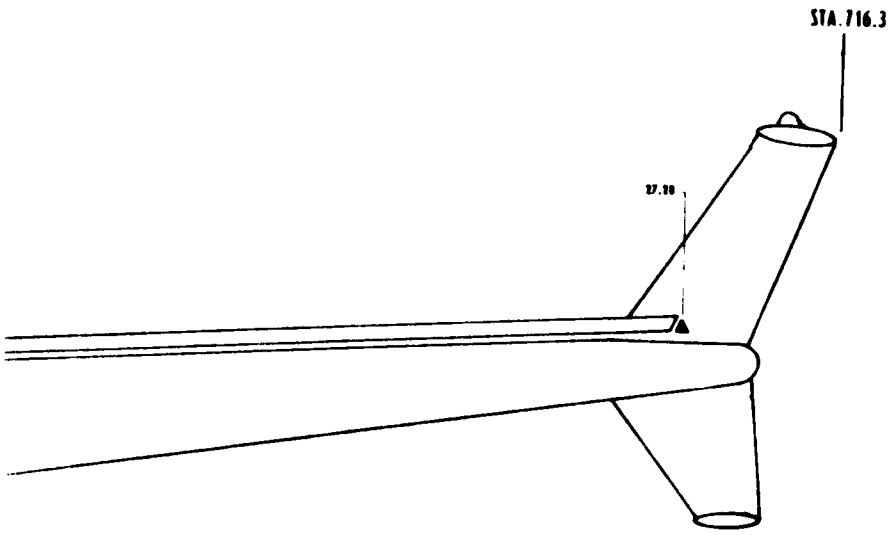

EGEND:

■ = PRESSURE TRANSDUCER
▲ = ACCELEROMETERS
● = STRAIN GAUGE
⬬ = DISPLACEMENT

(2)

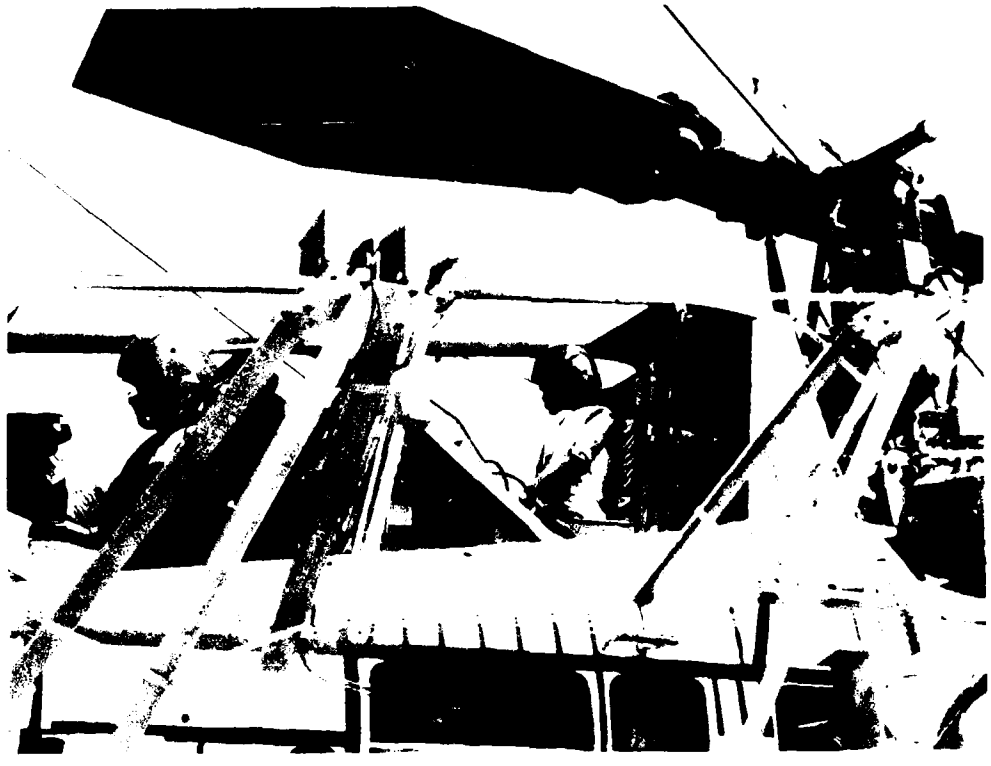

Figure 24. T-41 on-board high-speed camera installation.

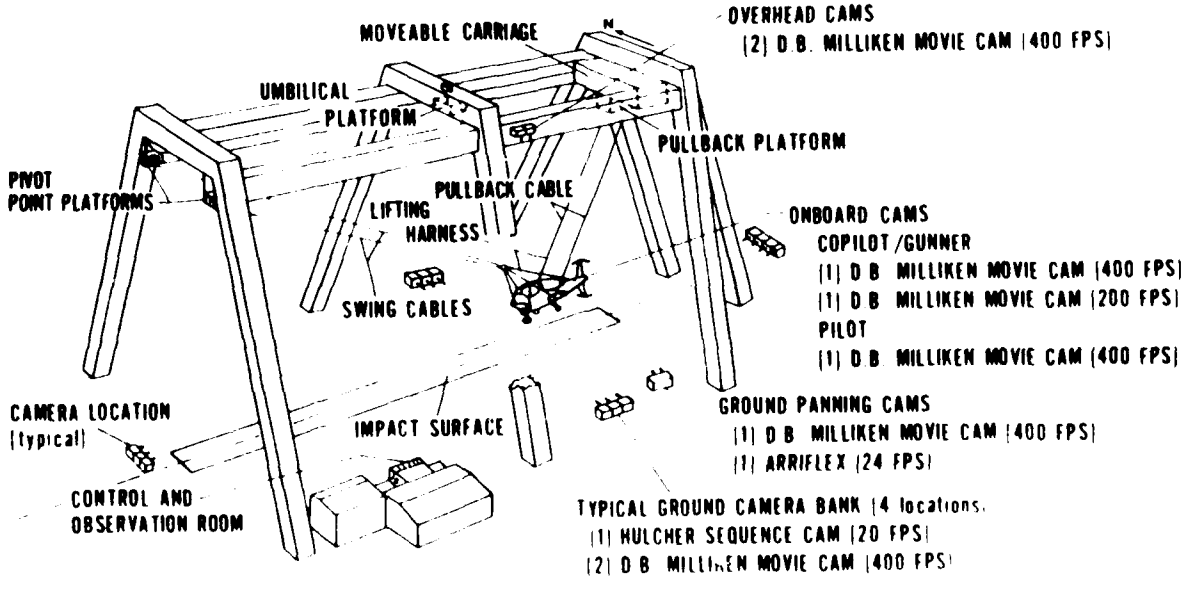

Figure 25. Crash facility layout and fixed camera positions.

TEST RESULTS

IMPACT

The crash test sequence began when the instrumentation recording equipment was started, approximately 30 seconds prior to releasing the helicopter. Release was initiated in the control room by a push switch that closed relays and sent signals from the pyrotechnic power supply to the guillotine cable cutters in the pullback harness. A second and third relay initiated ground-mounted and on-board camera coverage. As the helicopter descended to a point where the tail skid was approximately 3 feet above the impact surface, slack was removed from a lanyard attached to a tail boom mounted switch. At this time the lanyard key disengaged the switch, firing the swing cable harness pyrotechnic cable cutters and separating all harness cables from the test specimen. The helicopter then continued in free flight (except for two data umbilical cables) until impact.

Tail impact occurred at 1400.03.527 EDT with the main landing gear contacting 46 milliseconds later at 1400.03.573. The nose landing gear made contact 45 milliseconds later at 1400.03.618, and the peak acceleration recorded at the aircraft CG (39 G) occurred 54 milliseconds later at 1400.03.672. From tail impact, the helicopter traveled approximately 27 feet along the facility's concrete apron.

Actual impact conditions (Table 3) deviated considerably from those planned. A prevailing wind influence and an overestimation of aircraft aerodynamic drag were both causal factors. Resultant impact velocity was 60.1 ft/sec and the crash pulse contained 44 percent greater energy than that planned. Figure 26 is a bar chart comparing the T-41 crash pulse with two previous full-scale crash tests of CH-47 helicopters (T-40 and T-39).

TABLE 3. T-41 CRASH TEST PLANNED VERSUS ACTUAL IMPACT PARAMETERS

	Planned	Actual
Pitch angle, deg	+10	+9.25
Yaw angle, deg	0	0
Roll angle, deg	0	-0.5 (left)
Flight path angle, deg	-53.1	-53.0
Vertical velocity, ft/sec	40	48.0
Horizontal velocity, ft/sec	30	36.2
Resultant velocity, ft/sec	50	60.1

Figures 27 through 39 are a sequential set of photographs from the ground-mounted Hulcher camera viewing the aircraft's left side. Figure 29 was taken with a hand-held camera, manually triggered, and was later determined, through motion analysis, to have been taken at 135 milliseconds from tail impact. It has been inserted into the Hulcher sequence at the appropriate location.

On impact of the vertical tail, an immediate torsion was applied to the tail boom, since the vertical tail assembly is mounted from starboard flanges at the aft boom. This torsion caused a near total separation of the vertical tail boom and tail rotor gearbox assembly approximately at FS 638. Figure 40 shows the aircraft in its final position.

All three landing gear "blow-off" valves were observed to function as designed and, after stroking of the main gear, fuselage crushing occurred between FS 193 and FS 409 to an average depth of 5.5 inches through this zone. This was somewhat more crushing than was expected and reflects dissipation of the additional 44 percent of energy above that planned. Vertical loads transmitted into the upper fuselage are indicated by the data traces from vertical axis accelerometers mounted to locations on the airframe. Figure 41 illustrates the peak vertical accelerations at various points along the aircraft longitudinal axis.

Retention of high-mass components in a crash of this severity is always a critical aspect of an aircraft's crashworthiness potential. Superior restraint systems and load-control devices do the occupants little good if they find themselves in the path of an engine or transmission torn from its mounts. All of the high-mass items remained secured to their airframe mounts throughout the T-41 crash sequence. Postcrash inspection revealed no measurable deformation at the mounting locations. Shown below are the peak vertical loadings recorded for each of the high-mass items:

Nose gun turret	60.7 G
Right and left engines	38.3 G
Main transmission	30.0 G
Tail rotor gearbox	64.0 G

In general, the fuselage absorbed this very severe impact without any major structural failures that might have been hazardous to the crew. In addition to the tail boom failure described above, the nose failed at the FS 160.75 bulkhead due to vertical loads (see Figure 42). This failure was certainly caused, in part or in total, by the cantilevering effects of the extra 379 pounds of lead ballast mounted over the nose turret. The cockpit canopy frame deformed and distorted as shown in Figure 43. The dynamic deformation was enough that the forward lateral member struck the CPG helmet during the crash sequence, causing superficial damage to the IHADSS helmet (Figure 44). The excessive deformation of the canopy frame was caused by two test-related factors: (1) the removal of all canopy glass for photographic clarity took away structural stiffness, and (2) the external camera mounts designed for the YAH-63 were attached at four points to the upper canopy frame and thus placed an asymmetrical dynamic download on the frame. The left stub wing failed at its attachment point (Figure 45) to the main fuselage box structure and departed the aircraft. The right stub wing remained attached.

Only one of the three on-board cameras recorded the impact, and this camera lost power midway through the crash sequence. On-board cameras were driven off a 24-volt DC aircraft battery. The impact was severe enough that the battery cable was disconnected at its battery-end connector. The 186-fps D. B. Milliken camera at the CPG crew station recorded through approximately 280 milliseconds of the crash pulse before losing power. This period was sufficient to record the IBAHRS inflation and the seat stroking events.

Appendix B contains the output of all retrieved data channels that were processed by NASA-LRC and filtered to 60 Hz. This data filtered to higher frequencies is presented in Reference 7. The data recorded and processed by the Naval Air Development Center (IBAHRS-related data) is presented in Reference 8.

LANDING GEAR

On impact, the high closure velocity of the main and nose landing gear shock struts created sufficient hydraulic pressure to activate the "blow-off" relief valve mechanisms. As a result, after the tires contacted the surface, deflected, and bottomed on the rims, hydraulic fluid was vented through the valve orifices providing energy absorption and attenuation of the crash loads. Once the landing gear had absorbed a portion of the crash energy, gear failure occurred. Figure 46 shows the left main gear after failure of the shock strut upper attachment lug to the wing box structure as well as the drag link lower attachment lug to the shock strut. After failure, the shock strut and wheel assembly departed the aircraft. Figure 47 shows the right main gear having also failed the drag link lower attachment lug. The shock strut upper attachment was fractured but remained attached to the aircraft. The nose gear, shown posttest in Figure 48, failed at the forward attachment lug of the upper link (see Figure 3) and folded upward into the well. The structural fractures or failures present in all three landing gear members suggest that the excessive vertical velocity resulted in higher-than-design forces being transferred to the fuselage attachment points. This was due to loads generated by the venting action of the velocity dependent hydraulic orifices. Figure 49 shows the characteristic shape of the load-deflection curves for the main gear struts for two different crash orifice sizes predicted by Bell Helicopter Textron, Inc. (BHTI), and based on a drop test of the YAH-63 main gear strut from Reference 7. It should be noted that the proposed production YAH-63 landing gear design was to have incorporated mechanical tube-cutting crash energy attenuators that exhibit better load control and are not loading-rate sensitive.

Figure 50 is the vertical accelerometer time history (Channel 11) of the aircraft CG. The trace clearly shows the occurrences of initial impact, main landing gear stroking, nose gear impact, and the combined deceleration produced by nose gear stroking and fuselage crushing. The main landing gear appears to have achieved a peak deceleration of around 8 G, which was approximately the design level for the YAH-63. The effects of nose gear stroking are harder to distinguish since this event took place simultaneously with extensive fuselage crushing.

Berry, Cronkhite and Haas (Reference 7) made a determination of the total crash energy removed by the YAH-63 landing gear by integrating the vertical accelerometer trace of the pilot's bulkhead (Channel 40). Through this procedure they determined a fuselage contact velocity of 38 ft/sec after landing gear failure, resulting in a 10-ft/sec reduction in vertical velocity. This yielded a landing gear energy absorption capability equivalent to a 29.3 ft/sec vertical impact ($\sqrt{48^2 - 38^2} = 29.3$).

A similar analysis was performed for this report, except that the vertical acceleration of the aircraft CG was selected as the parameter most representative of landing gear loads. Figure 50 clearly shows the triangular deceleration pulse produced by the main landing gear stroking from 46 through 91 milliseconds. The pulse is well-defined and, when integrated, yields a vertical velocity change. Since all deceleration during this period is caused solely by main gear stroking, there are no other interactions to clutter the results. Figure 51 shows the vertical velocity decay resulting from the above integration. The final velocity of 42.0 ft/sec occurs at nose gear impact. The nose gear contribution to overall energy absorption is masked by other events as mentioned earlier in this discussion. For this reason, the nose gear energy absorption was derived using a fairly straightforward ratio process described in the following paragraphs.

In preparation for T-41, BHTI performed a drop test of a full-scale main landing gear strut. The test was for the purpose of sizing the blow-off valve orifice so that peak loads developed during a 40-ft/sec vertical impact could be controlled. Results of this drop test are reported in Reference 7. Based on drop test performance, BHTI generated strut load-deflection curves for the orifice sizing ultimately selected for T-41. After T-41, the curves were revised to reflect the higher loads due to the higher-than-planned 48-ft/sec vertical impact velocity. These curves for one main gear strut and the nose gear strut are shown in Figure 52. The curves were integrated to give the predicted energy absorption capability of one main gear (and then doubled for two) and then the nose gear. These values were then ratioed to determine the nose gear energy capability with respect to that absorbed by the mains. This percentage was 28.2.

The vertical velocity of 42.0 ft/sec at nose gear contact corresponds to a main gear energy absorption of 115,539 ft-lb (the kinetic energy difference between main and nose gear contact). If the assumption is made that the stroking nose gear adds an additional 28.2 percent of energy absorption, then the total landing gear attenuation becomes 115,539 ft-lb + 32,582 ft-lb = 148,121 ft-lb. Equating $1/2mV^2$ to this total yields an equivalent landing gear energy absorption capability of 26.3 ft/sec. Compared with the 29.3 ft/sec reported in Reference 7, this is 19.4 percent lower in energy. However, this calculation of 26.3 ft/sec still shows the YAH-63 to have exceeded the MIL-STD-1290 landing gear requirement of 20 ft/sec by 73 percent in energy capability.

COPILOT/GUNNER (FORWARD) CREW STATION

Forces due to the excessive crash energy (beyond a 95th percentile potentially survivable pulse) caused problems in acquiring on-board film data for both the

CPG and the pilot crew stations. The two cameras operating at 372 fps suffered a power interruption after the on-board battery connections were damaged and did not record past the initial onset pulse. The third camera, the D. B. Milliken covering the copilot/gunner at 186 fps, continued functioning until approximately 280 milliseconds after tail impact. The camera mount distorted severely and changed the viewing perspective during the pulse, but certain events were readily observable. Shortly after main gear touchdown (46 ms from tail impact) the IBAHRS sensor triggered the inflatable restraint and the right bag inflated at 80 milliseconds after tail impact. The left bag failed to inflate because the gas generator on that side did not function. The unit was later test-fired normally by the Naval Air Development Center in a laboratory. One possible explanation for the malfunction during T-41 is excessive moisture build-up within the triggering electrical connector for this gas generator. The climate was quite humid and several hard rains had occurred in the days preceding the test. A complete description of the IBAHRS experiment during T-41 is found in Reference 8.

Decelerative loadings on the CPG dummy were examined in some detail in an attempt to define the dummy's deceleration environment and to assess the potential for injury had a human occupant been present. As a consequence of the excessive vertical energy, the AH-64 crew seat traveled through its entire available stroking distance of 12.3 inches and "bottomed" at the limits of the seat bucket travel. The residual energy dissipated resulted in a bottoming pulse clearly shown in the vertical acceleration traces of the seat pan and dummy pelvis.

Figure 53 shows the CPG seat pan vertical pulse resulting from the seat mounting bulkhead input acceleration, which is shown as the solid line. The corresponding CPG dummy pelvis acceleration trace is shown in Figure 54. Both figures are expanded from NADC data plots from Reference 8, which were digitally filtered to 100 Hz. This differs from channels covered with NASA-processed data, which was digitally filtered to 60 Hz. Figure 54 in particular shows evidence of a relatively smooth "ride" on the part of the dummy up until the seat bottoming event. The stroking G load varied between 14 and 19 until the bottoming pulse resulted in a 31 G peak. In the case of the seat pan accelerations shown in Figure 53, the trace is more erratic due primarily to the rapid seat bucket acceleration excursions that occur initially while the seat cushion and dummy buttocks are being compressed, coupling the dummy to the seat during the initial loading of the dummy occupant. This trace shows the stroking G load to vary between 3 and 27 until the bottoming pulse resulted in a 40 G peak.

The Army's current crashworthy crew seat specification, MIL-S-58095 (Reference 4), uses seat pan vertical acceleration as its injury criteria. Accelerations parallel to the aircraft vertical axis are of paramount concern, since with proper restraint the occupants can withstand the full 95th percentile survivable crash acceleration conditions in the lateral (Gy) and longitudinal (Gx) directions with no energy absorption. Such is not the case with vertical accelerations. The thoracic and lumbar vertebrae of the occupant, which must support the upper torso mass while loaded as a column, are susceptible to compression and flexion-induced fractures. MIL-S-58095 requires that, for a

42-ft/sec aircraft vertical impact, an energy-absorbing mechanism limit vertical accelerations at the seat pan according to the Eiband criteria (Reference 9) shown in Figure 55.

These criteria establish the noninjurious upper limit for vertical accelerations transmitted to the occupant to magnitudes of less than 23 G for time durations exceeding 6 milliseconds. Whether it is realistic to apply this criterion to accelerations experienced by the seat pan is currently being reviewed by the Tri-Services and the FAA. Under current guidelines, however, the AH-64 crew seat installed in the CPG cockpit provided noninjurious loads until the excessive impact vertical energy caused bottoming of the seat. At that time the 23 G limit was exceeded for 18 milliseconds. Plotting this pulse on the Eiband curve defines the "seat pan" line shown in Figure 56. If the CPG dummy pelvis trace from Figure 54 is used as an indicator of actual occupant loads, then the 23 G criterion was exceeded for 16 milliseconds and the bottoming pulse defines the "dummy pelvis" line shown in Figure 56. Either way, the indication is that by the Eiband criteria, the CPG bottoming pulse placed him in the area of moderate back injury.

The Naval Air Development Center used the CPG seat pan acceleration data to develop the curve for the dynamic response index (DRI) shown in Figure 57. The DRI is a dimensionless parameter resulting from a single lumped mass, damped spring model of the body mass acting on the human spine. It represents the human response to short duration accelerations applied in an upward vertical direction parallel to the spine. The U.S. Air Force developed the DRI parameter and uses it as one of its ejection seat acceptance parameters. As is seen by the figure, the peak DRI of 26.6 occurred when the CPG seat ran out of stroke and bottomed at 209 milliseconds after tail impact.

Figure 58, from Reference 10, is an injury rate comparison of military pilot ejectees and human cadavers versus DRI. For live pilots, DRIs of greater than 24 correspond to spinal injury rates of greater than 50 percent. It is clear, then, that due to the excess energy present in T-41, 12 inches of vertical seat stroke at 14.5 G was not adequate to keep the seat from bottoming and creating a hazardous condition for the CPG occupant.

The results of the CPG strike envelope relative to the optical relay tube (ORT) were inconclusive. During the main impact, the styrofoam ORT mock-up broke into pieces, dislodged, and separated from its mount. A combination of factors during impact--early separation of the ORT mock-up and extreme distortion of the on-board camera mounts--made it impossible to plot the CPG dummy's strike envelope in relation to the ORT. In any event, the asymmetrical IBAHRS inflation would have invalidated the CPG strike envelope if it had been obtained.

PILOT (AFT) CREW STATION

The input vertical pulse characteristics transmitted to the seat by the pilot's seat-mounting bulkhead were considerably different from those at the CPG bulkhead. Comparison of the two bulkhead peak vertical accelerations (Channel 2 with Channel 6) shows that the pilot's bulkhead received only 70

percent (38.0 vs. 54.5 G) of the peak G loading experienced by the CPG bulkhead. Several reasons are offered in explanation of this peak G differential. The nose landing gear strut assembly was attached to the aircraft at the CPG bulkhead, allowing direct transmission of nose gear shock loads into the bulkhead. On impact of the main landing gear, the aircraft pivoted about its lateral axis so that it was experiencing rotation when the nose gear hit. The CPG bulkhead is 61 inches forward of the pilot's bulkhead and, therefore, impacted at a slightly higher velocity. Finally, in an impact of this severity, there was undoubtedly airframe longitudinal deformation aft of the nose gear which served to attenuate loads at the pilot's bulkhead.

Both of the pilot's seat energy attenuators buckled in compression after stroking only 2.5 inches. Figure 59 is a close-up of the buckled right-side attenuator. In spite of this failure, the seat appeared to continue absorbing energy during this buckling event. Figure 60 is an overlay of the pilot's seat pan vertical acceleration and the crew seat bulkhead (input) acceleration. Peak seat bucket vertical acceleration was 17 G. Also, the pilot's seat began stroking at 139 milliseconds after tail impact, 13 milliseconds after the CPG seat began stroking. As these vertical loads do not exceed the 23 G Eiband criterion, the pilot should have survived this impact with no spinal injury. As was the case with the CPG, the pilot's lateral and longitudinal loads were well within noninjurious tolerance for a properly restrained human.

FUEL SYSTEM

The YAH-63 fuel system, which was designed to the Army's crashworthy fuel system requirements of MIL-T-27422B (Reference 11), generally performed well despite the 44 percent excessive energy (beyond that planned) present in the actual crash pulse. Pressure sensors (described in Appendix A) were located internal to each fuel tank to measure the hydraulic ram pressure time histories. The forward fuel tank sensor was located at WL 54.8 and the aft tank sensor at WL 55.8. Both fuel tank bottoms were located at WL 40. The forward fuel tank pressure peaked at 115 psig at 133 milliseconds after tail impact, or 87 milliseconds after main gear impact. Aft fuel tank pressure peaked at 102 psig at 140 milliseconds after tail impact, or 94 milliseconds after main gear impact. The cable to the aft tank pressure transducer was severed due to structural damage at approximately 150 milliseconds after tail impact, and it is estimated that the pressure peak in this tank was correctly recorded just prior to the drop-out.

Three breakaway/self-sealing valves in the lower fuselage area were broken and sealed off completely, as designed. One leak in the forward fuel tank area did occur, allowing a steady escape of green colored water. This leak was relatively small--estimated at 1 gallon per minute. The source was located only after disassembly of the aircraft's belly structure. A fuel sump lower cover located approximately 20 inches aft of the forward fuel tank forward bulkhead (FS 275) and 9 inches inboard of the left keel beam (BL 24) had fractured along its aluminum mounting flange. The fuel leakage was confined to the flange area and there was no penetration of the fuel tank material. The sump cover was located immediately above the ejectable ammo tray which is designed to house ammunition for the 30mm nose gun.

The ammo tray of this prototype helicopter was definitely not developed or refined into a production configuration and was somewhat "cobbled" together to expedite the prototype construction. In the area of the forward fuel tank sump cover, a number of aluminum angles had been pieced together to form a stringer along the upper section of the ammo tray. It was the structural break-up of this segmented stringer that was responsible for the sump cover flange fracture. Figure 61 is a view looking from inside the fuel tank at the elliptical sump cover and its fractured flange; Figure 62 is the view looking up from outside the sump cover; and Figure 63 shows the approximate relative relationship of a typical segmented stringer and the sump cover plate.

With consideration being given to the nonstandard nature of the ammo tray construction and to the higher-than-design severity of this crash pulse onto a nonyielding surface, the performance of the crashworthy fuel system was successful.

BRASSBOARD FLIGHT DATA RECORDER (FDR)

Representatives of Hamilton Standard Division of United Technologies Corporation processed the recorded signal received from CPG bulkhead accelerometers. Figure 64 shows the FDR's vertical accelerometer output filtered to 100 Hz (Channel 73) compared with the NADC 100 Hz data for a different accelerometer at the same location (Channel 64). FDR data for the longitudinal accelerometer at the CPG bulkhead is shown compared with Channel 66 data in Figure 65. The FDR vertical acceleration was very representative of the pulse trend recorded on Channel 64. The amplitude of peak accelerations, however, was usually higher by as much as a factor of 2. This could probably be improved with attention to accelerometer selection and calibration. FDR longitudinal acceleration tracked the Channel 66 trace well except for two or three unexplained departures. The concept of recording a crash pulse in solid-state digital memory is certainly viable, judging from the T-41 results.

FLIGHT INCIDENT RECORDER/CRASH POSITION LOCATOR (FIR/CPL)

The tail-low impact activated the frangible switch at FS 680, which in turn triggered the pyrotechnic ejection of the FIR/CPL airfoil. The airfoil impacted the concrete surface near the point of aircraft impact. The impact loading was later determined to be approximately 300 G. Figure 66, taken by NATC personnel at 191 milliseconds after tail impact, shows the airfoil in mid-flight just prior to ground impact. The airfoil came to rest 14 feet from the aircraft, and the 243.5 MHz emergency radio transmission was successfully received by a Naval aircraft orbiting at 10,000 feet in the vicinity of the test site. The test signal was allowed to transmit for about 30 minutes after impact and then turned off. There was very little damage to the airfoil, and all data in the memory module was later shown to be intact. The FIR/CPL system is currently planned for production installation on U.S. Navy SH-60 B/F and HCS helicopters. Additional information regarding the FIR/CPL experiment is available from Mr. Daniel M. Watters, now with Helicopter Combat Support Squadron Sixteen, NAS, Pensacola, Florida.

EMERGENCY LOCATOR TRANSMITTER (ELT)

Interest in the ELT experiment centered mainly on the two banks of triggering switches that were undergoing functional checks. Each bank contained eight switches (production and experimental). Specific detailed results on the ELT experiment are available through Mr. Huey Carden, NASA-LRC.

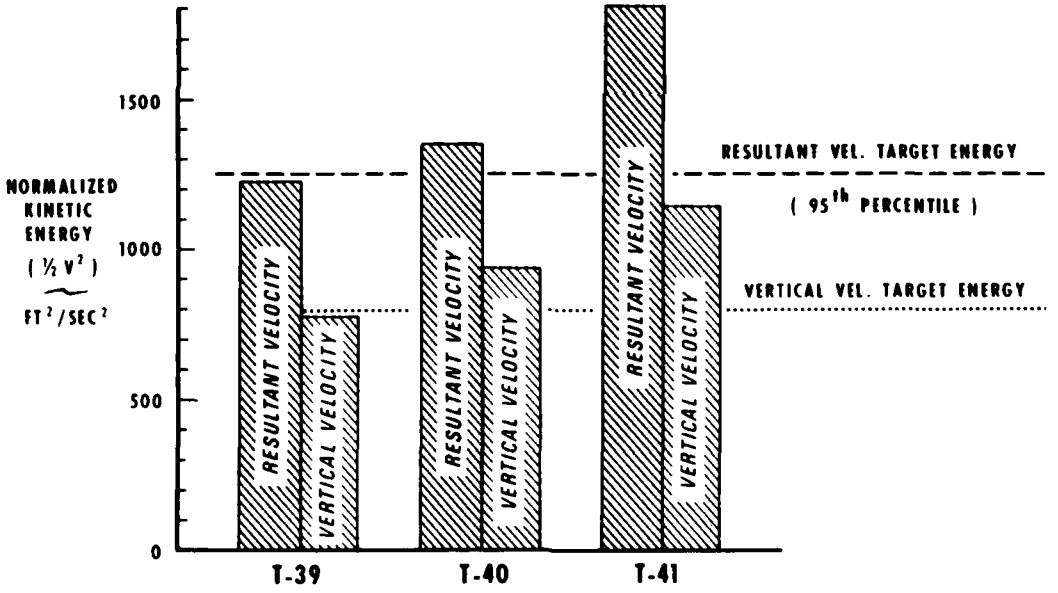

Figure 26. Relative energy in impact pulse for three Army/NASA crash tests.

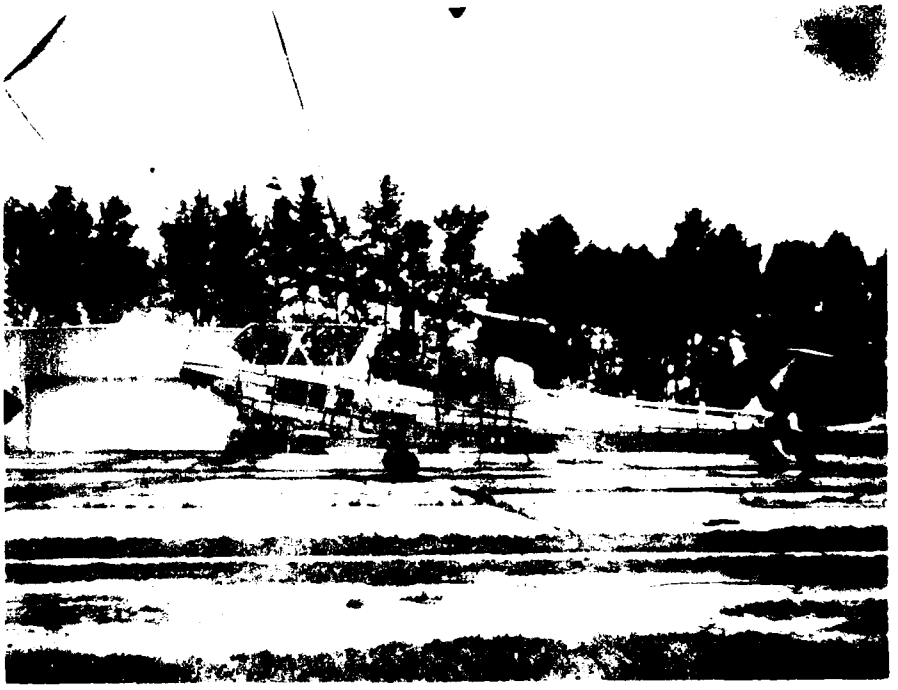

Figure 27. T-41 Hulcher photo (tail impact +44 ms).

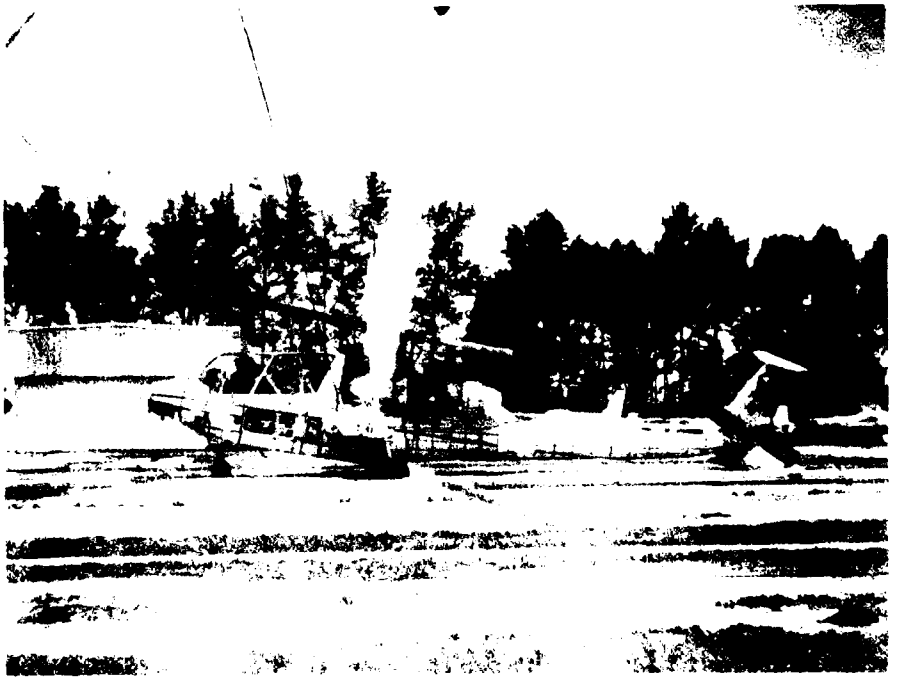

Figure 28. T-41 Hulcher photo (tail impact +94 ms).

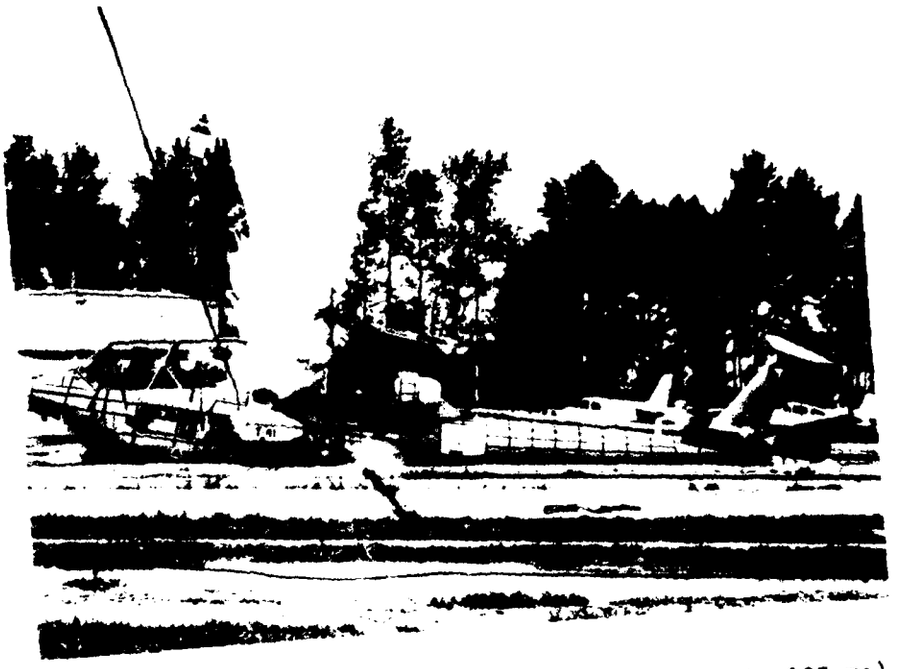

Figure 29. T-41 still camera photo (tail impact +135 ms).

Figure 30. T-41 Hulcher photo (tail impact +144 ms).

Figure 31. T-41 Hulcher photo (tail impact +194 ms).

Figure 32. T-41 Hulcher photo (tail impact +244 ms).

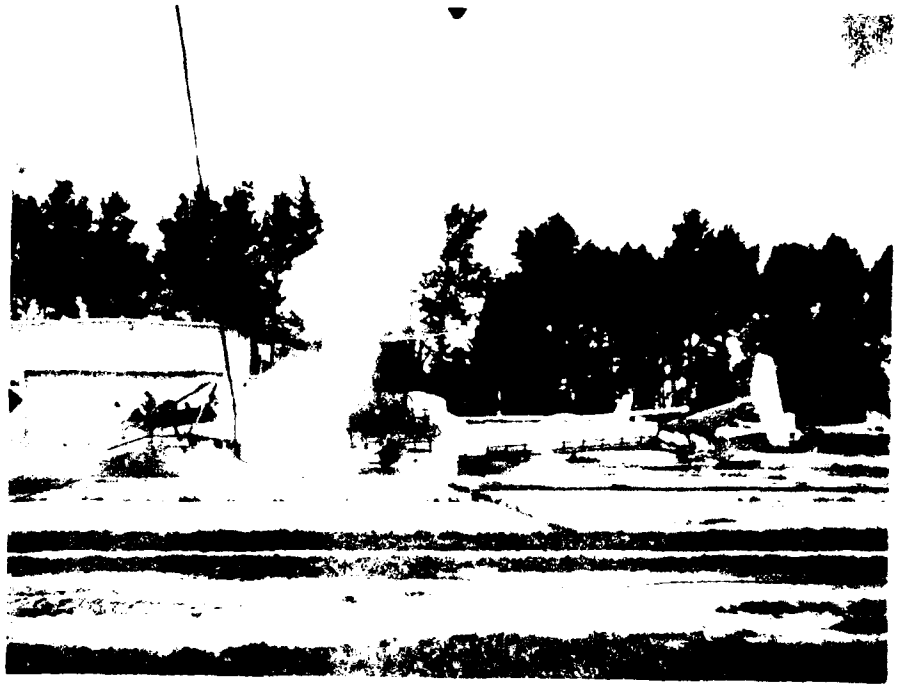

Figure 33. T-41 Hulcher photo (tail impact +294 ms).

Figure 34. T-41 Hulcher photo (tail impact +344 ms).

Figure 35. T-41 Hulcher photo (tail impact +394 ms).

Figure 36. T-41 Hulcher photo (tail impact +444 ms).

Figure 37. T-41 Hulcher photo (tail impact +494 ms).

Figure 38. T-41 Hulcher photo (tail impact +544 ms).

Figure 39. T-41 Hulcher photo (tail impact +594 ms).

Figure 40. YAH-63 in final posttest position.

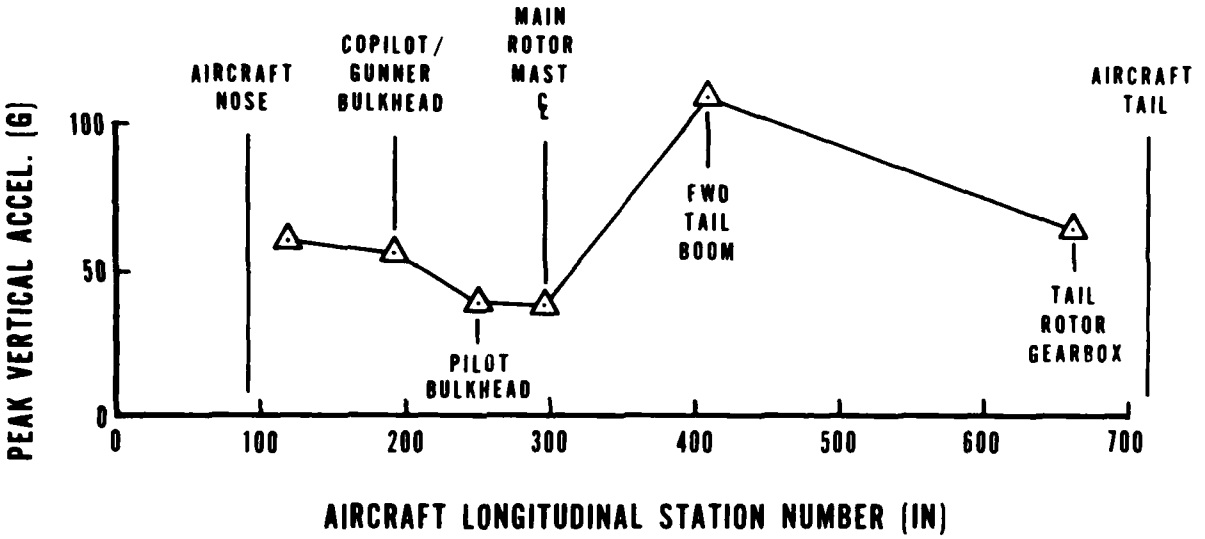

Figure 41. YAH-63 peak vertical acceleration.

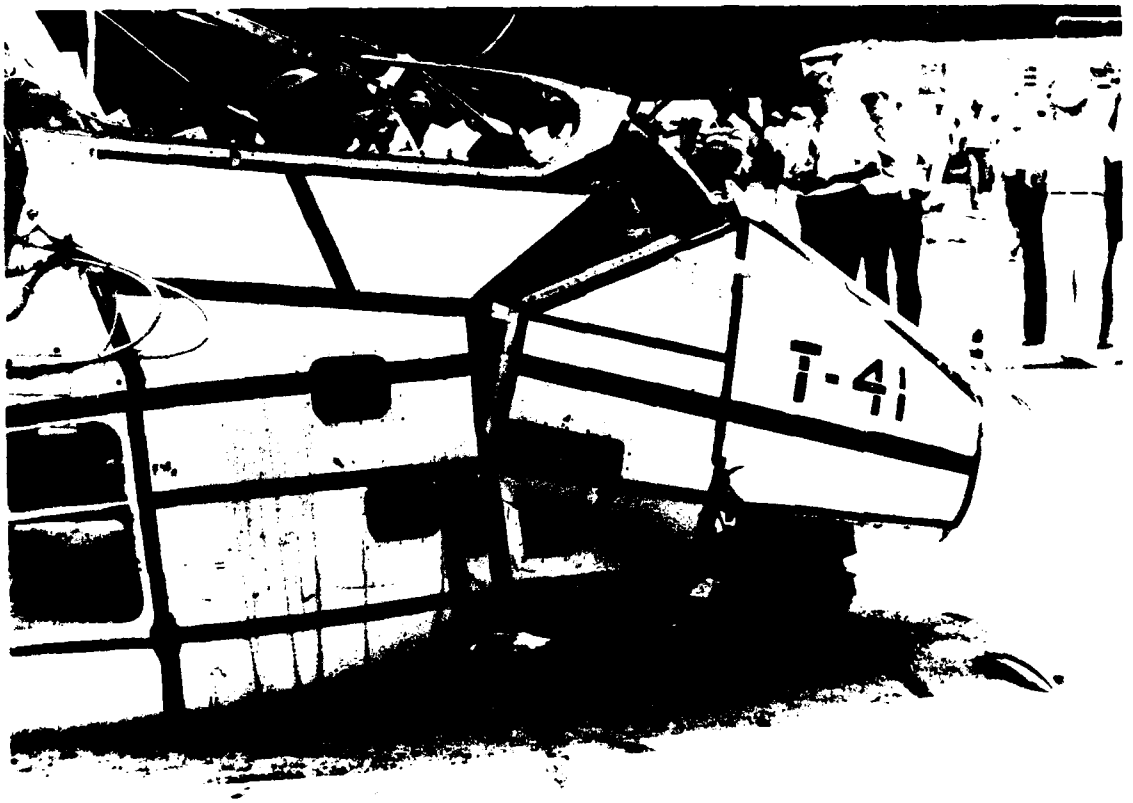

Figure 42. YAH-63 failed nose section.

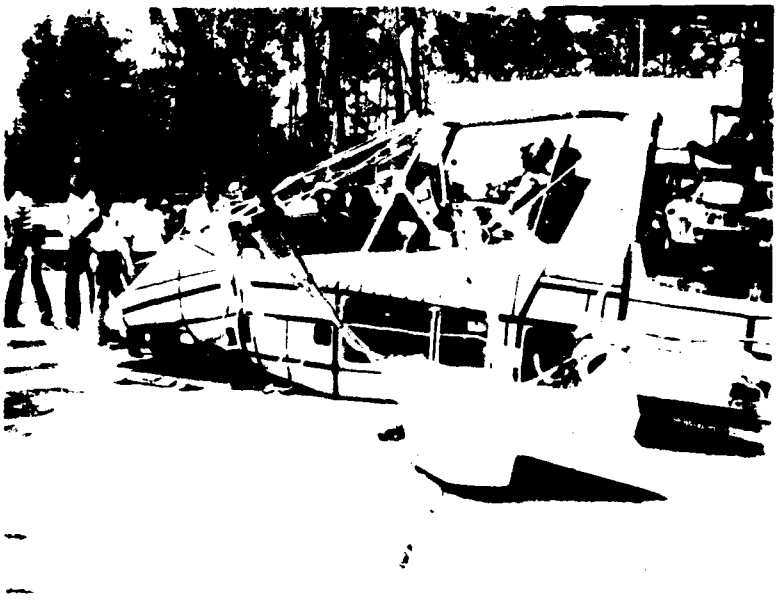

Figure 43. YAH-63 crew stations with deformed canopy frame.

Figure 44. Superficial damage to visor cover of IHADSS helmet (aft crew station).

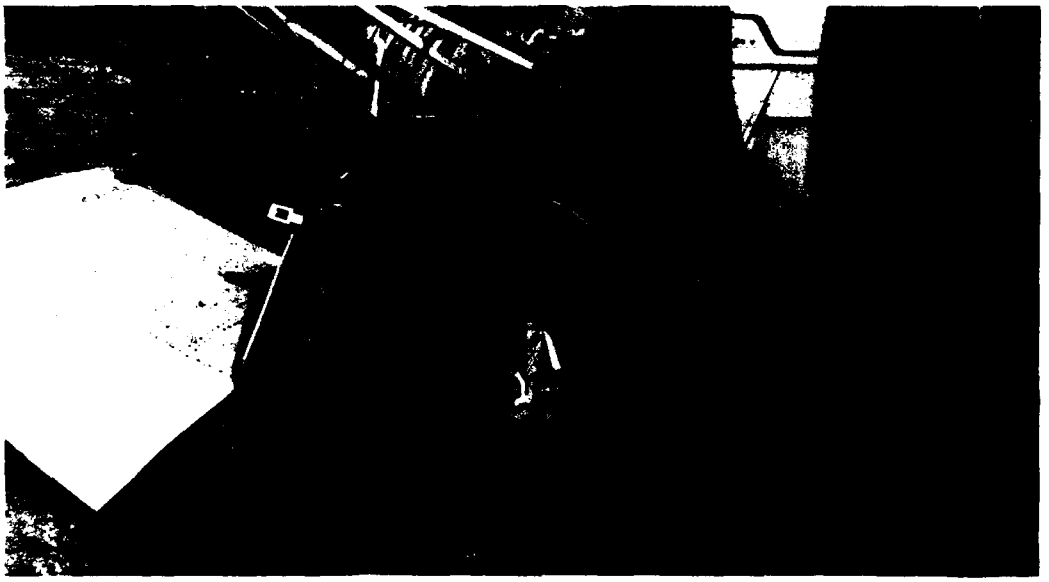

Figure 45. Left stub wing failure at attachment point.

Figure 46. Failed attachment fitting of left main gear strut.

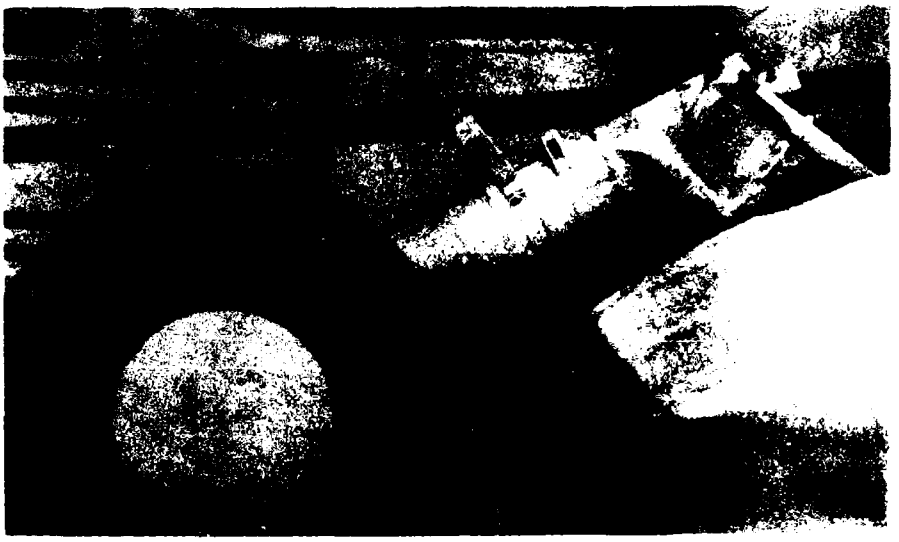

Figure 47. Right main gear strut after failure of drag link lower attachment lug.

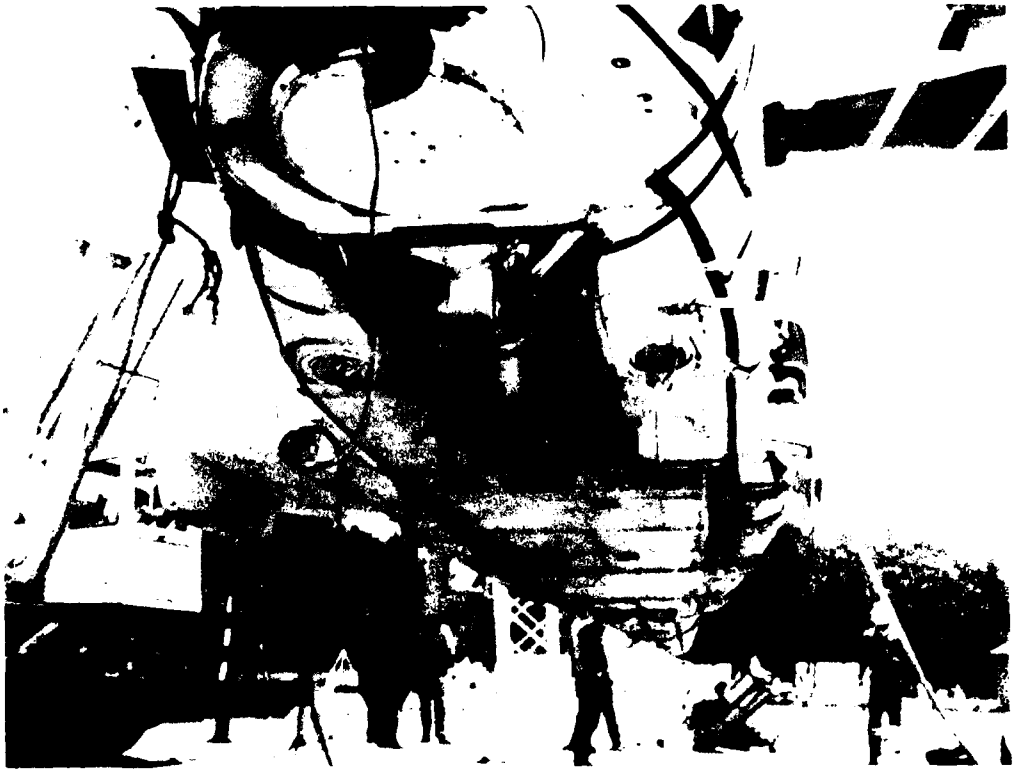

Figure 48. Nose gear after failure and folding into well.

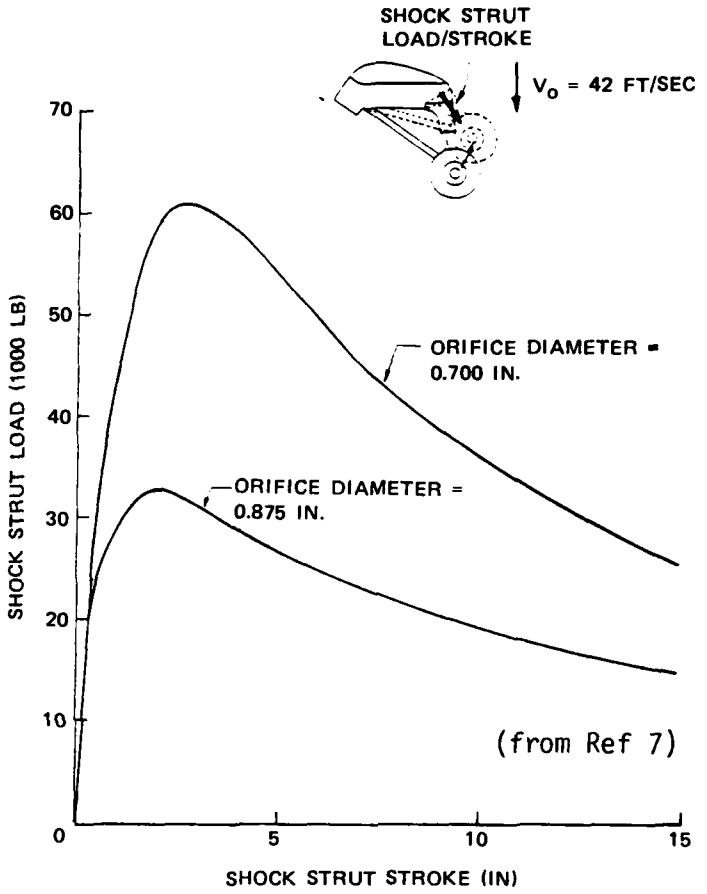

Figure 49. Main gear load deflection for 42 ft/sec vertical sink speed.

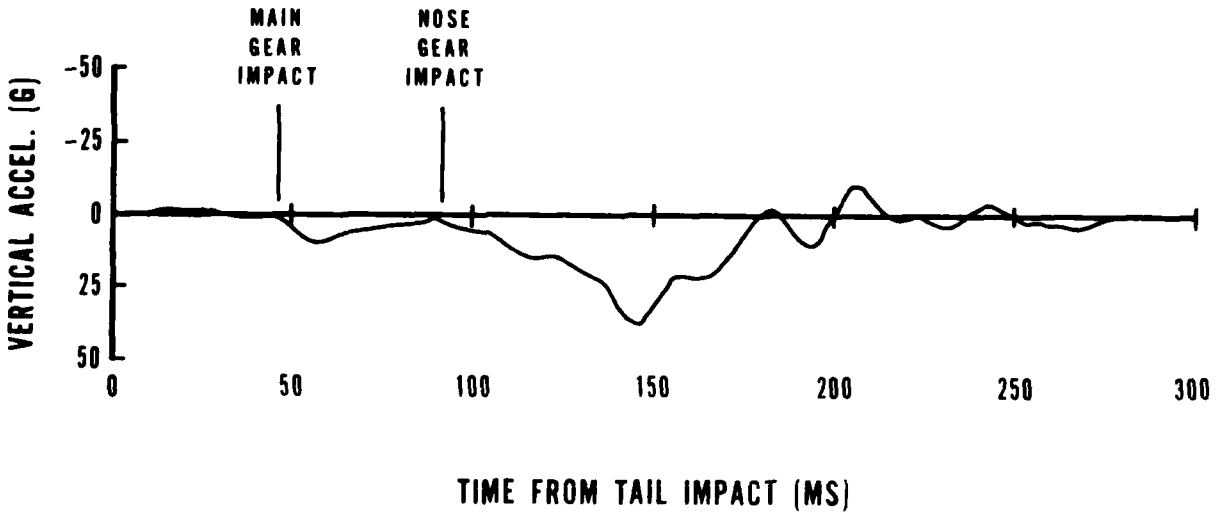

Figure 50. Vertical acceleration at aircraft center of gravity.

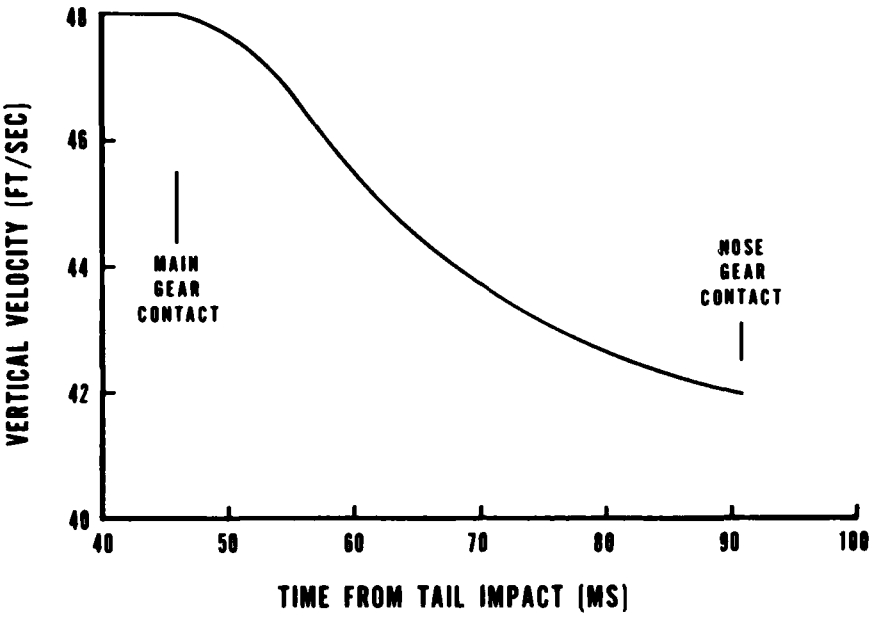

Figure 51. YAH-63 vertical velocity change during main gear stroking.

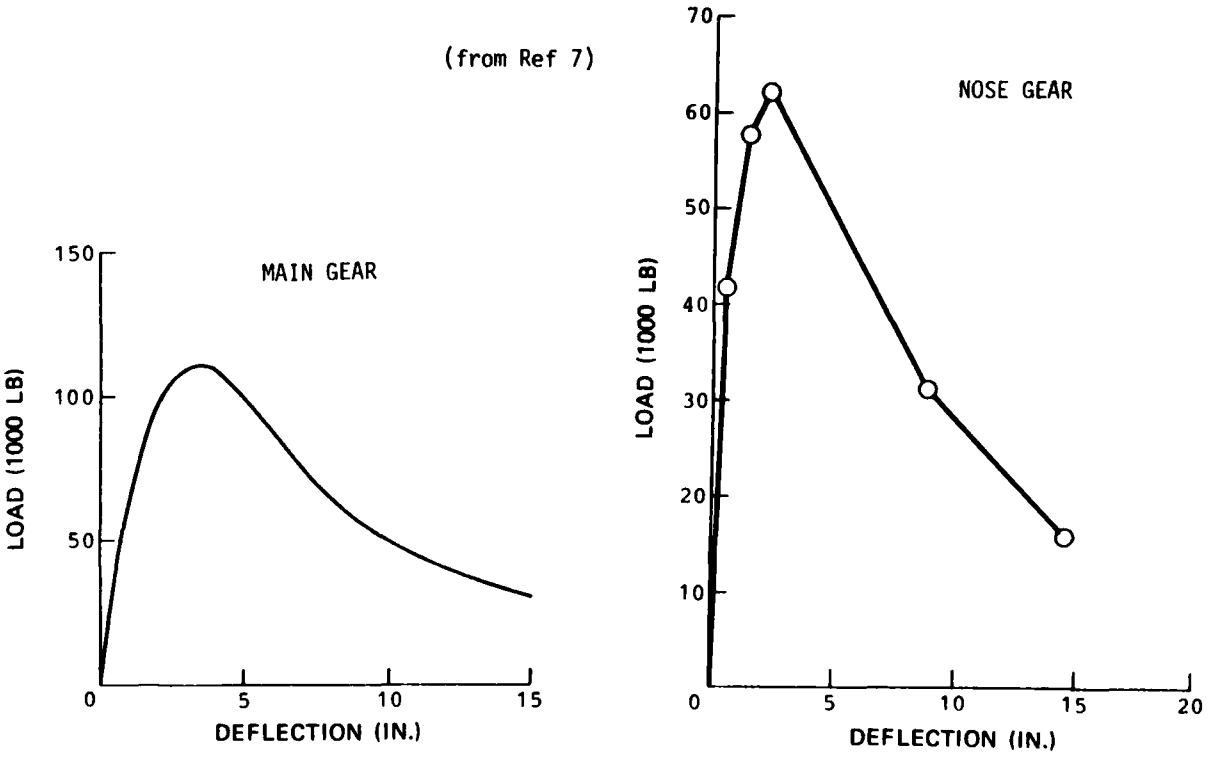

Figure 52. Predicted YAH-63 landing gear load deflection at T-41 sink speed.

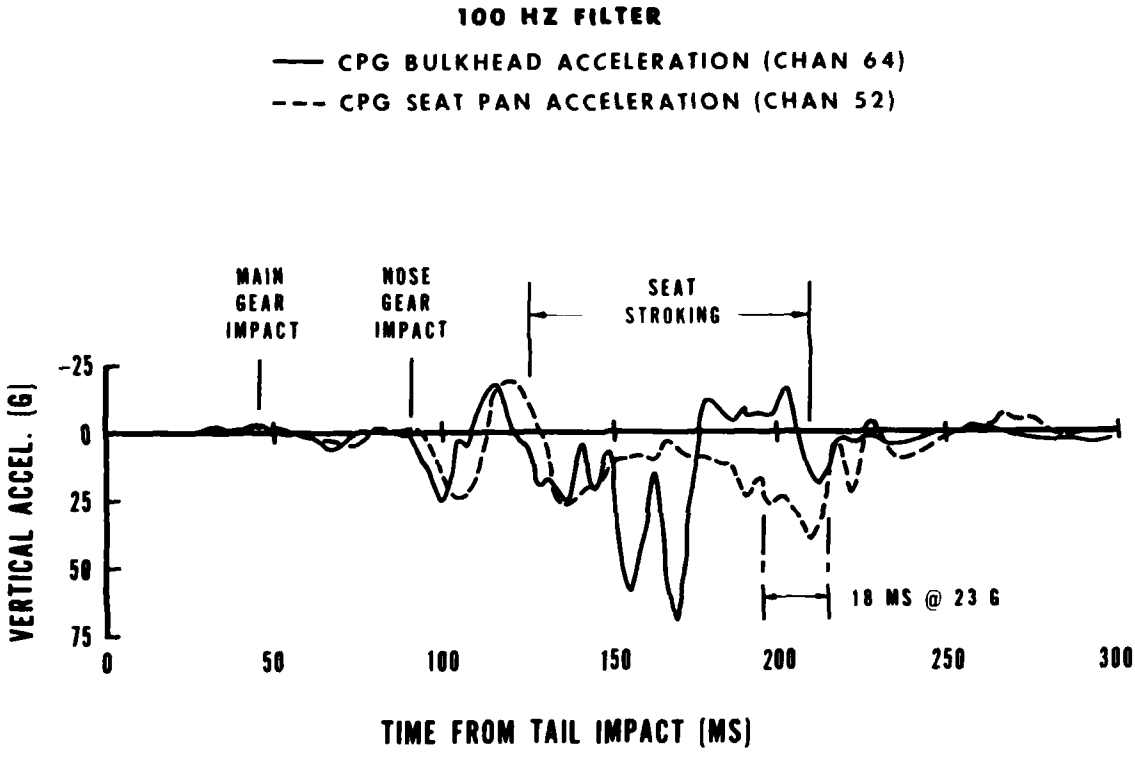

Figure 53. CPG bulkhead vertical pulse and seat pan response.

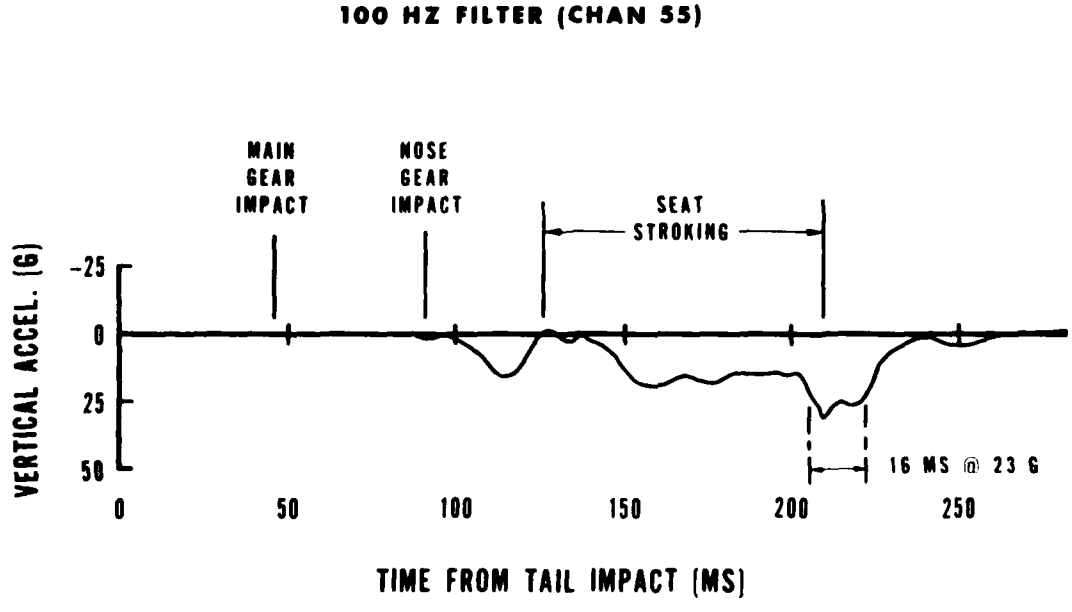

Figure 54. CPG dummy pelvis vertical acceleration.

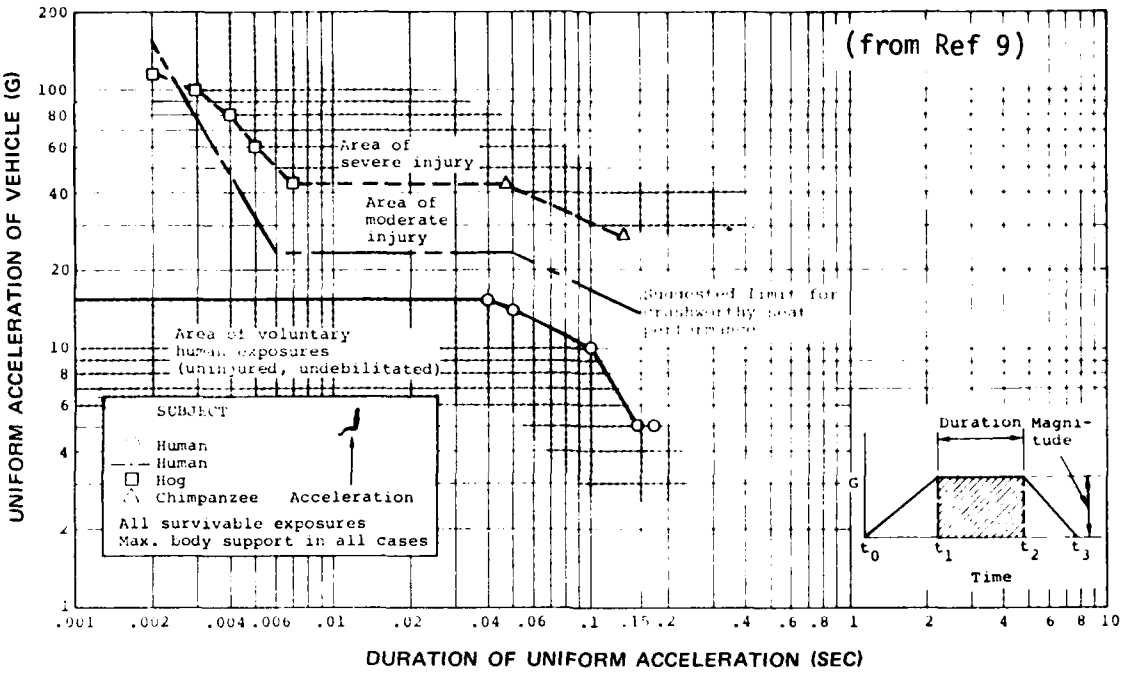

Figure 55. Duration and magnitude of headward acceleration endured by various subjects.

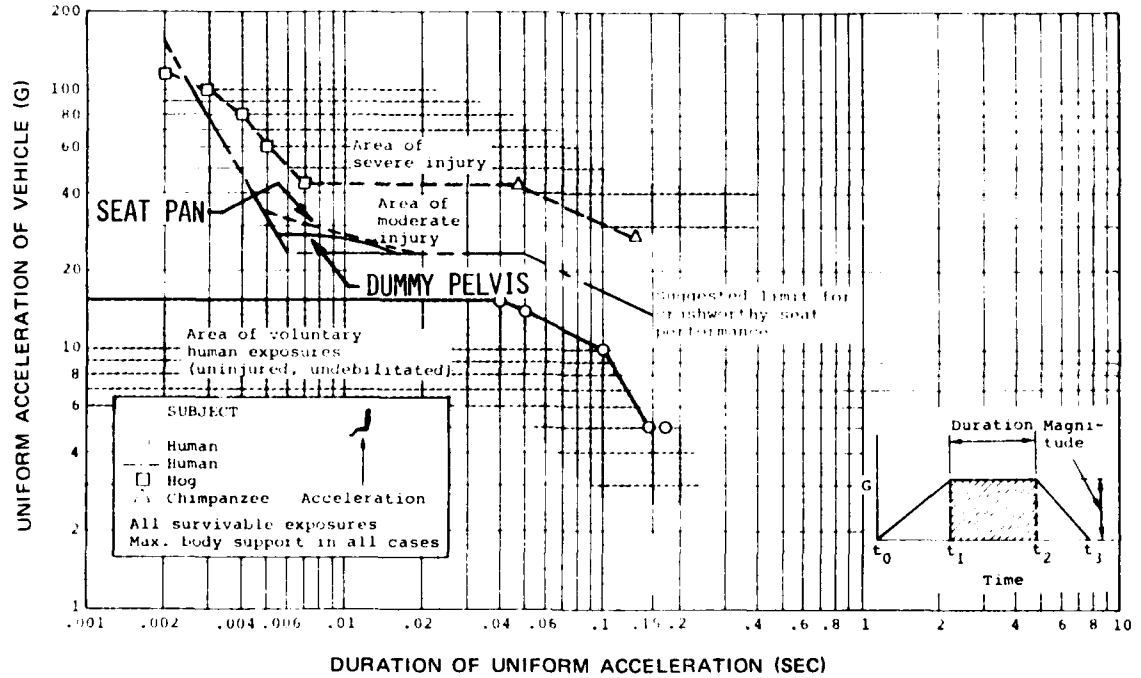

Figure 56. CPG seat pan and dummy pelvis accelerations superimposed on Eiband curve.

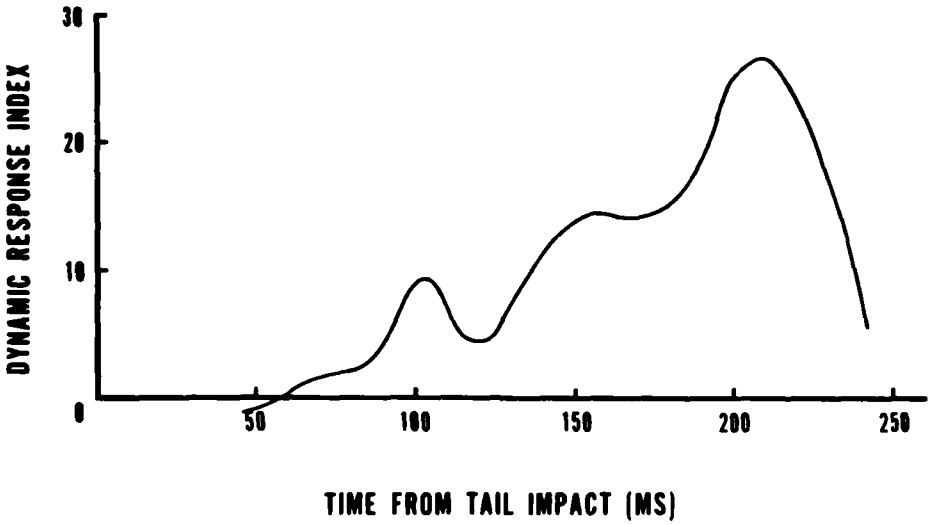

Figure 57. CPG seat pan dynamic response index.

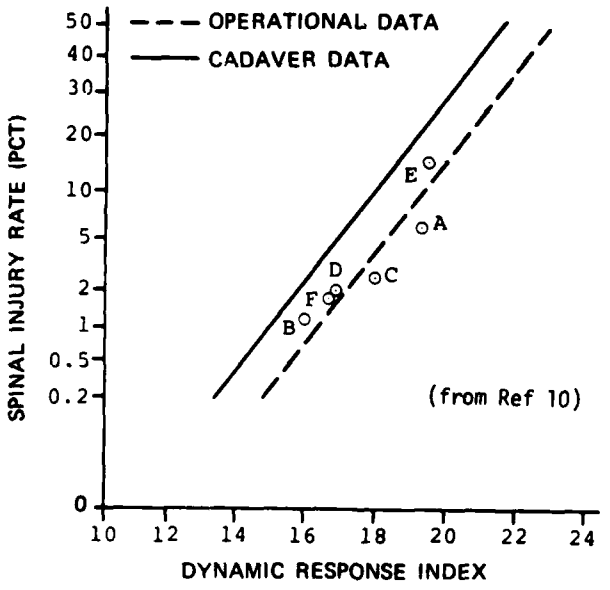

Aircraft type	Nonfatal ejections
A*	64
B*	62
C	65
D*	89
E	33
F	48

*Denotes rocket catapult

Figure 58. Probability of spinal injury estimated from laboratory data compared to operational experience.

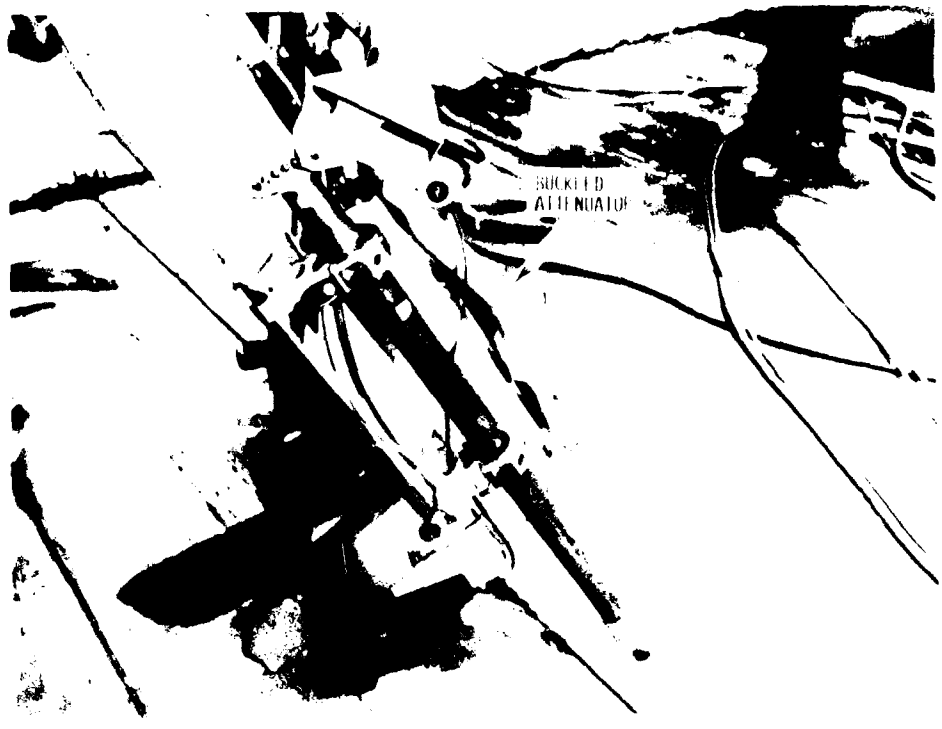

Figure 59. Posttest view of pilot (aft) crew seat showing buckled attenuator.

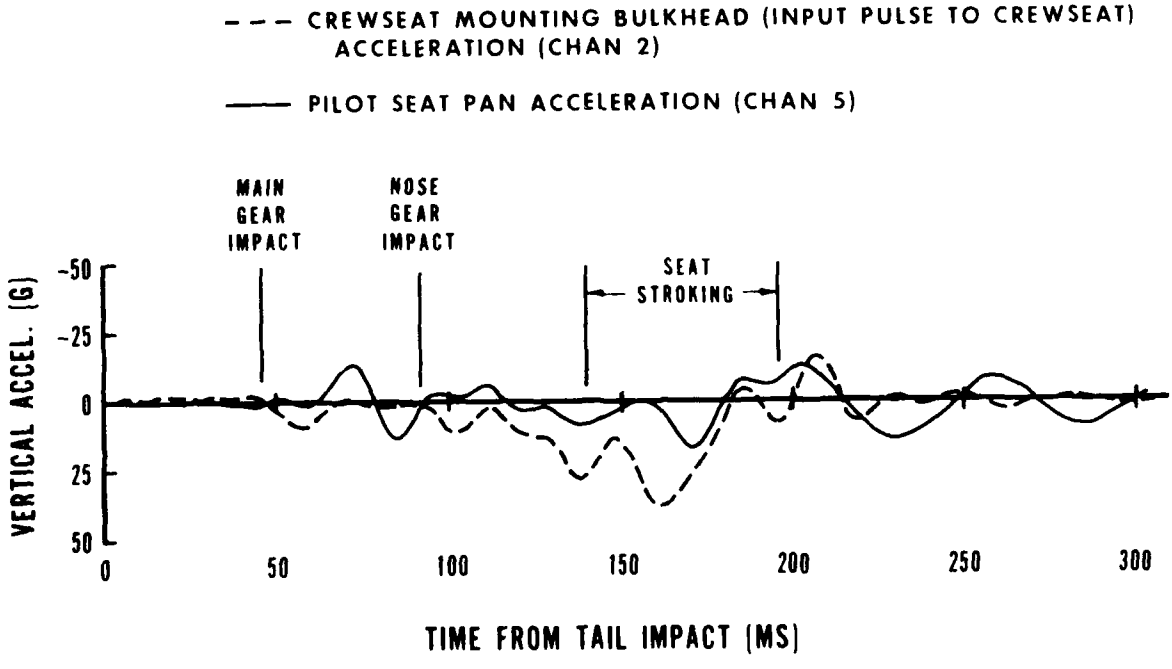

Figure 60. Pilot bulkhead and seat pan vertical accelerations.

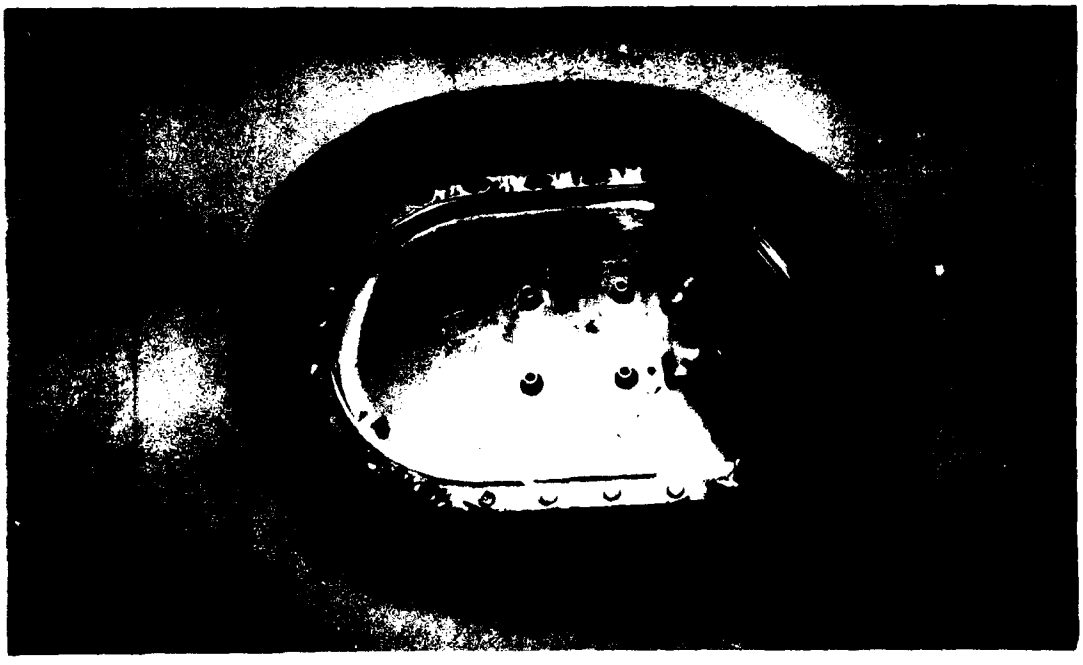

Figure 61. Forward fuel tank sump cover with fractured flange (viewed from inside fuel tank).

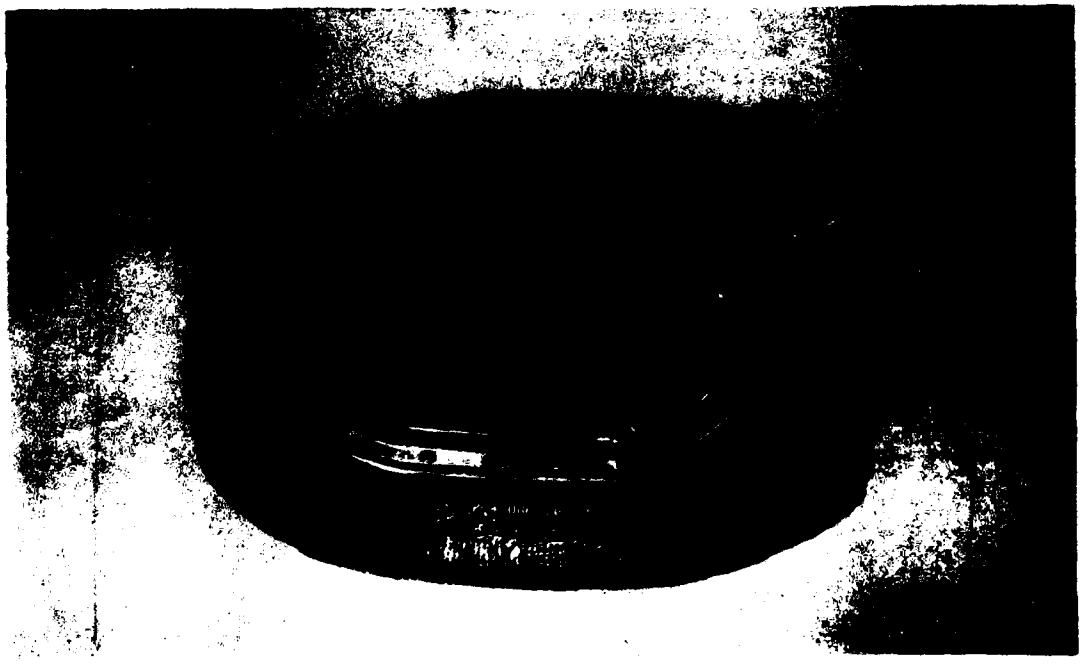

Figure 62. Forward fuel tank sump cover with fractured flange (viewed external to fuel tank).

Figure 63. Relative relationship of typical ammo tray stringer to forward fuel tank sump cover.

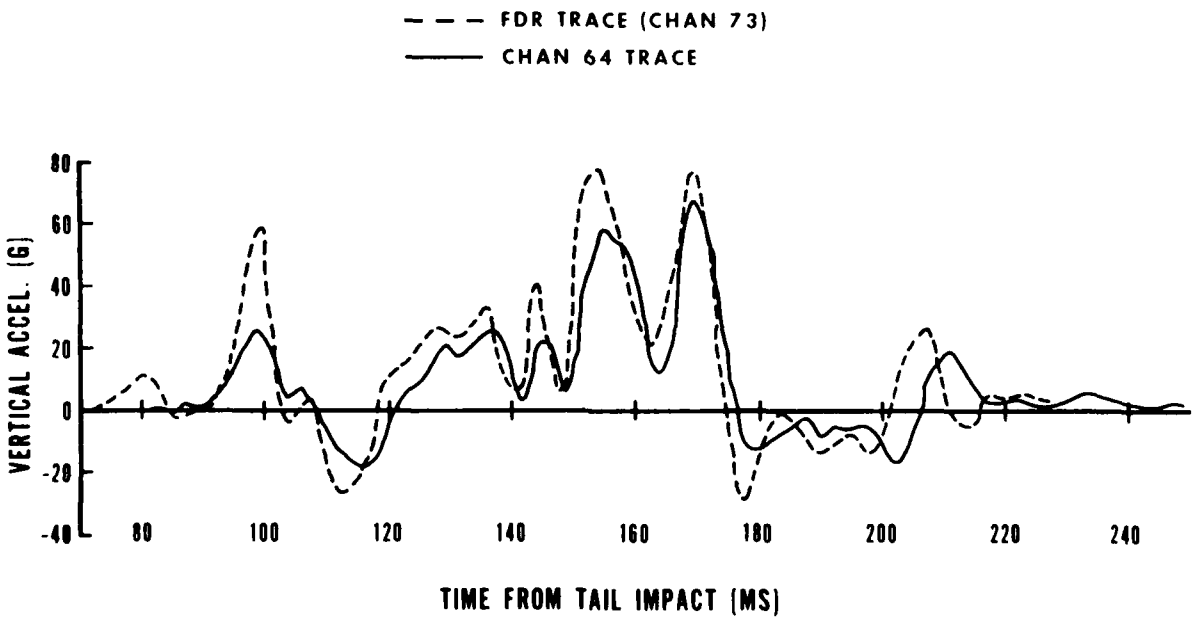

Figure 64. FDR vertical acceleration comparison at CPG bulkhead.

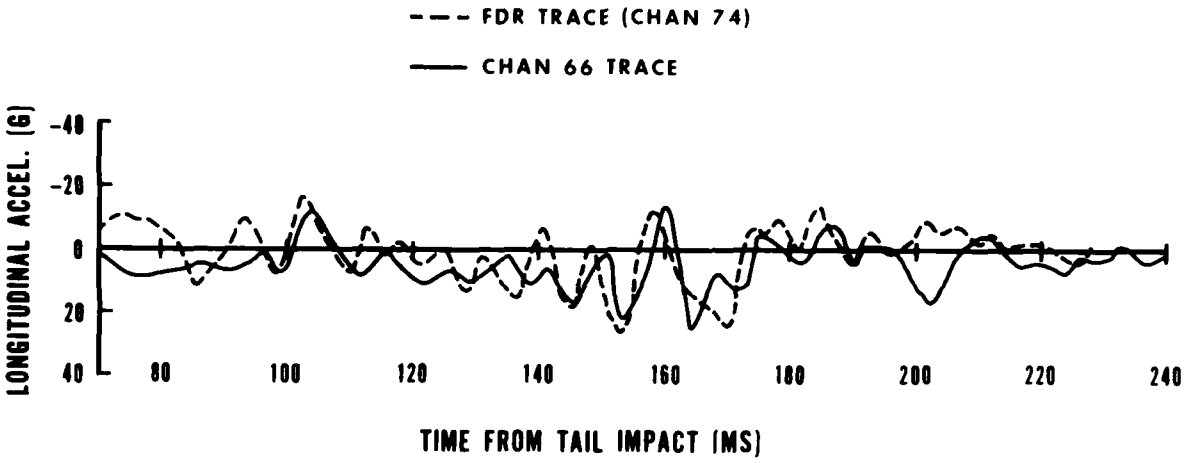

Figure 65. FDR longitudinal acceleration comparison at CPG bulkhead.

Figure 66. Starboard view of impact showing FIR/CPL in mid-flight (tail impact +191 ms).

CONCLUSIONS

1. T-41 produced the first real-world dynamic impact data on an aircraft having crashworthiness included in its basic design.

2. T-41 data provided a valid basis for correlation with computer program KRASH predictions and subsequent improvements to the math model.

3. The T-41 crash pulse contained 44 percent more energy than that planned, placing the impact severity considerably above the 95th percentile potentially survivable level.

4. The YAH-63 crashworthy landing gear, energy absorbing fuselage structure, and AH-64 crew seat performed at or above their design levels of energy absorption.

5. The YAH-63 crew seat (aft cockpit) failed to stroke in its prescribed manner due to malfunctioning inversion tube attenuators of an obsolete design.

6. The YAH-63 fuel system experienced a small leak in the forward fuel tank sump fitting. The fitting was fractured during the break-up of a nonproduction ammunition tray. There was, however, no penetration of the fuel tank material.

7. T-41 provided a realistic test-bed for evaluating the performance of several crash survivability experiments installed and monitored by the U.S. Army, U.S. Navy, and NASA-LRC.

REFERENCES

1. Turnbow, J. W., et al., Crash Survival Design Guide, Dynamic Science Division of Marshall Industries, USAAMRDL Technical Report 71-22, Eustis Directorate, U.S. Army Air Mobility Research and Development Laboratory, Fort Eustis, Virginia, October 1971, AD 733358.

2. Military Standard MIL-STD-1290(AV), Light Fixed and Rotary-Wing Aircraft Crashworthiness, Department of Defense, Washington, D.C., 25 January 1974.

3. Burrows, L., Lane, R., and McElhenney, J., CH-47 Crash Test (T-40) Structural, Cargo Restraints, and Aircrew Inflatable Restraint Experiments, USARTL TR 78-22, Applied Technology Laboratory, U.S. Army Research and Technology Laboratories (AVRADCOM), Fort Eustis, Virginia, April 1978, AD A055804.

4. Military Specification MIL-S-5895(AV), Seat System: Crashworthy, Non-Ejection, Aircrew, General Specification for, Department of Defense, Washington, D.C., 27 August 1971.

5. McElhenney, J. R., IBAHRS - An Inflatable Restraint System for Helicopter Aircrewmembers, Naval Air Development Center, Report No. NADC-82046-60, Warminster, Pennsylvania, 18 February 1982.

6. Ask, H.R., White, D. L., and Berwick, K. E., Advanced Crash Survivable Flight Data Recorder and Accident Information Retrieval System (AIRS), Hamilton Standard Division of United Technologies Corp., USAAVRADCOM TR 81-D-20, Applied Technology Laboratory, U.S. Army Research and Technology Laboratories (AVRADCOM), Fort Eustis, Virginia, August 1981, AD A105510.

7. Berry, V. L., Cronkhite, J. D., and Haas, T. J., YAH-63 Helicopter Simulation and Analysis, Bell Helicopter Textron, Inc., USAAVRADCOM TR 81-D-27, Applied Technology Laboratory, U.S. Army Research and Technology Laboratories (AVRADCOM), Fort Eustis, Virginia, February 1983, AD A107576.

8. Domzalski, Leon, Inflatable Body and Head Restraint System (IBAHRS): YAH-63 Crash Test, Naval Air Development Center, Report No. NADC-84141-60, Warminster, Pennsylvania, June 1984.

9. Eiband, A. M., Human Tolerance to Rapidly Applied Accelerations: A Summary of the Literature, NASA Memorandum 5-19-59E, National Aeronautics and Space Administration, Washington, D. C., June 1959.

REFERENCES - Continued

10. Brinkley, J. W., and Shaffer, J. T., Dynamic Simulation Techniques for the Design of Escape Systems: Current Applications and Future Air Force Requirements, Aerospace Medical Research Laboratory, AMRL Technical Report 71-29-2, Wright-Patterson Air Force Base, Ohio, December 1971, AD 740439.

11. Military Specification MIL-T-27422B Amendment 1, Tank, Fuel, Crash-Resistant, Aircraft, Department of Defense, Washington, D.C., 13 April 1971.

10
F

APPENDIX A
INSTRUMENTATION

GENERAL

T-41 measurements were obtained using five basic type transducers: accelerometers, load cells, strain gages, displacement sensors, and pressure sensors. The locations of these transducers are depicted in Figure 23. All sensors were connected to remote conditioning and recording equipment via a multipair, shielded umbilical cable system. Four magnetic tape recorders were employed, three supplied and operated by AATD and one by NASA personnel. The AATD signal conditioning and recording equipment was positioned in an instrumentation type trailer configured to meet this project's requirements. The NASA equivalent equipment was positioned in their permanently configured crash test site control room and was basically operated in accordance with their usual recording procedures. All aircraft instrumentation and supporting umbilical cabling was configured and installed by AATD personnel. NASA and AATD instrumentation technicians worked closely together during the calibration and data acquisition phases of the test. See Table A-1 for T-41 channel assignments plus other pertinent data relative to each data channel.

AVIATION APPLIED TECHNOLOGY DIRECTORATE (ARMY/AATD) RECORDING SYSTEM

The AATD data recording system is graphically depicted in Figure A-1. Data was recorded from accelerometers, load cells, pressure, strain gage and displacement type sensors, using designated tape recorders A, B, and C plus an oscillograph designated recorder E. IRIG-B Time Code 100 kHz tape speed compensation and voice narrative data was also placed on all magnetic tape machines which were configured to IRIG intermediate band standards. All circuits were individual four-wire plus shield and drain, and excitation was provided to each individual channel by each channel's bridge conditioning/amplifier unit. Recorder E measured selected on-line NADC channels plus Channels 77 through 80.

ACCELEROMETER CIRCUITS

Nineteen channels of vertical, lateral and longitudinal aircraft component structural, anthropomorphic dummy, and loads acceleration data were recorded. Four Endevco model 2260A-250 piezoresistive type accelerometers were used to provide redundant transmission, pilot seat, and rear bulkhead (Channels 40-43) high frequency (2000 Hz) coverage. The high signal, low-impedance output (nominal 1.6MV/g) was fed through junction boxes and 300 feet of four-wire shielded (per channel) umbilical cable into Calex model 165B strain gage conditioning amplifiers and ultimately into either a Honeywell 101 or a Bell & Howell MARS 2000 FM Magnetic Tape Recorder. Fifteen CEC-4-202 damped strain gage type accelerometers (100 to 250g) were used to provide NADC with triaxial loads data relative to the copilot seat bottom; associated mounting bulkhead; and copilot dummy's pelvis, thorax and head positions (Channels 52-66). The sensor outputs were boosted to the record level by Accudata 218 signal conditioning amplifiers. Calibrations were accomplished the day prior to the drop by using either DC voltage insertion (Endevco 2260A-250) or shunt

resistance (CEC4-202) techniques, setting the signal conditioning amplifier gain, and then recording by the respective mag tape data channel. Calibration levels were selected, in most cases, to be within 75 percent of established FM band edge limits. Recorders A, B, C, and D functions and calibration data are shown in Tables A-2 through A-5.

Strain Gage Circuits

Eight strain gage channels (44-51) were employed to measure axial load strain on the main transmission support links, crash links, and the pilot seat energy attenuator columns. Micro-measurements (MM) type EA-13-125TB-350/W 350 ohm 2 element rosette gages were used in a full active bridge axial arrangement as the crash link and energy attenuator sensors, while MM type EA-06-125TB-350/W gages were used in a similar arrangement for the transmission crash links. These bridge sensors were fed through aircraft and recording trailer J-boxes, then conditioned by Honeywell Model Accudata 218 gage control/amplifiers and recorded on tape recorder A. Each circuit's excitation voltage was provided by the Accudata 218 conditioners, and excitation voltage control was remote sensed at the sensor bridge. Shunt resistance type calibrations were performed the day prior to the test, and each of these gaged aircraft members had been dynamically calibrated in the lab prior to installation. See Table A-2 for the applicable function and calibration data.

Load Cells (Tensiometers)

Four circuits operating either GSE Model 2500 4k or 5k pound seat belt tensiometers or the NADC designed webbing load cells provided NADC with tension loads for the copilot shoulder strap and negative-G harness straps (Channels 67-70). The sensor outputs were fed via the umbilical cable arrangement to the Honeywell Model 218 signal conditioning amplifier to recorder C. Calibrations were performed using the shunt resistance technique. See Table A-4 for applicable function and calibration data. Two additional channels (77 and 78) using load cell type sensors were employed to measure the NADC copilot seat left and right attenuator loads. The output from these strain gage type 2k pound sensors was fed directly into oscillograph recorder E only. Shunt type calibrations were applied the day of the test.

Pressure Sensors

NADC employed two 25-psi CEC 4-326 pressure transducers as IBAHRS left and right bladder inflation detectors (Channels 71 and 72). The output from these sensors was fed via the normal J-box and umbilical cable route to Honeywell Accudata 218 strain gage/conditioning amplifiers and then into recorder C. Shunt reistance calibration techniques were employed, and applicable function and calibration data can be found in Table A-4.

Displacement and Impact Switch Sensors

A spring recoil linear potentiometer type transducer was used to measure the NADC copilot seat displacement (Channel 79). The sensor output was fed directly into oscillograph recorder E only. The NADC impact sense pulse circuit was intended to establish an initial aircraft touch-down time but was eliminated on test day due to installation technical problems. Aircraft

touch-down time was ultimately detected using the tail rotor gearbox vertical accelerometer (Channel 27) output.

NASA Recording System

Figure A-2 generally depicts the NASA recording system. Four types of transducers representing 41 channels of Army data were recorded (accelerometers, strain gage, pressure and displacement sensors) on magnetic tape recorder D. The NASA control room equipment used for this test was that which is normally used to support all test site activities. The permanently installed system had been reconfigured prior to T-41 to include a Honeywell model 96, 28-channel IRIG standardized magnetic tape recording system. All umbilical cable incoming data is conditioned by NASA designed/built adjustable gain (1 to 1000) signal conditioning amplifiers and fed into a metroplex 100 series standard multiplex system which resulted in five data channels and one tape compensation subcarrier being placed on one direct record tape channel. The NASA multiplex subcarrier frequencies are 25, 40, 55, 70, 85, and 100 kHz (compensation). Data recorded under this system is limited to 720 Hz band pass. The power for 33 on-board sensors is fed down the umbilical cable to a 10 VDC regulator mounted within the J-box and then buss fed to each of 33 sensors requiring 10 VDC. Another J-box regulator that was fed from a second DC source via the umbilical cable provided 12 VDC for eight pressure and displacement sensors.

ACCELEROMETERS

Twenty-nine single-axis accelerometers (Channels 1-29) were employed to measure aircraft structural and anthropomorphic dummy loads. Endevco 2260A 250g piezoresistive accelerometers were used, fed through junction boxes and the 700-foot NASA umbilical cable to the NASA control room where the signals were conditioned, multiplexed, and placed on magnetic tape recorder D. These data are limited to 720 Hz (±3 dB) due to the signal condition filtering band pass. The voltage insertion calibration method was employed prior to drop day and the calibration levels were selected to fit within the limitations of the fixed gain signal conditioning amplifiers. Recorder D functions and calibration data are presented in Table A-5.

PRESSURE SENSORS

Five sensors were used to measure hydraulic ram pressure in the forward and rear fuel tanks (Channels 30 and 31) and oil pressure in the landing gear struts (Channels 32-34). Two CEC 4-317 250-psi strain gage type sensors were used to measure the fuel tank pressures while Kistler type 202A1 piezotron 5000 psi with 7000 psi overrange capabilities along with the required 549C impedance converter/coupler were used to measure the landing gear oil strut pressures. The Kistler piezotron system's output (6.5VC @ 7000 psi) was too high for the NASA recording system so a resistive divide-by-three attenuator network was placed in line at the aircraft J-box. The 549C couplers were mounted in a protected aircraft location, and the resulting low impedance output was fed via the umbilical cable to the NASA control room. Shunt and voltage insertion techniques were used to apply the sensor calibrations prior to test day (see Table A-5 for calibration particulars).

STRAIN GAGE CIRCUITS

Two strain gage channels (75 and 76) were used to measure axial load strains on the main landing gear drag struts. MM type EA-13-125TB-350 gages were used to construct a full bridge axial arrangement circuit. The sensor output was fed through the umbilical cable arrangement and conditioned in the same manner as the other sensors. A shunt type calibration technique was used, and Table A-5 reflects calibration data particulars.

DISPLACEMENT CIRCUITS

Five displacement circuits were employed to measure crew seat stroking (Channels 35 and 36) and degrees of angular rotation on the three landing gear points (Channels 37, 38, and 39). Waters Manufacturing 0.5 percent linear motion position (push rod type) transducers, in conjunction with interface circuitry which supplied span, sensitivity, and calibration control features, provided the crew seat displacement measurement capability of 0 to 18 inches. Beckman Helipot model 5710 single turn wire-wound 0.5 percent potentiometers were used in conjunction with the same interface circuitry to measure the degrees of displacement from true vertical on the three landing gear points. All five sensors and the mating interface circuitry were calibrated as a unit to ensure linearity over the complete range of the control. In addition, after the landing gear stroke sensors were installed, all wheels of the aircraft were jacked up, leveled, and the individual wheels calibrated (millivolt vs degrees) from a true vertical position. For mag tape signal calibrations, signal insertions of a known voltage equal to some number of degrees were injected into the individual circuits (see Table A-5 for calibration specifics).

ON-BOARD PHOTOGRAPHIC CONTROL

The crashworthy photographic control box which contained circuitry used to control the three on-board high-speed 16mm cameras was provided by NASA and installed by AATD instrumentation personnel. A pre-drop system check was performed to ensure overall operation and proper time sequencing. The on-board cameras can be seen on the aircraft's left side adjacent to the crew compartments.

ON-BOARD BATTERY SOURCES

Two on-board 24 VDC NiCad Batteries were positioned at station 232 on WL 40 directly beneath the rear crew seat. The batteries were mounted in a cradle lined with high density polyurethane cushioning material and held in place by two threaded tie-down posts which secured the battery tie-down flanges. Aircraft-approved locking type connectors were used for connection. Battery 1 provided 24 VDC power for all three on-board cameras while Battery 2 provided the same for the NADC and Naval Air Test Center experiments. Figure A-3 shows the basic on-board power distribution system.

DATA ACQUISITION

All channels were calibrated as shown in Tables A-2 through A-5. A 100 kHz signal was recorded on each tape recorder for speed compensation and noise

reduction purposes. IRIG-B timing information was recorded on each tape recorder to facilitate data reduction and event occurrence definition. Also, an audio narrative sequence was included on each tape recorder to provide for tape data marking and to facilitate more rapid data reduction.

DATA RECORDING PROBLEMS

The following instrumentation malfunctions occurred on the identified channels. In all cases except one, data was recorded until the described failure occurred.

1. Channel 1: Cable severed by structural damage 0.20 second after impact.

2. Channel 31: Cable severed due to structural damage 0.150 second after impact.

3. Channel 33: Polarity reversed due to wire reversal.

4. Channel 34: Cable severed at approximately 0.300 second after impact.

5. Channel 38: Channel failed when aircraft was being raised to drop height position. Cause unknown.

6. Channel 39: Cable cut as landing gear separated from aircraft at 0.180 second after impact.

7. Channel 45: Data exceeded record capability (2700 lb) for approximately 3 to 4 milliseconds. Low-frequency filtering plus interpolation can resolve this problem.

8. Channels 52, 53, and 54: Accelerometer mounting block separated from the seat pan bottom as the seat exterior fiberglass wrapping material to which it was secured separated from the basic composite seat structure. This separation occurred at approximately 0.200 second after impact.

9. Channel 72: Recorder C11 FM recorder card defective. Data can probably be obtained by using noise filtering techniques.

10. Channels 75 and 76: Cable cuts due to mass structure failure at approximately 0.125 and 0.115 second, respectively, after impact.

11. On-board cameras: All cameras lost 24 VDC battery power shortly after impact, limiting post impact data to just a few frames. The aircraft-approved battery feed cable connector failed on impact as the connector locking screw post sheared, releasing the connector and feed cable.

AIRCRAFT INSTRUMENTATION MOUNTING AND CABLING TECHNIQUES

All aircraft sensors to the umbilical junction box were Beldon type 8434 four-wire shielded instrumentation cable with the exception of three piezotron pressure sensors which used Microdot type coaxial cable from the sensor to the

impedance converter module. All on-board wiring was bundled and positioned with extra slack at expected heavy stress points using plastic cable ties, masking tape, and aircraft-type cable clamps.

All accelerometer mount blocks were fastened to their mounting positions by 1/4 or 3/8 inch hardware or adhesive bonding using 3M Scotch-Weld Epoxy Resin Structural Adhesive, Type 2216B/A. The accelerometers were mounted to the mount blocks using the manufacturer-supplied 10/32 mounting stud, threading that to the mount block, and securing it at approximately 18 in-lb. In the case of the Endevco 2260A-250 accelerometers, the manufacturer-supplied miniature cable was hand-wire-spliced to the Belden 8434 instrumentation cable and then run to the aircraft J-box.

All strain gage tranducers were bonded to the test members using standard preparation, methods, and materials as recommended by manufacturers such as Micro-Measurements, Inc. The MM strain gages were finger pressure adhesively bonded using MM M-Bond 200, and were moisture and physically protected with M-Coat A and/or M-Coat G coatings. All strain gage axial measurement circuits were connected to the aircraft J-box with Belden 8434 through an in-line connector arrangement (see Figure A-4 for a typical strain gage circuit installation).

Conventional mounting techniques were used for the pressure transducer load cells and most of the displacement sensors. For the landing gear strut displacement, the single turn linear potentiometers used as the transducer were mounted such that the landing gear circular rotation caused a corresponding degree change on the transducer's shaft. See Figure A-5 for a view of the right main gear (Channel 38) sensor arrangement

The AATD, NASA, and NADC aircraft cable J-boxes were mounted between stations 193 and 250, centered on WL 80 on the aircraft's right side (see Figure A-6). The individual 12- and 16-gage aluminum and galvanized steel boxes were fastened to a 1/4-inch, 64x30-inch aluminum plate which was secured to the aircraft by picking up existing aircraft hard mount points. The mounting plate was topped and 3/8 inch fine thread bolts secured the boxes to the plate. The AATD and NASA J-boxes were commercially procured (Hoffman Engineering) weather-proof electrical box shells and the four smaller NADC boxes were NADC-fabricated using 10-gage aluminum. The umbilical cables into the NASA and NADC J-boxes were thru-aircraft type circular connectors, while the AATD umbilical cable was hard wired directly into the box terminal strips. The NADC boxes' interior wire was not accessible, and all calibrations (shunt type) were applied at the signal conditioning amplifier end within the instrumentation trailer. The other two boxes, which were AATD constructed, had heavy-duty terminal strip hardware secured plus voltage regulators, attenuator networks and balancing circuits, which were readily accessible for calibration and checkout requirements.

The AATD, NADC, and NASA instrumentation umbilical cables were attached to both aircraft wing store leading edges at three points, using improvised light sheet metal strips bolted in place and lined with flex padding. The cables were secured with vinyl tape, and the left side cable (AATD/NADC) was fed to the aircraft J-boxes mounted on the right side through a 3-inch aluminum conduit which was layered through the aircraft interior at station 257.

Sufficient cable slack was left in the cable run points to preclude pull tearing of the cables. At crash impact the left wing separated from its mount points, but the left umbilical cable slack was sufficient to allow the cable to float with the damage and thus remain electrically intact.

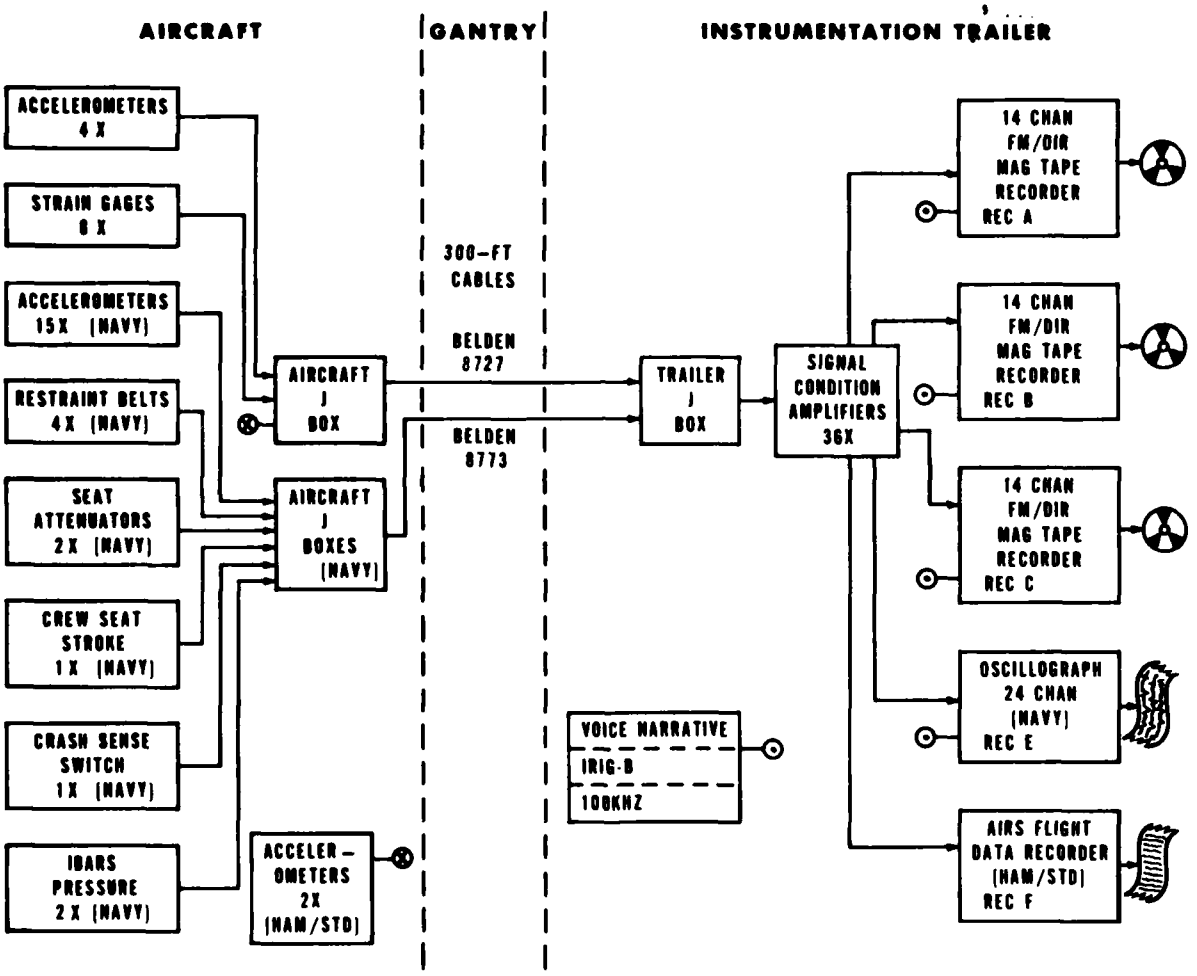

Figure A-1. AATD recorded data.

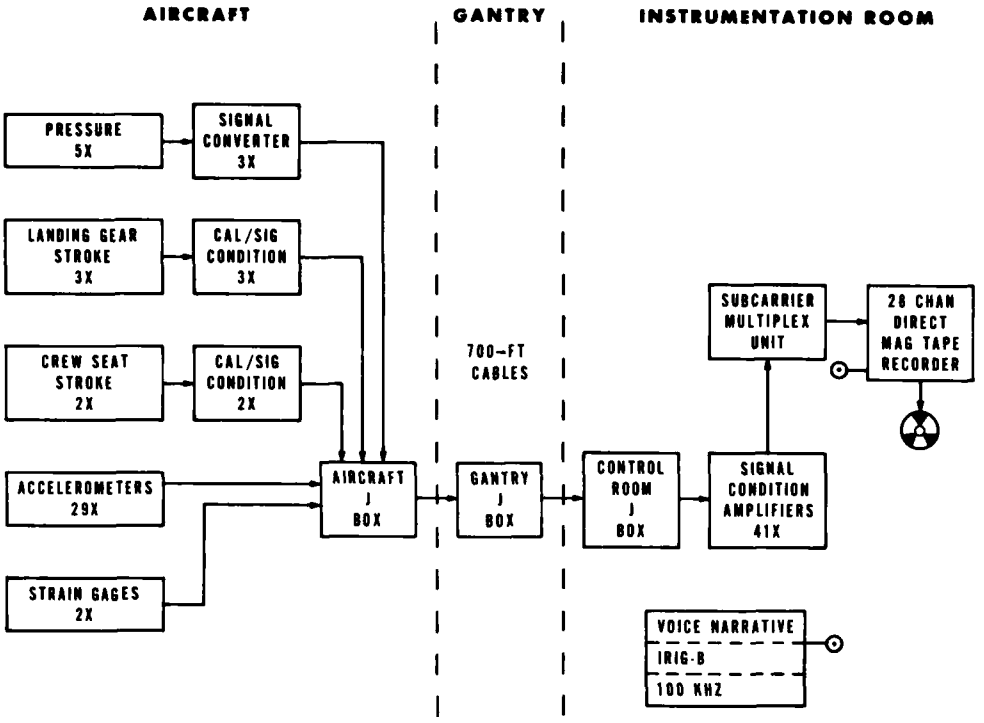

Figure A-2. NASA recorded data.

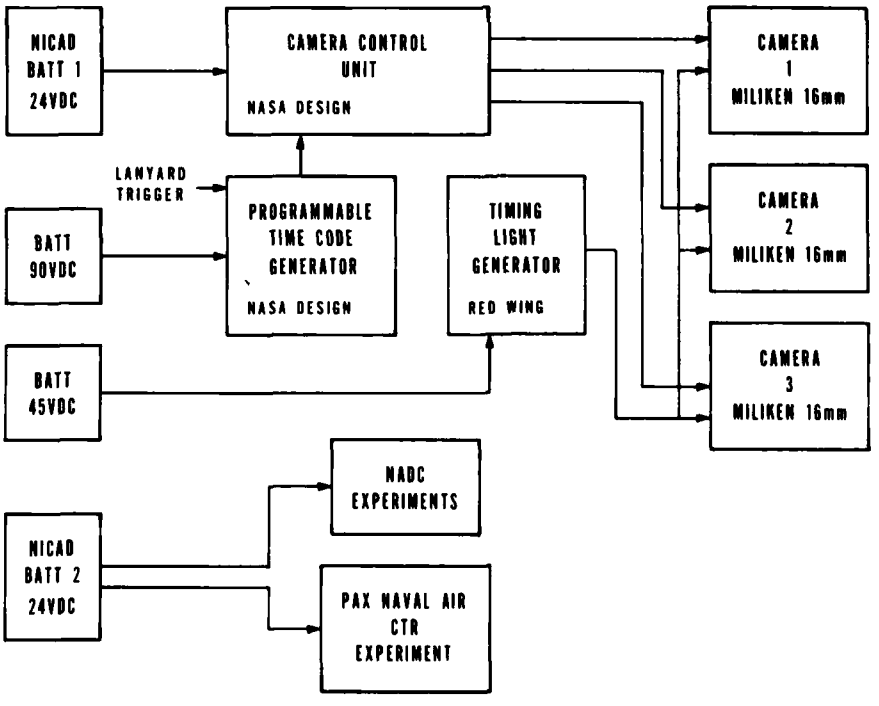

Figure A-3. On-board battery and camera control systems.

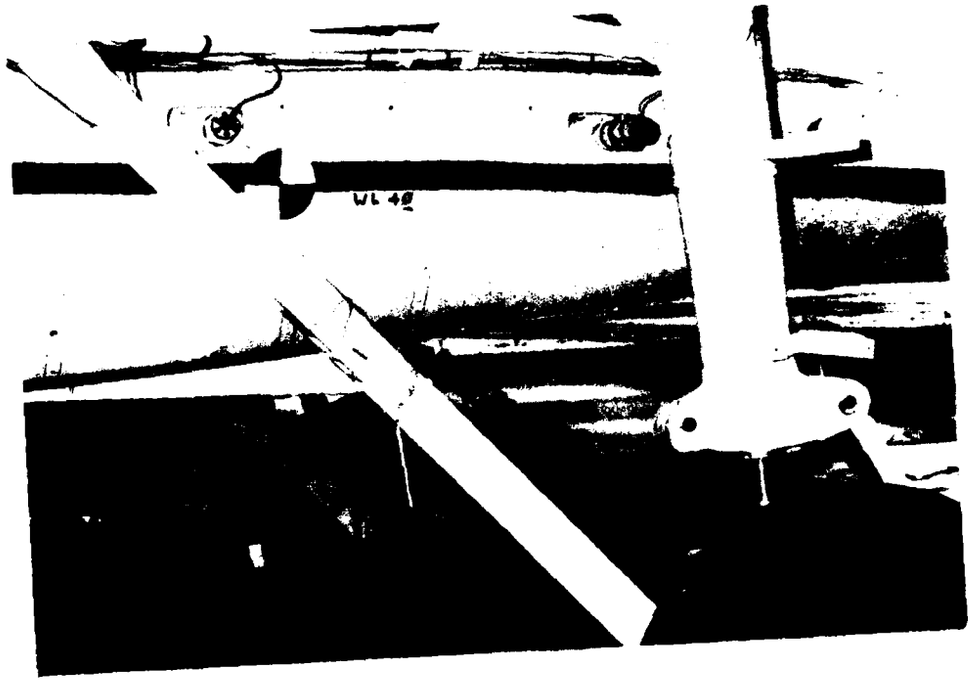

Figure A-4. Typical strain gage circuit and fuel tank pressure sensor.

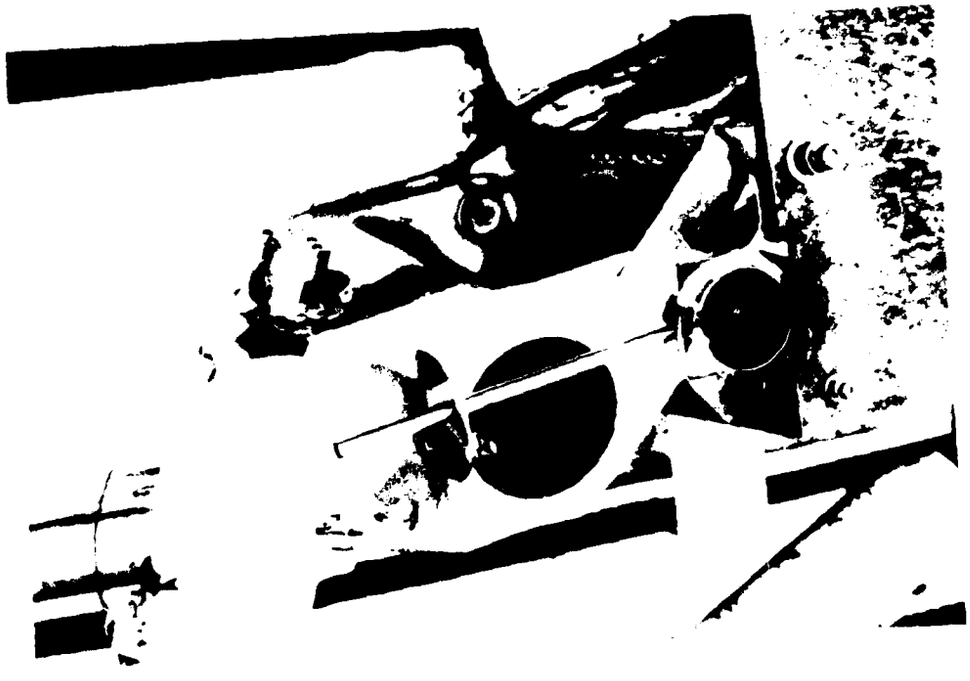

Figure A-5. Right main landing gear displacement sensor.

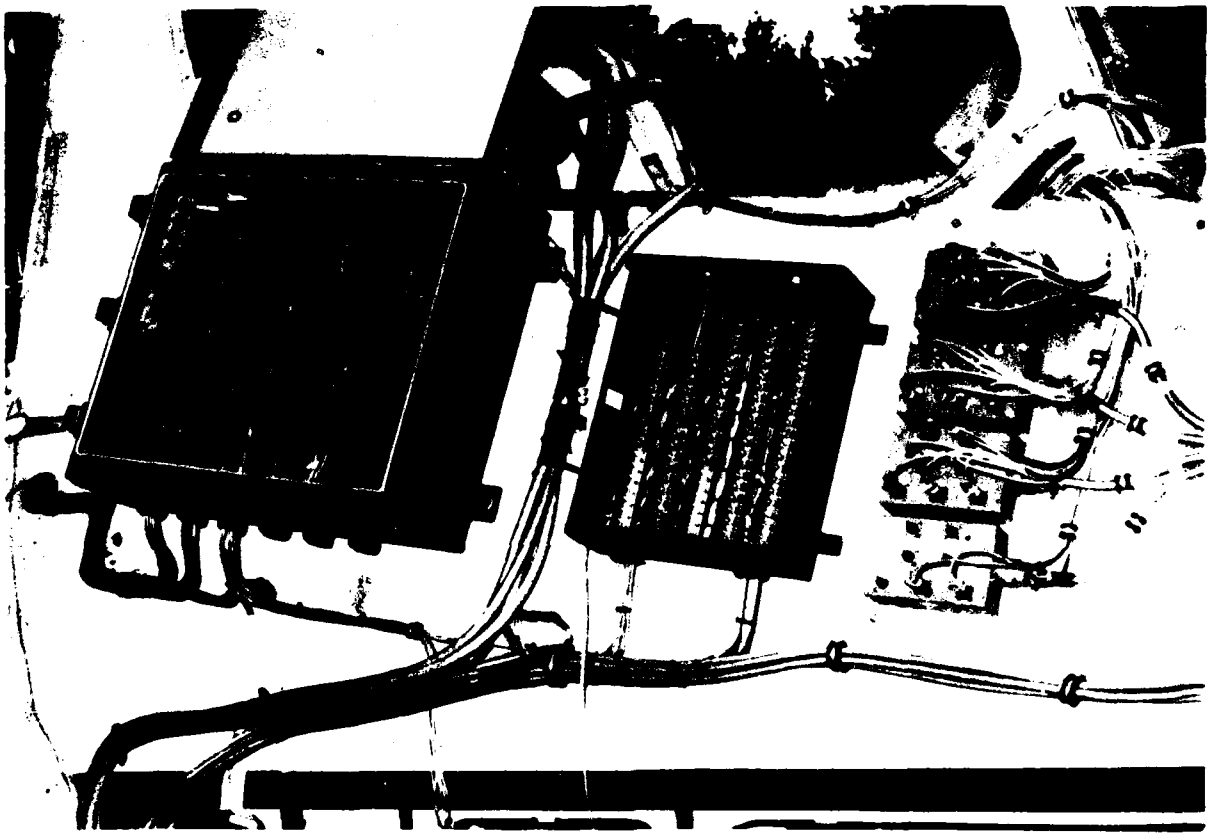

Figure A-6. Aircraft umbilical tie-box arrangements.

TABLE A-1. T-41 CHANNEL DESIGNATIONS

Channel	Parameter	Descriptor	Fuselage Station	Recording Channel	Sensitivity	Recording Responsibility
01	Nose gun turret	V	120	D1A	250 g	N
02	Pilot bulkhead	V	251	D1B	250 g	N
03	Pilot bulkhead	LA	251	D1C	250 g	N
04	Pilot bulkhead	LO	251	D1D	250 g	N
05	Pilot seat bot rev pol	V	244	D1E	250 g	N
06	Copilot bulkhead	V	193	D2A	250 g	N
07	Right wing store outer	V	280	D2B	250 g	N
08	Right wing store outer	LO	280	D2C	250 g	N
09	Left wing store outer	V	280	D2D	250 g	N
10	Left wing store outer	LO	280	D2E	250 g	N
11	Aircraft CG	V	290	D3A	250 g	N
12	Aircraft CG	LA	290	D3B	250 g	N
13	Aircraft CG	LO	290	D3C	250 g	N
14	Transmission CG rev pol	V	300	D3D	250 g	N
15	Transmission CG	LA	300	D3E	250 g	N
16	Transmission CG	LO	300	D4A	250 g	N
17	Main rotor hub	LA	300	D4B	250 g	N
18	Main rotor hub	LO	300	D4C	250 g	N
19	Center fuselage	V	411	D4D	250 g	N
20	Pilot pelvis	V	244	D4E	250 g	N
21	Pilot pelvis	LO	244	D5A	250 g	N
22	Pilot chest	V	244	D5B	250 g	N
23	Pilot chest rev pol	LO	244	D5C	250 g	N
24	Pilot head	V	244	D5D	250 g	N
25	Pilot head	LA	244	D5E	250 g	N
26	Pilot head	LO	244	D6A	250 g	N
27	Tail rotor gearbox	V	665	D6B	250 g	N
28	Tail rotor gearbox	LA	665	D6C	250 g	N
29	Pilot seat bot	LO	244	D6D	250 g	N
30	Forward fuel cell	P	292	D6E	250 psi	N
31	Rear fuel cell	P	322	D7A	250 psi	N
32	Nose gear strut	P	160	D7B	7000 lb	N
33	Right gear strut	P	314	D7C	7000 lb	N
34	Left gear strut	P	314	D7D	7000 lb	N
35	Pilot seat stroke	DP	244	D7E	18 in	N
36	Copilot seat stroke	DP	183	D8A	18 in	N
37	Nose gear stroke	DP	185	D8B	90 deg	N
38	Right main gear stroke	DP	314	D8C	90 deg	N
39	Left main gear stroke	DP	314	D8D	90 deg	N
40	Pilot bulkhead	V	251	A9	250 g	A
41	Transmission CG	LO	300	A10	250 g	A
42	Transmission CG rev pol	V	300	A11	250 g	A
43	Pilot seat bot rev pol	V	244	B1	250 g	A
44	Left pilot seat atten axial	SG	244	A1	2700 lb	A
45	Right pilot seat atten axial	SG	244	A2	2700 lb	A
46	Right fwd trans link, axial	SG	265	A3	150k lb	A
47	Right rear trans link, axial	SG	330	A4	150k lb	A
48	Left fwd trans link, axial	SG	265	A5	150k lb	A
49	Left rear trans link, axial	SG	330	A6	150k lb	A

TABLE A-1. Continued.

Channel	Parameter	Descriptor	Fuselage Station	Recording Channel	Sensitivity	Recording Responsibility
50	Right trans crash link, axial	SG	300	A7	75k lb	A
51	Left trans crash link, axial	SG	300	A8	75k lb	A
52	Copilot seat pan	V	183	B2	100 g	A
53	Copilot seat pan	LA	183	B3	100 g	A
54	Copilot seat pan	LO	183	B4	100 g	A
55	Copilot pelvis	V	183	B5	100 g	A
56	Copilot pelvis	LA	183	B6	100 g	A
57	Copilot pelvis	LO	183	B7	100 g	A
58	Copilot chest	V	183	B8	100 g	A
59	Copilot chest	LA	183	B9	100 g	A
60	Copilot chest	LO	183	B10	100 g	A
61	Copilot head	V	183	B11	100 g	A
62	Copilot head	LA	183	C1	100 g	A
63	Copilot head	LO	183	C2	100 g	A
64	Copilot bulkhead	V	212	C3	250 g	A
65	Copilot bulkhead	LA	212	C4	250 g	A
66	Copilot bulkhead	LO	212	C5	250 g	A
67	Copilot lap belt, right	SG	183	C6	4000 lb	A
68	Copilot lap belt, left	SG	183	C7	4000 lb	A
69	Copilot shoulder	SG	183	C8	5000 lb	A
70	Copilot neg g strap	SG	183	C9	4000 lb	A
71	IBAHRS pressure, right	P	183	C10	100 psi	A
72	IBAHRS pressure, left	P	183	C11	100 psi	A
73	AIRS crash sensor	V	212	F1	50 g	C
74	AIRS crash sensor	LA	212	F2	50 g	C
75	Right main lg strut, axial	SG	308	D8-5	75k lb	N
76	Left main lg strut, axial	SG	308	D9-1	75k lb	N
77	Copilot atten, right	SG	183	E1	2000 lb	A
78	Copilot atten, left	SG	183	E2	2000 lb	A
79	Copilot seat stroke	DP	183	E3	20 in	A
80	Crash sensor pulse	SW	183	E4	Off On	A

A – Army
N – NASA
C – Contractor

DP – Displacement position
LA – Lateral
LO – Longitudinal

P – Pressure
SG – Strain gage
SW – Switch

TABLE A-2. RECORDER A FUNCTIONS AND CALIBRATION DATA

Data Channel	Tape Track	Transducer Location	Axis	Range	Tape DC Cal (V)	Tape Equivalent	Polarity
44	A-1	Left pilot seat atten SG, axial	–	2720 lb	1.300	2500 lb	Tension
45	A-2	Right pilot seat atten SG, axial	–	2720 lb	1.300	2500 lb	Tension
46	A-3	Right fwd trans link SG, axial	–	65.2k lb	1.300	60k lb	Tension
47	A-4	Right rear trans link SG, axial	–	65.2k lb	1.300	60k lb	Tension
48	A-5	Left fwd trans link SG, axial	–	65.2k lb	1.300	60k lb	Tension
49	A-6	Left rear trans link SG, axial	–	65.2k lb	1.300	60k lb	Tension
50	A-7	Right trans crash link SG, axial	–	43.5k lb	1.300	40k lb	Tension
51	A-8	Left trans crash link SG, axial	–	43.5k lb	1.300	40k lb	Tension
40	A-9	Pilot bulkhead, accel	V	272 g	1.300	250 g	+ (Base down)
41	A-10	Trans CG, accel	LO	272 g	1.300	250 g	+ (Base rear)
42	A-11	Trans CG, accel	V	272 g	1.300	250 g	+
–	A-12	100 kHz ± 1 kHz tape speed	–	–	1.414	–	NA
–	A-13	Voice narrative	–	–	5.000	–	NA
–	A-14	IRIG-B time code	–	–	1.414	–	NA

TABLE A-3. RECORDER B FUNCTIONS AND CALIBRATION DATA

Data Channel	Tape Track	Transducer Location	Axis	Range	Tape DC Cal (V)	Tape Equivalent	Polarity
43	B-1	Pilot seat bot accel	V	272 g	1.390	250 g	–
52	B-2	Copilot seat pan, accel	V	100 g	1.110	78.6 g	+
53	B-3	Copilot seat pan, accel	LA	100 g	1.060	74.8 g	+
54	B-4	Copilot seat pan, accel	LO	100 g	1.140	80.4 g	+
55	B-5	Copilot pelvis, accel	V	100 g	1.070	75.4 g	+
56	B-6	Copilot pelvis, accel	LA	100 g	1.100	77.7 g	+
57	B-7	Copilot pelvis, accel	LO	100 g	1.130	79.6 g	+
58	B-8	Copilot chest, accel	V	100 g	1.080	76.7 g	+
59	B-9	Copilot chest, accel	LA	100 g	1.140	80.9 g	+
60	B-10	Copilot chest, accel	LO	100 g	1.080	76.6 g	+
61	B-11	Copilot head, accel	V	100 g	1.110	78.6 g	+
–	B-12	100 kHz ± 1 kHz tape speed	–	–	1.414	–	NA
–	B-13	Voice narrative	–	–	5.000	–	NA
–	B-14	IRIG-B time code	–	–	1.414	–	NA

TABLE A-4. RECORDER C FUNCTIONS AND CALIBRATION DATA

Data Channel	Tape Track	Transducer			Tape		Polarity
		Location	Axis	Range	DC Cal (V)	Equivalent	
62	C-1	Copilot head	LA	100 g	1.120	78.9 g	+
63	C-2	Copilot head	LO	100 g	1.120	79.0 g	+
64	C-3	Copilot bulkhead	V	250 g	1.240	219.4 g	+
65	C-4	Copilot bulkhead	LA	150 g	0.950	101 g	+
66	C-5	Copilot bulkhead	LO	250 g	1.200	212 g	+
67	C-6	Copilot lap belt, right	–	3000 lb	0.790	1675 lb	Tension
68	C-7	Copilot lap belt, left	–	3000 lb	0.780	1658 lb	Tension
69	C-8	Copilot shoulder	–	5000 lb	0.480	1686 lb	Tension
70	C-9	Copilot negative G strap	–	3000 lb	0.780	1653 lb	Tension
71	C-10	IBAHRS pressure, right	–	50 psi	1.310	46.4 psi	Pressure
72	C-11	IBAHRS pressure, left	–	50 psi	1.290	45.7 psi	Pressure
–	C-12	100 kHz ± 1 kHz tape speed	–	–	1.414	–	NA
–	C-13	Voice narrative	–	–	5.000	–	NA
–	C-14	IRIG-B time code	–	–	1.414	–	NA

TABLE A-5. RECORDER D FUNCTIONS AND CALIBRATION DATA

Data Channel	Tape Track	Transducer			Tape		Polarity
		Location	Axis	Range	DC Cal (V)	Equivalent	
1	D1-1	Nose gun turret	V	211 g	1.300	194 g	+ (Base down)
2	D1-2	Pilot bulkhead	V	225 g	1.300	207 g	+
3	D1-3	Pilot bulkhead	LA	227 g	1.300	209 g	+ (Base left)
4	D1-4	Pilot bulkhead	LO	230 g	1.300	211 g	+ (Base rear)
5	D1-5	Pilot seat bottom	V	230 g	1.300	211 g	–
6	D2-1	Copilot bulkhead	V	237 g	1.300	218 g	+
7	D2-2	Right wing outer store	V	250 g	1.300	242 g	+
8	D2-3	Right wing outer store	LO	250 g	1.300	245 g	+
9	D2-4	Left wing outer store	V	250 g	1.300	246 g	+
10	D2-5	Left wing outer store	LO	250 g	1.300	250 g	+
11	D3-1	Aircraft CG	V	250 g	1.100	212 g	+
12	D3-2	Aircraft CG	LA	250 g	1.100	217 g	+
13	D3-3	Aircraft CG	LO	250 g	1.100	217 g	+
14	D3-4	Transmission CG	V	250 g	1.100	217 g	–
15	D3-5	Transmission CG	LA	250 g	1.100	225 g	+
16	D4-1	Transmission CG	LO	250 g	1.100	228 g	+
17	D4-2	Main rotor hub	LA	250 g	1.100	231 g	+

TABLE A-5. Continued.

Data Channel	Tape Track	Transducer			Tape		Polarity
		Location	Axis	Range	DC Cal (V)	Equivalent	
18	D4-3	Main rotor hub	LO	250 g	1.100	234 g	+
19	D4-4	Center fuselage	V	250 g	1.100	248 g	+
20	D4-5	Pilot pelvis	V	213 g	1.100	166 g	+
21	D5-1	Pilot pelvis	LO	219 g	1.300	201 g	+
22	D5-2	Pilot chest	V	250 g	1.300	280 g	+
23	D5-3	Pilot chest	LO	250 g	1.300	234 g	–
24	D5-4	Pilot head	V	221 g	1.300	203 g	+
25	D5-5	Pilot head	LA	250 g	1.300	230 g	+
26	D6-1	Pilot head	LO	235 g	1.300	216 g	+
27	D6-2	Tail rotor gearbox	V	234 g	1.300	215 g	+
28	D6-3	Tail rotor gearbox	LA	221 g	1.300	203 g	+
29	D6-4	Pilot seat bottom	LO	224 g	1.300	206 g	+
30	D6-5	Forward fuel cell	–	214 psi	0.826	125 psi	pos press
31	D7-1	Rear fuel cell	–	223 psi	0.794	125 psi	pos press
32	D7-2	Nose gear strut	–	7000 psi	2.226	7000 psi	pos press
33	D7-3	Right main strut	–	7000 psi	2.107	7000 psi	pos press
12 F 34	D7-4	Left main strut	–	7000 psi	2.157	7000 psi	pos press
35	D7-5	Pilot seat stroke	–	18 in	2.000	18 in	+
36	D8-1	Copilot seat stroke	–	18 in	2.000	18 in	+
37	D8-2	Nose gear stroke	–	90 deg	1.800	65.4 deg	+
38	D8-3	Right main stroke	–	90 deg	1.710	61.7 deg	+
39	D8-4	Left main stroke	–	90 deg	1.700	61.9 deg	+
75	D8-5	Right main strut, axial	–	75k lb	1.880	75k lb	Tension
76	D9-1	Left main strut, axial	–	75k lb	1.910	75k lb	Tension
–	27	Voice narrative	–	–	1.414	–	NA
–	28	IRIG-B time code	–	–	1.414	–	NA

APPENDIX B
NASA-PROCESSED DATA

This appendix contains the output of all retrieved data channels that were processed by NASA-LRC and filtered to 60 Hz.

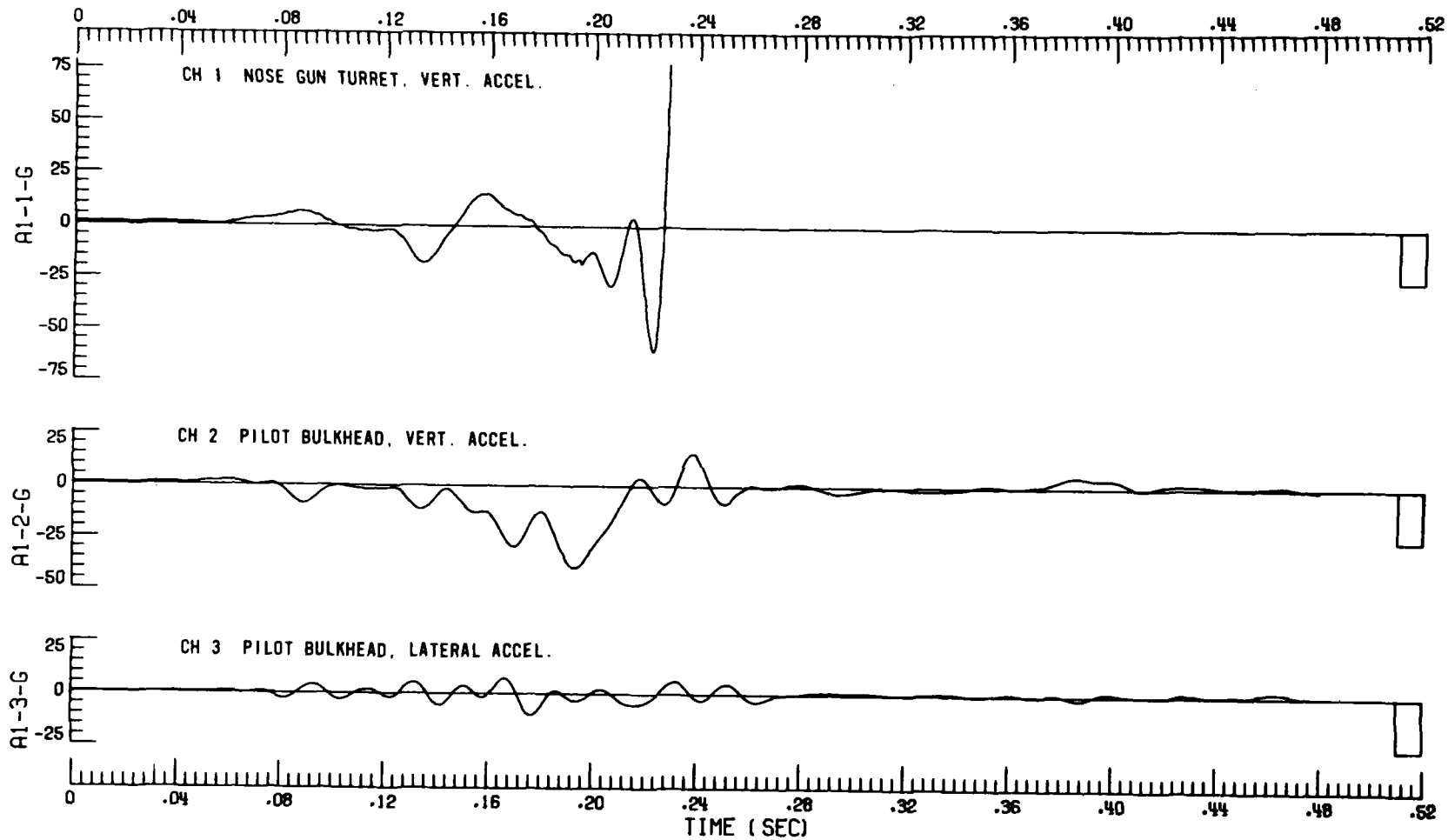
0
.04
.08
.12
.16
.20
.24
.28
.32
.36
.40
.44
.48
.52
CH 1 NOSE GUN TURRET, VERT. ACCEL.
A1-1-G
75
50
25
0
-25
-50
-75
CH 2 PILOT BULKHEAD, VERT. ACCEL.
A1-2-G
25
0
-25
-50
CH 3 PILOT BULKHEAD, LATERAL ACCEL.
A1-3-G
25
0
-25
TIME (SEC)

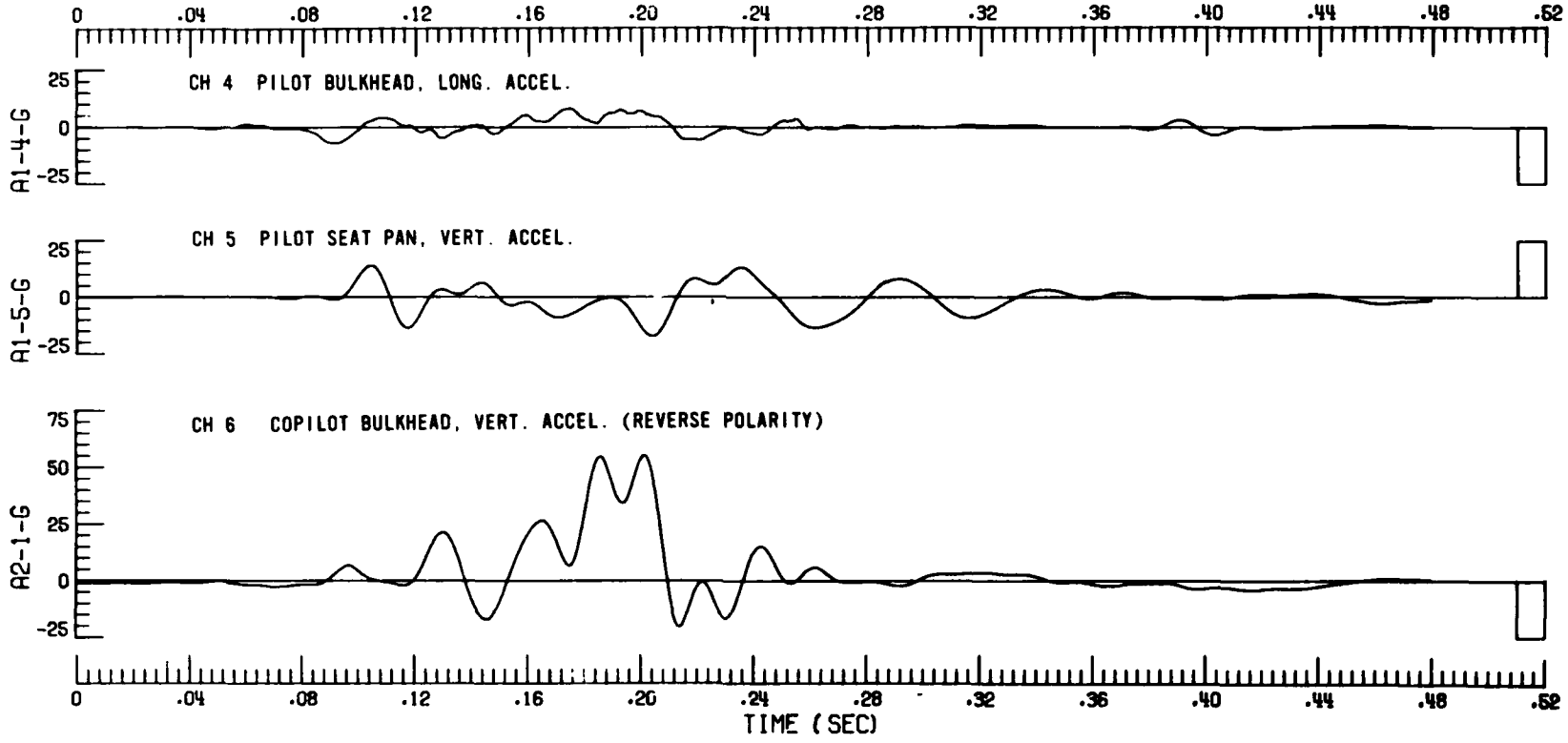
0
.04
.08
.12
.16
.20
.24
.28
.32
.36
.40
.44
.48
.52
CH 4 PILOT BULKHEAD, LONG. ACCEL.
A1-4-G
25
0
-25
CH 5 PILOT SEAT PAN, VERT. ACCEL.
A1-5-G
25
0
-25
CH 6 COPILOT BULKHEAD, VERT. ACCEL. (REVERSE POLARITY)
A2-1-G
75
50
25
0
-25
TIME (SEC)

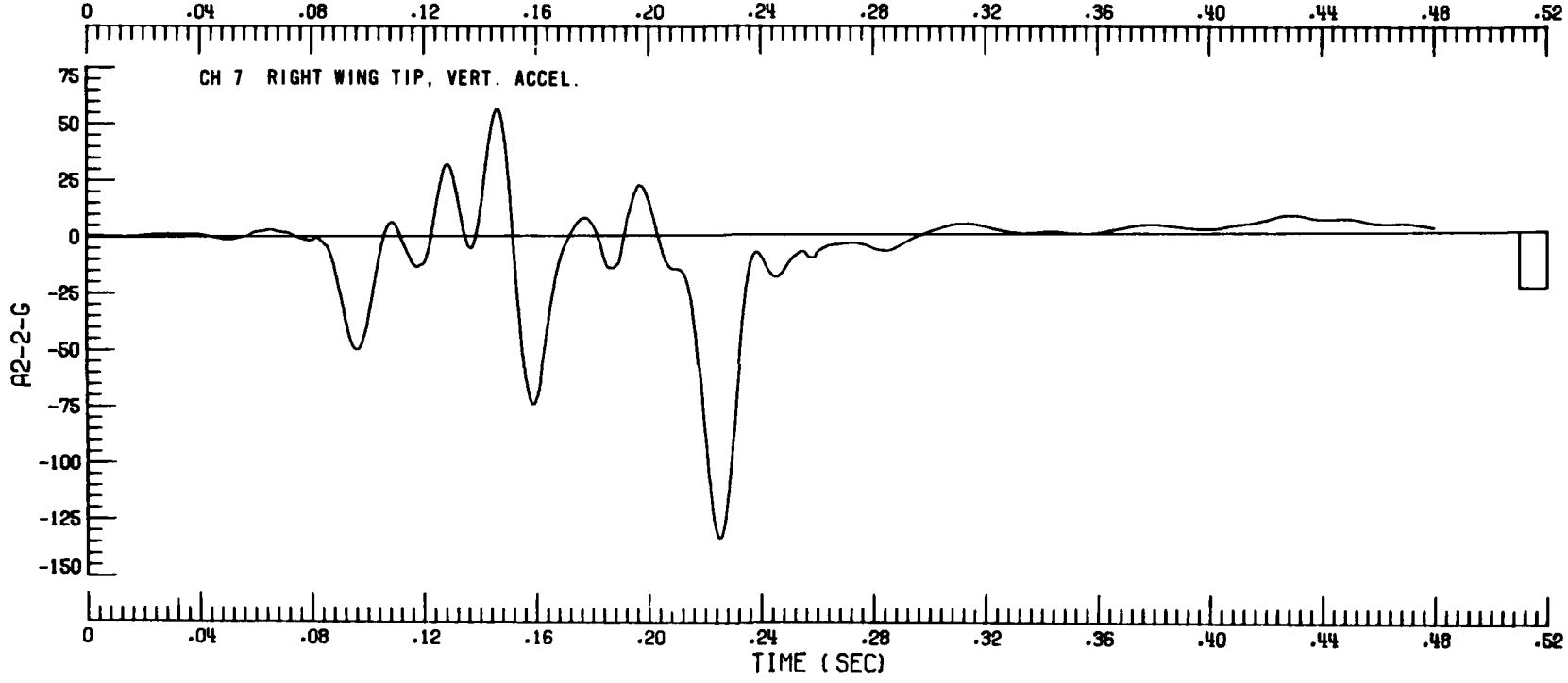
CH 7 RIGHT WING TIP, VERT. ACCEL.
A2-2-G
75
50
25
0
-25
-50
-75
-100
-125
-150
0
.04
.08
.12
.16
.20
.24
.28
.32
.36
.40
.44
.48
.52
TIME (SEC)

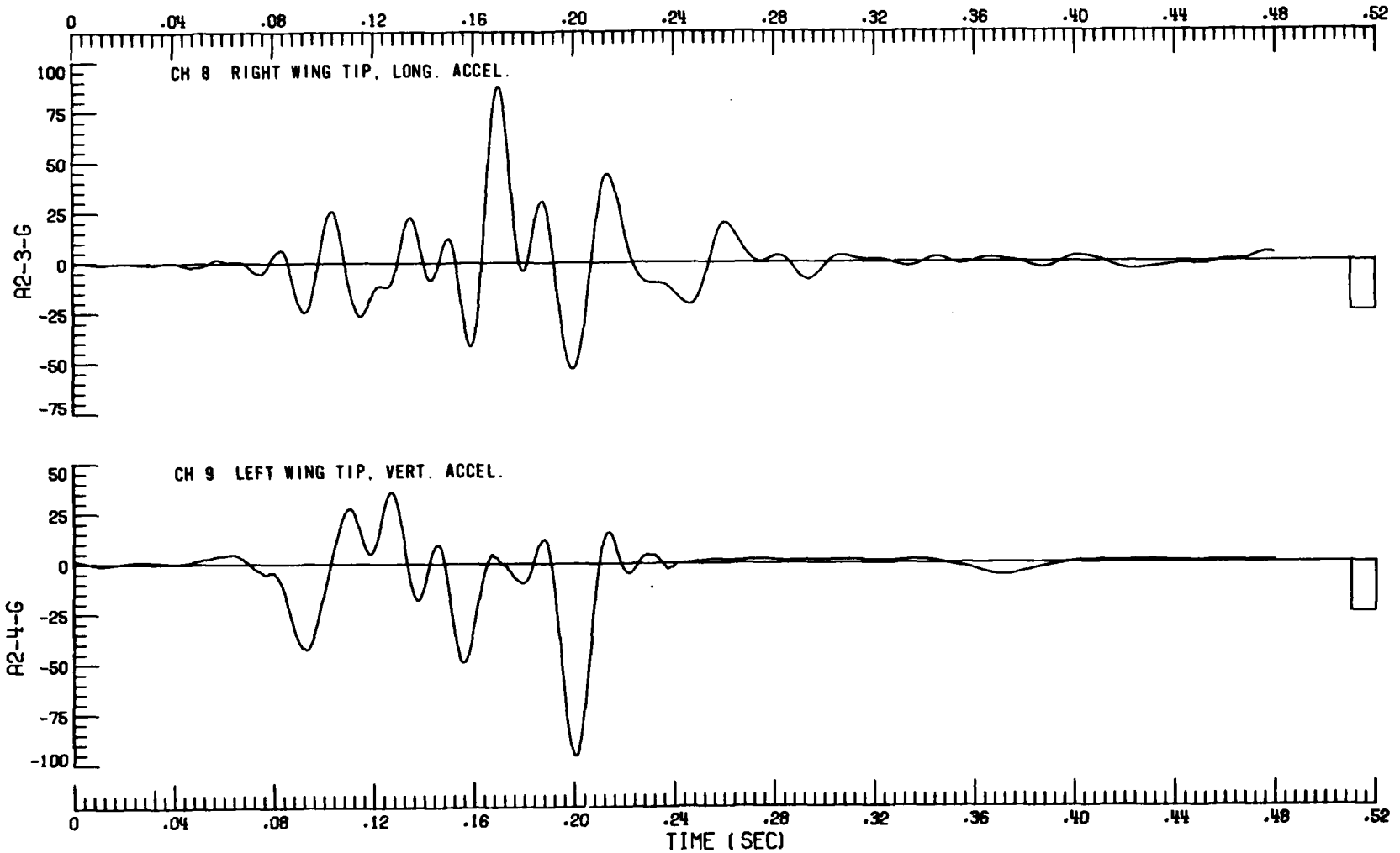
0
.04
.08
.12
.16
.20
.24
.28
.32
.36
.40
.44
.48
.52
CH 8 RIGHT WING TIP, LONG. ACCEL.
100
75
50
25
0
-25
-50
-75
A2-3-G
CH 9 LEFT WING TIP, VERT. ACCEL.
50
25
0
-25
-50
-75
-100
A2-4-G
TIME (SEC)

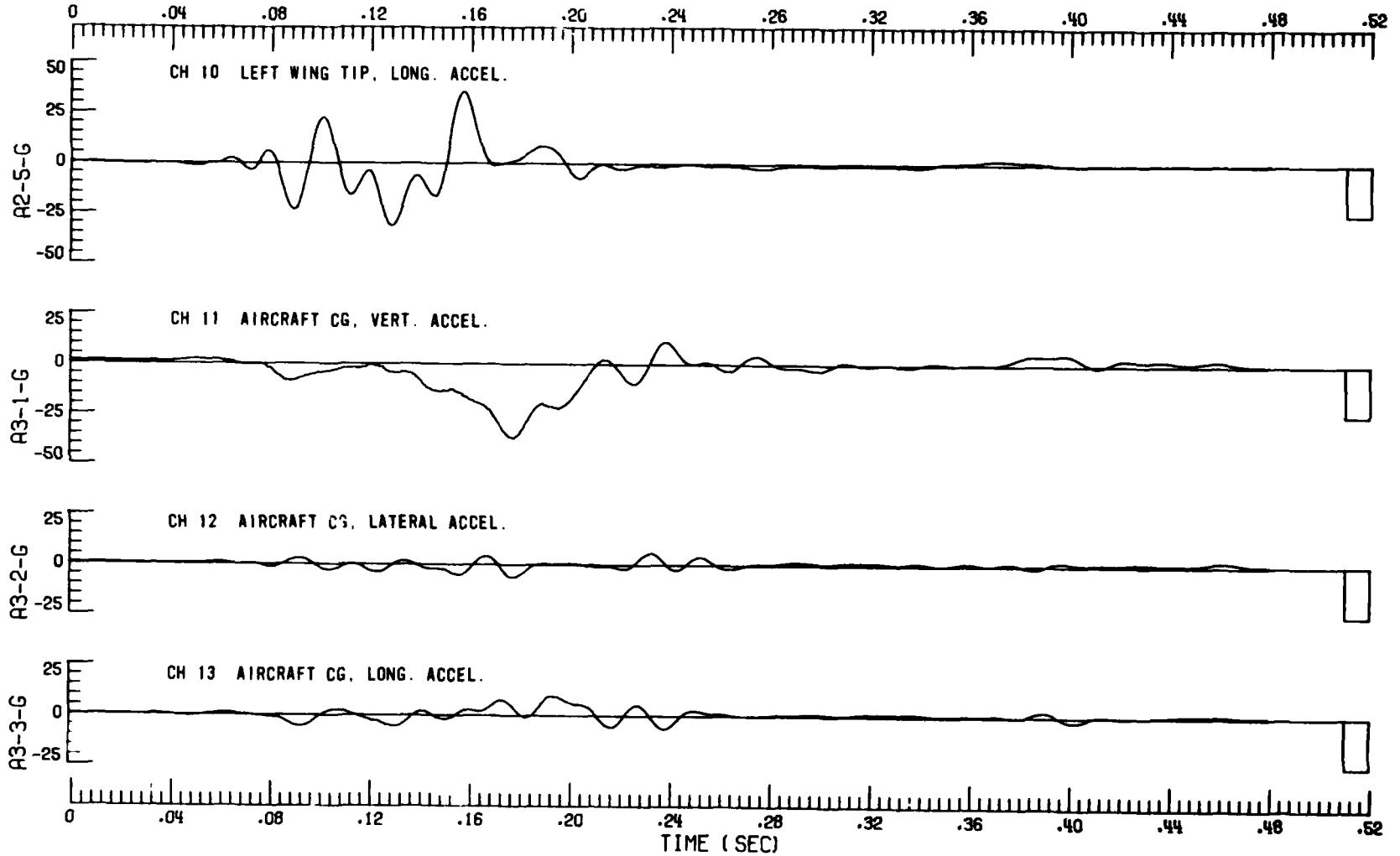
0
.04
.08
.12
.16
.20
.24
.26
.32
.36
.40
.44
.48
.52
CH 10 LEFT WING TIP, LONG. ACCEL.
A2-5-G
50
25
0
-25
-50
CH 11 AIRCRAFT CG, VERT. ACCEL.
A3-1-G
25
0
-25
-50
CH 12 AIRCRAFT CG, LATERAL ACCEL.
A3-2-G
25
0
-25
CH 13 AIRCRAFT CG, LONG. ACCEL.
A3-3-G
25
0
-25
0
.04
.08
.12
.16
.20
.24
.28
.32
.36
.40
.44
.48
.52
TIME (SEC)

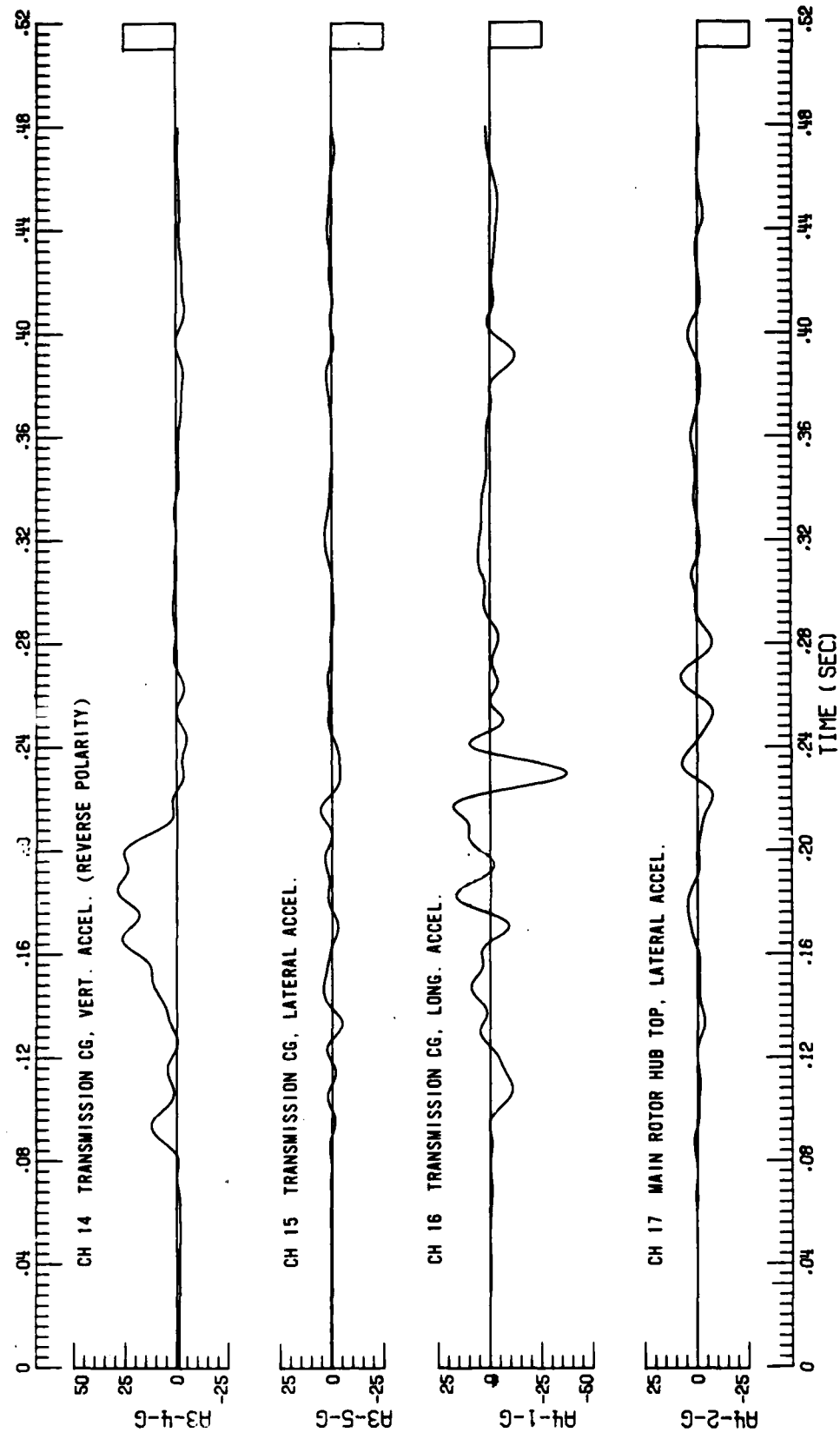
CH 14 TRANSMISSION CG, VERT. ACCEL. (REVERSE POLARITY)
A3-4-G
50
25
0
-25
CH 15 TRANSMISSION CG, LATERAL ACCEL.
A3-5-G
25
0
-25
CH 16 TRANSMISSION CG, LONG. ACCEL.
A4-1-G
25
0
-25
-50
CH 17 MAIN ROTOR HUB TOP, LATERAL ACCEL.
A4-2-G
25
0
-25
0
.04
.08
.12
.16
.20
.24
.28
.32
.36
.40
.44
.48
.52
TIME (SEC)

13
F

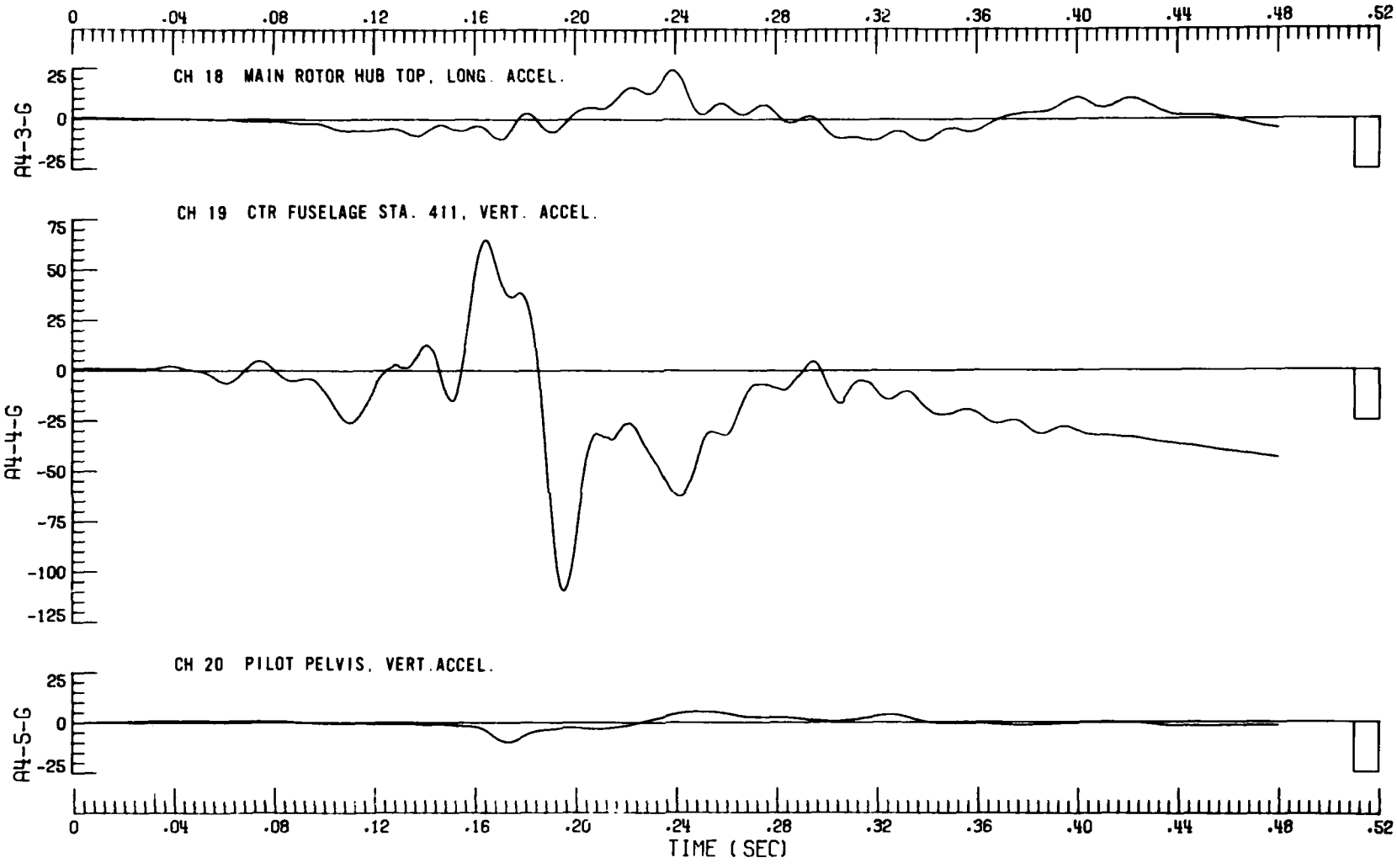
0
.04
.08
.12
.16
.20
.24
.28
.32
.36
.40
.44
.48
.52
CH 18 MAIN ROTOR HUB TOP, LONG. ACCEL.
A4-3-G
25
0
-25
CH 19 CTR FUSELAGE STA. 411, VERT. ACCEL.
A4-4-G
75
50
25
0
-25
-50
-75
-100
-125
CH 20 PILOT PELVIS, VERT.ACCEL.
A4-5-G
25
0
-25
TIME (SEC)

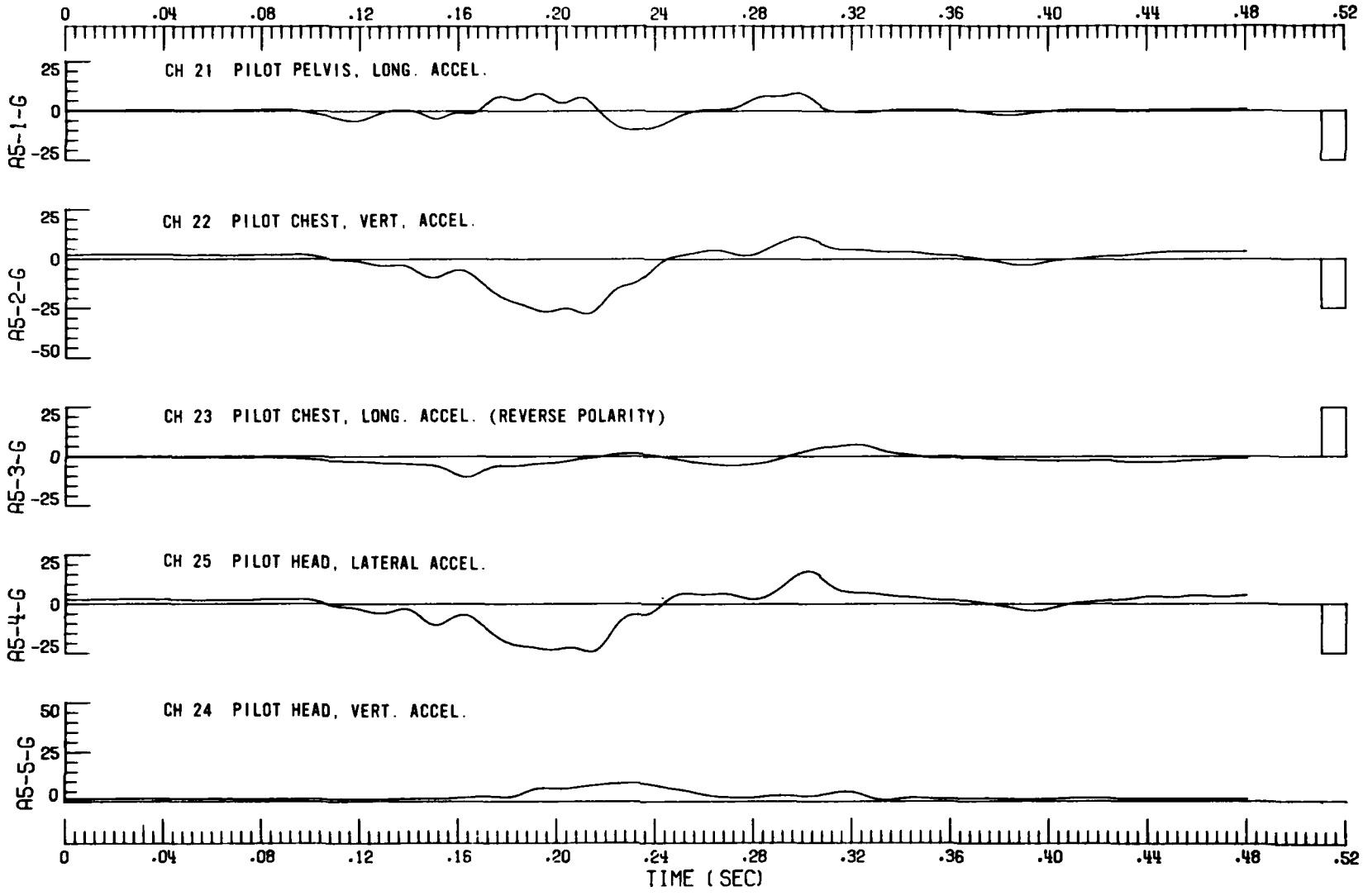
0
.04
.08
.12
.16
.20
24
.28
.32
.36
.40
.44
.48
.52
CH 21 PILOT PELVIS, LONG. ACCEL.
A5-1-G
25
0
-25
CH 22 PILOT CHEST, VERT. ACCEL.
A5-2-G
25
0
-25
-50
CH 23 PILOT CHEST, LONG. ACCEL. (REVERSE POLARITY)
A5-3-G
25
0
-25
CH 25 PILOT HEAD, LATERAL ACCEL.
A5-4-G
25
0
-25
CH 24 PILOT HEAD, VERT. ACCEL.
A5-5-G
50
25
0
TIME (SEC)

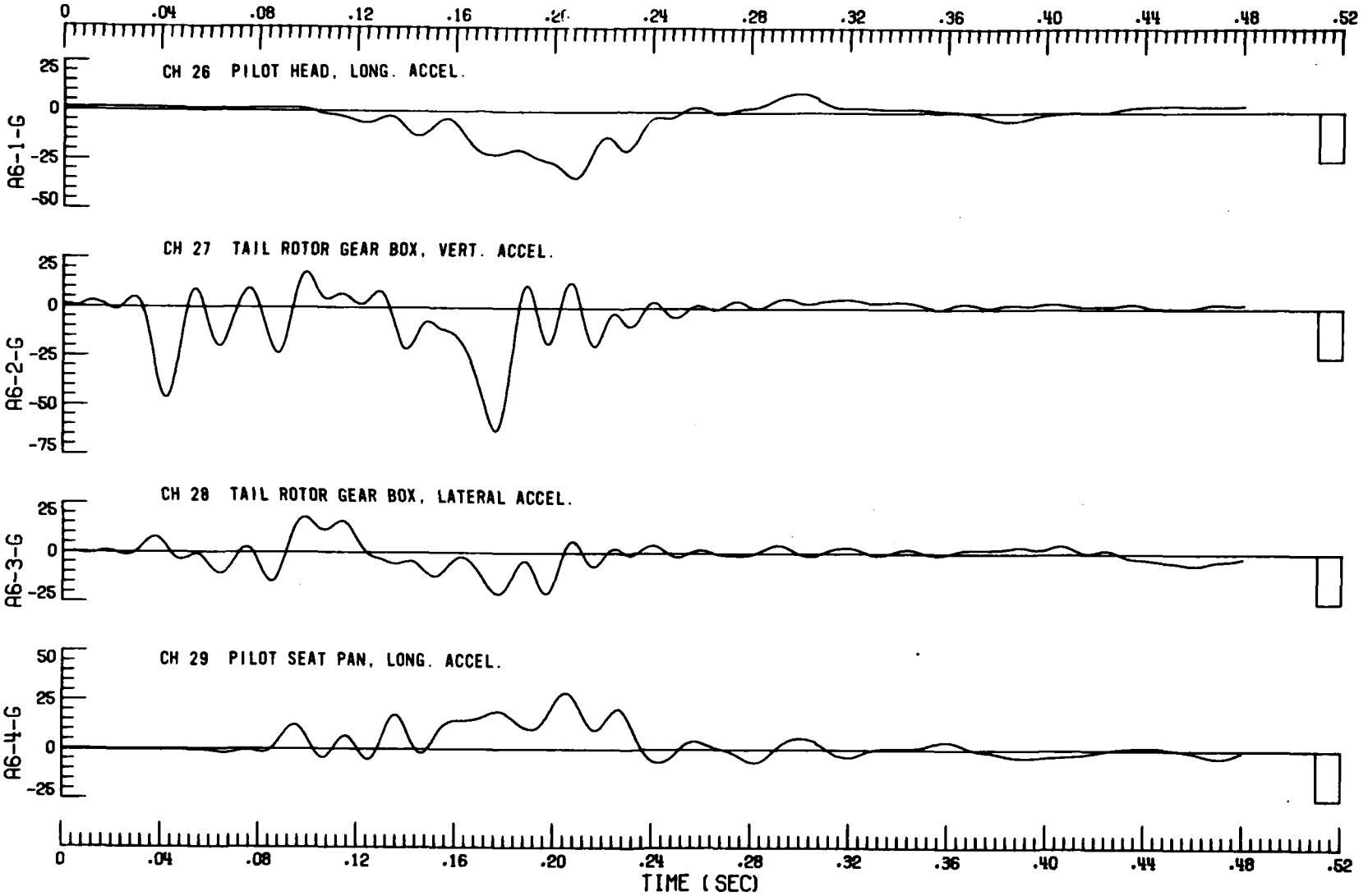
0 .04 .08 .12 .16 .20 .24 .28 .32 .36 .40 .44 .48 .52
CH 26 PILOT HEAD, LONG. ACCEL.
A6-1-G
25 0 -25 -50
CH 27 TAIL ROTOR GEAR BOX, VERT. ACCEL.
A6-2-G
25 0 -25 -50 -75
CH 28 TAIL ROTOR GEAR BOX, LATERAL ACCEL.
A6-3-G
25 0 -25
CH 29 PILOT SEAT PAN, LONG. ACCEL.
A6-4-G
50 25 0 -25
0 .04 .08 .12 .16 .20 .24 .28 .32 .36 .40 .44 .48 .52
TIME (SEC)

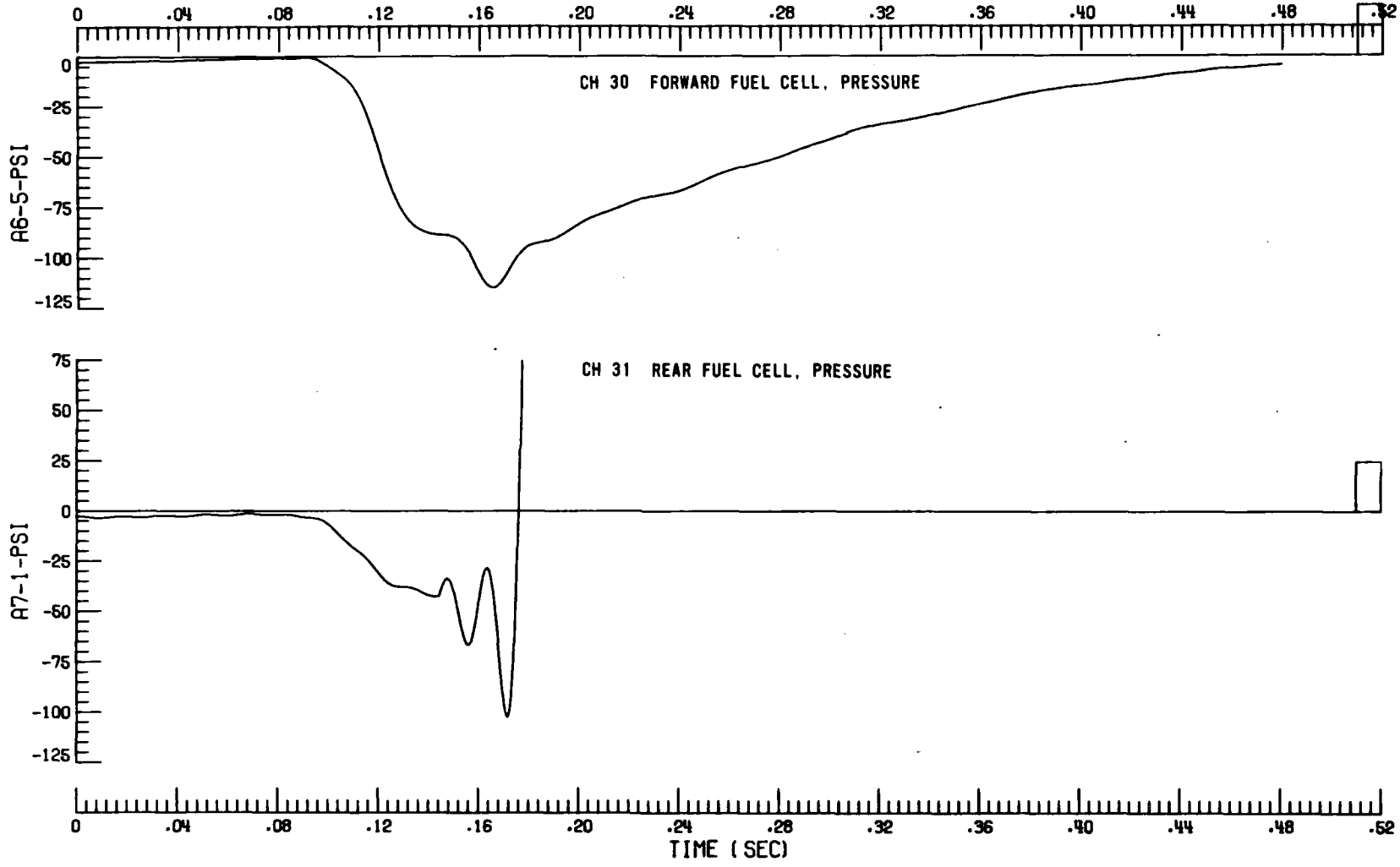
CH 30 FORWARD FUEL CELL, PRESSURE
A6-5-PSI
0
-25
-50
-75
-100
-125
CH 31 REAR FUEL CELL, PRESSURE
A7-1-PSI
75
50
25
0
-25
-50
-75
-100
-125
0
.04
.08
.12
.16
.20
.24
.28
.32
.36
.40
.44
.48
.52
TIME (SEC)

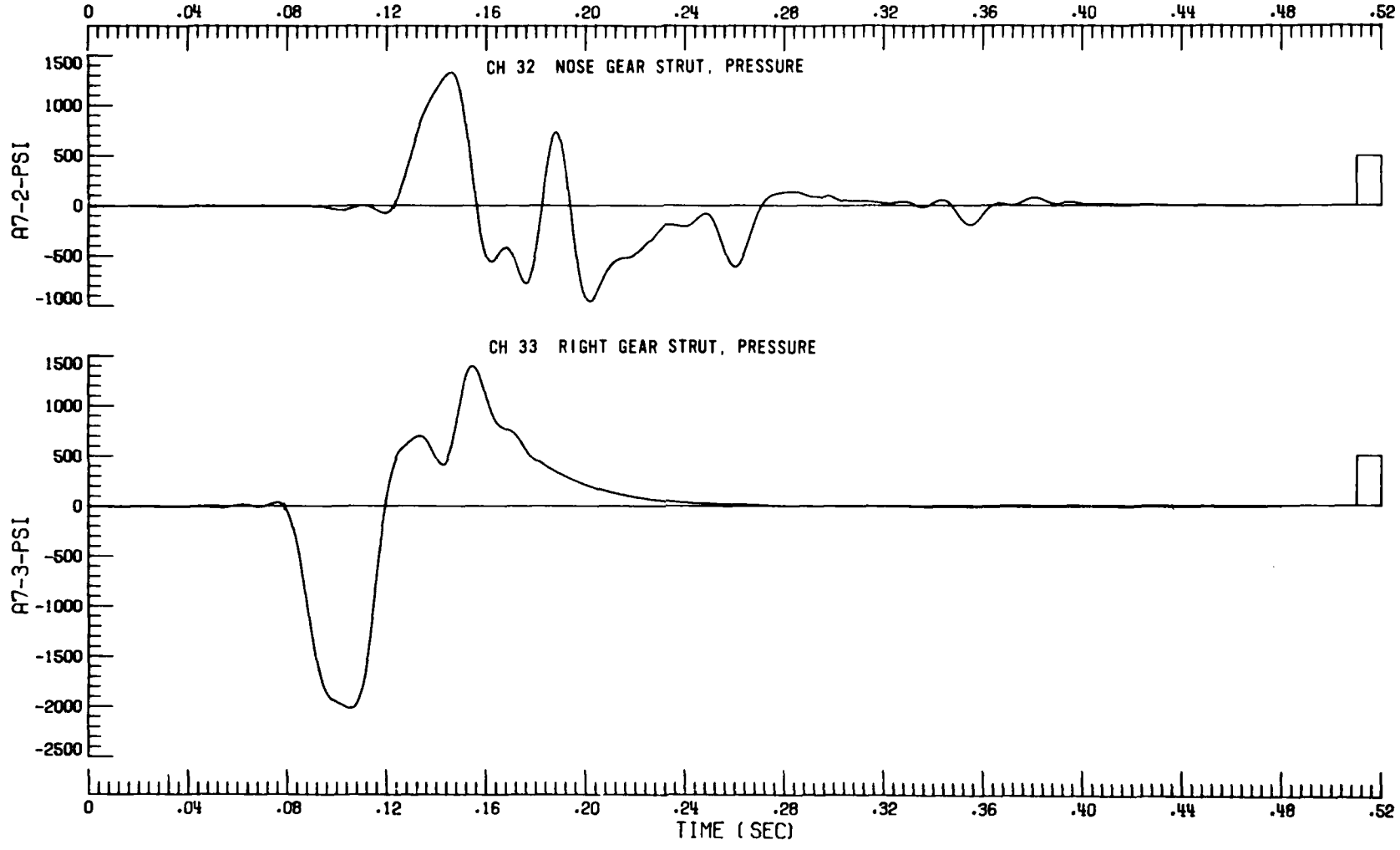
CH 32 NOSE GEAR STRUT, PRESSURE
A7-2-PSI
1500
1000
500
0
-500
-1000
CH 33 RIGHT GEAR STRUT, PRESSURE
A7-3-PSI
1500
1000
500
0
-500
-1000
-1500
-2000
-2500
0
.04
.08
.12
.16
.20
.24
.28
.32
.36
.40
.44
.48
.52
TIME (SEC)

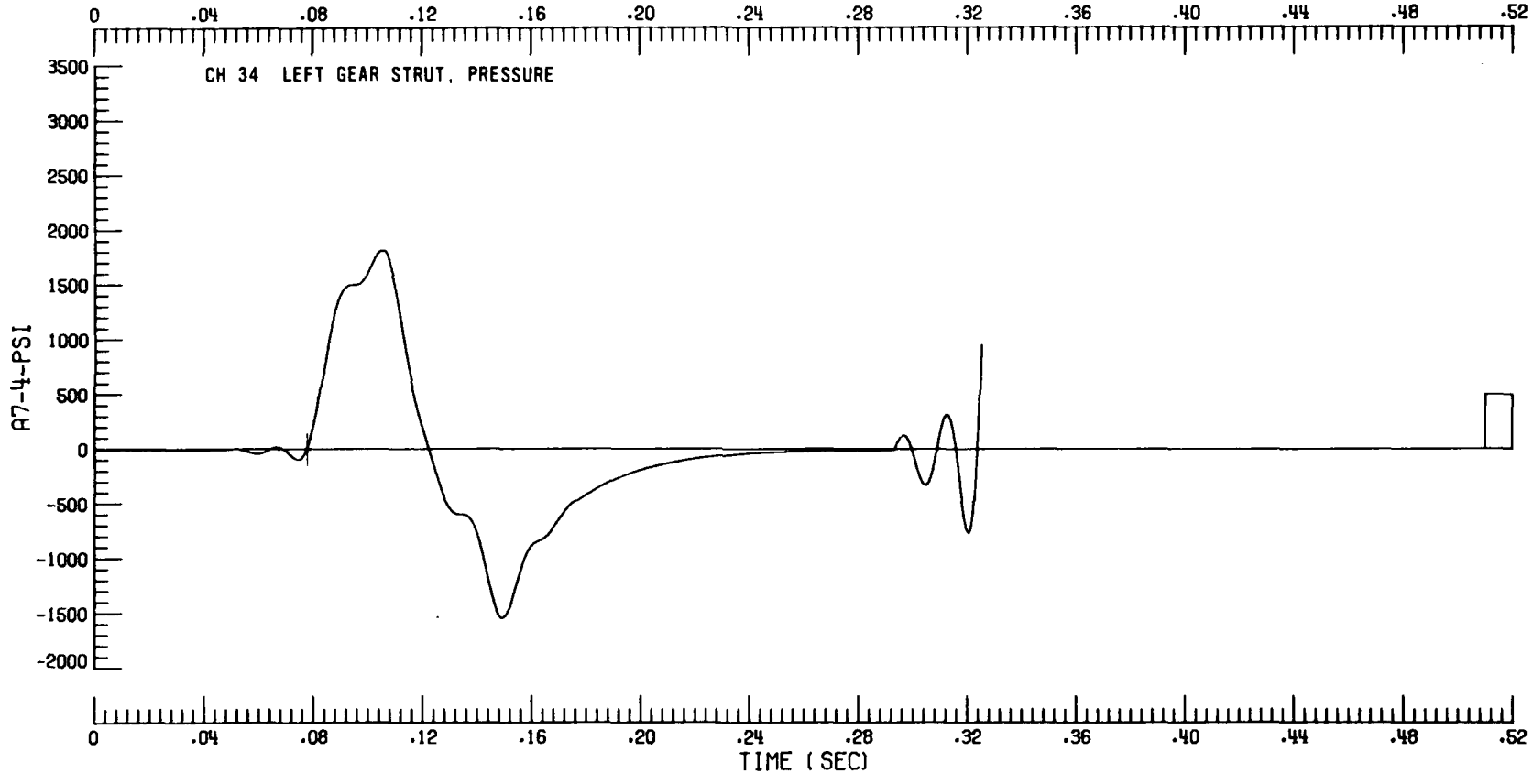
CH 34 LEFT GEAR STRUT, PRESSURE
A7-4-PSI
3500
3000
2500
2000
1500
1000
500
0
-500
-1000
-1500
-2000
0
.04
.08
.12
.16
.20
.24
.28
.32
.36
.40
.44
.48
.52
TIME (SEC)

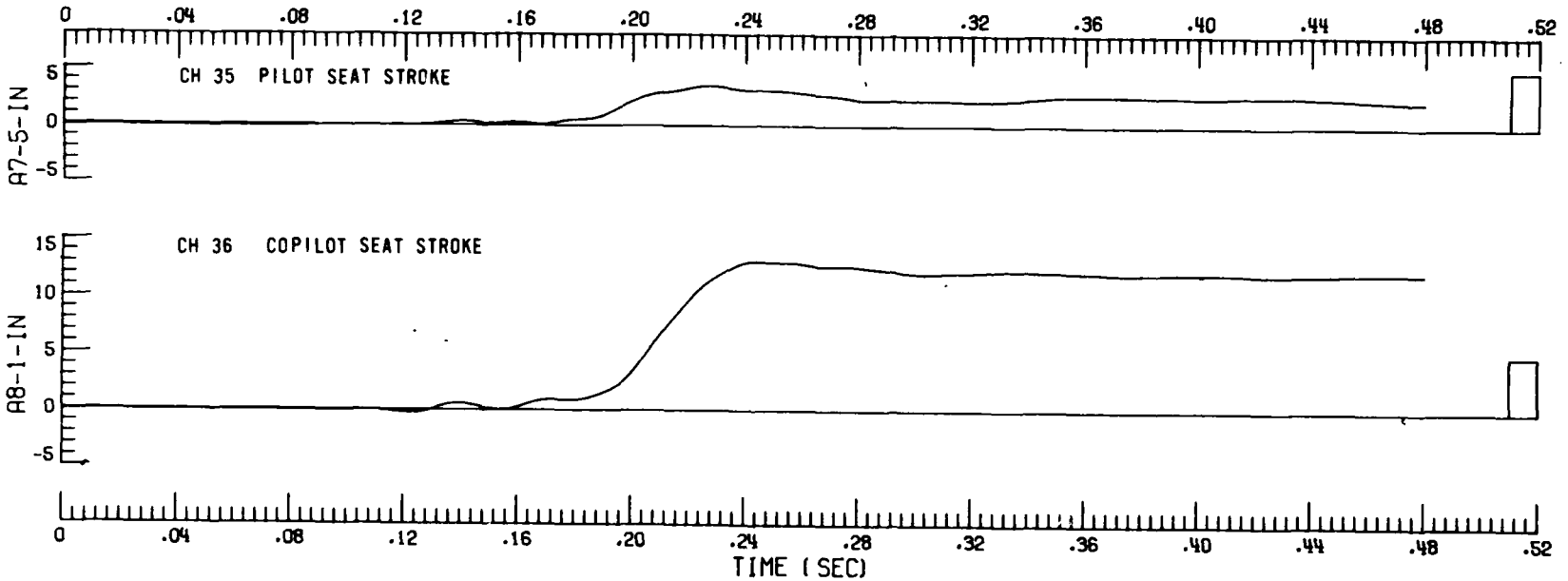
0
.04
.08
.12
.16
.20
.24
.28
.32
.36
.40
.44
.48
.52
CH 35 PILOT SEAT STROKE
A7-5-IN
5
0
-5
CH 36 COPILOT SEAT STROKE
A8-1-IN
15
10
5
0
-5
TIME (SEC)

AD-A167 813 FULL-SCALE CRASH TEST (T-41) OF THE YAH-63 ATTACK HELICOPTER(U) ARMY AVIATION SYSTEMS COMMAND ST LOUIS MO K F SMITH APR 86 USAAVSCOM-TR-86-D-2 2/2

UNCLASSIFIED F/G 1/3 NL

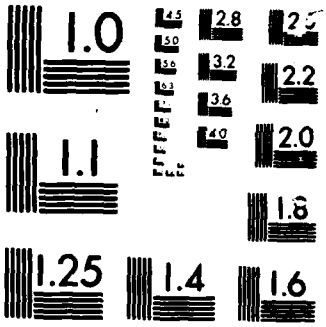

MICROCOPY CHART

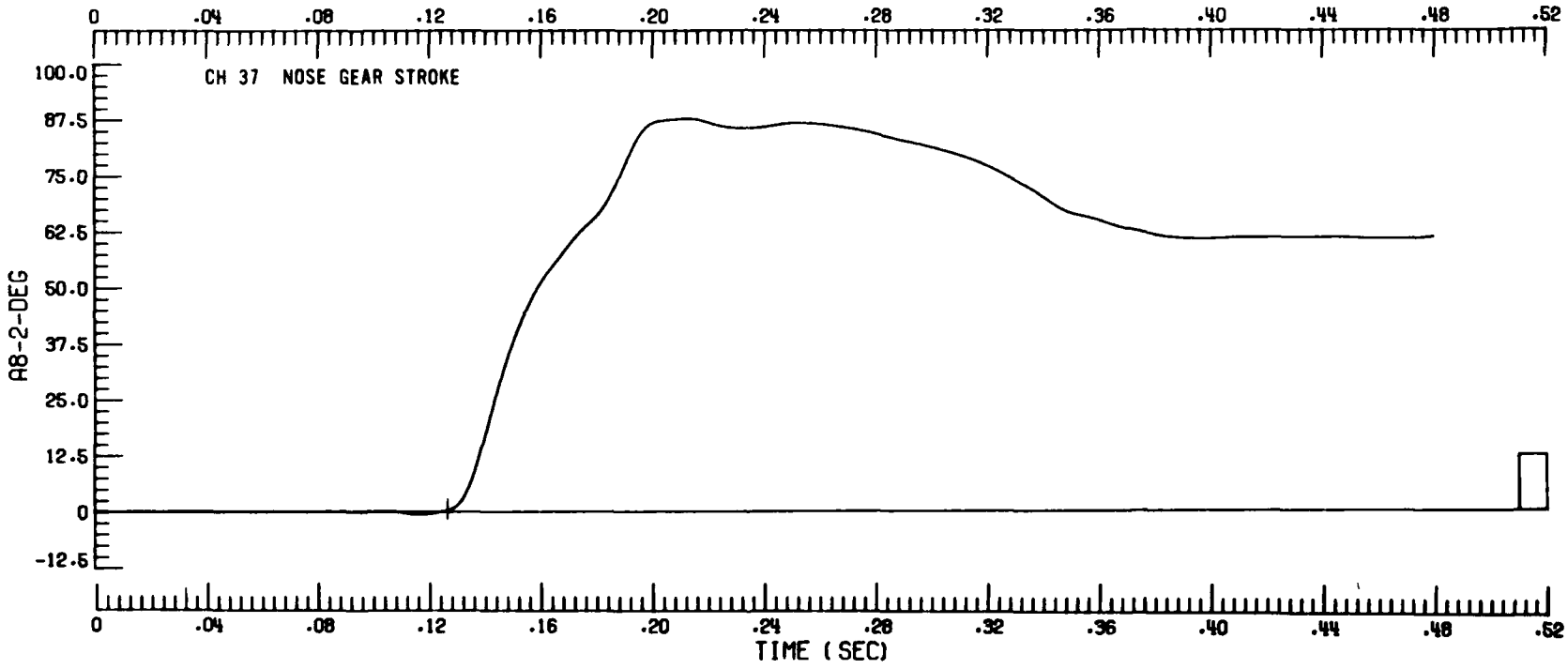
CH 37 NOSE GEAR STROKE
AB-2-DEG
100.0
87.5
75.0
62.5
50.0
37.5
25.0
12.5
0
-12.5
0
.04
.08
.12
.16
.20
.24
.28
.32
.36
.40
.44
.48
.52
TIME (SEC)

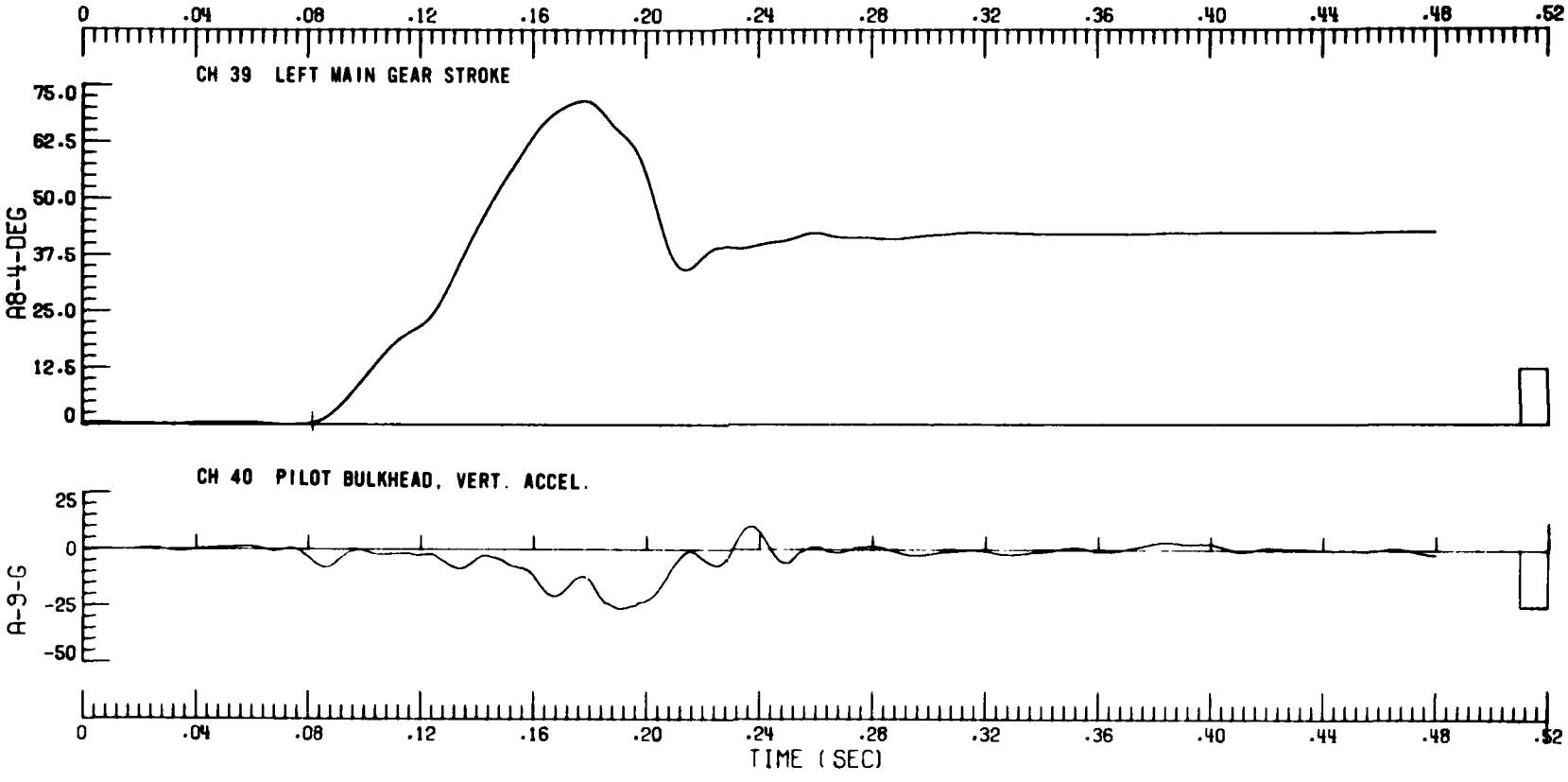
0
.04
.08
.12
.16
.20
.24
.28
.32
.36
.40
.44
.48
.52
CH 39 LEFT MAIN GEAR STROKE
75.0
62.5
50.0
37.5
25.0
12.5
0
A8-4-DEG
CH 40 PILOT BULKHEAD, VERT. ACCEL.
25
0
-25
-50
A-9-G
TIME (SEC)

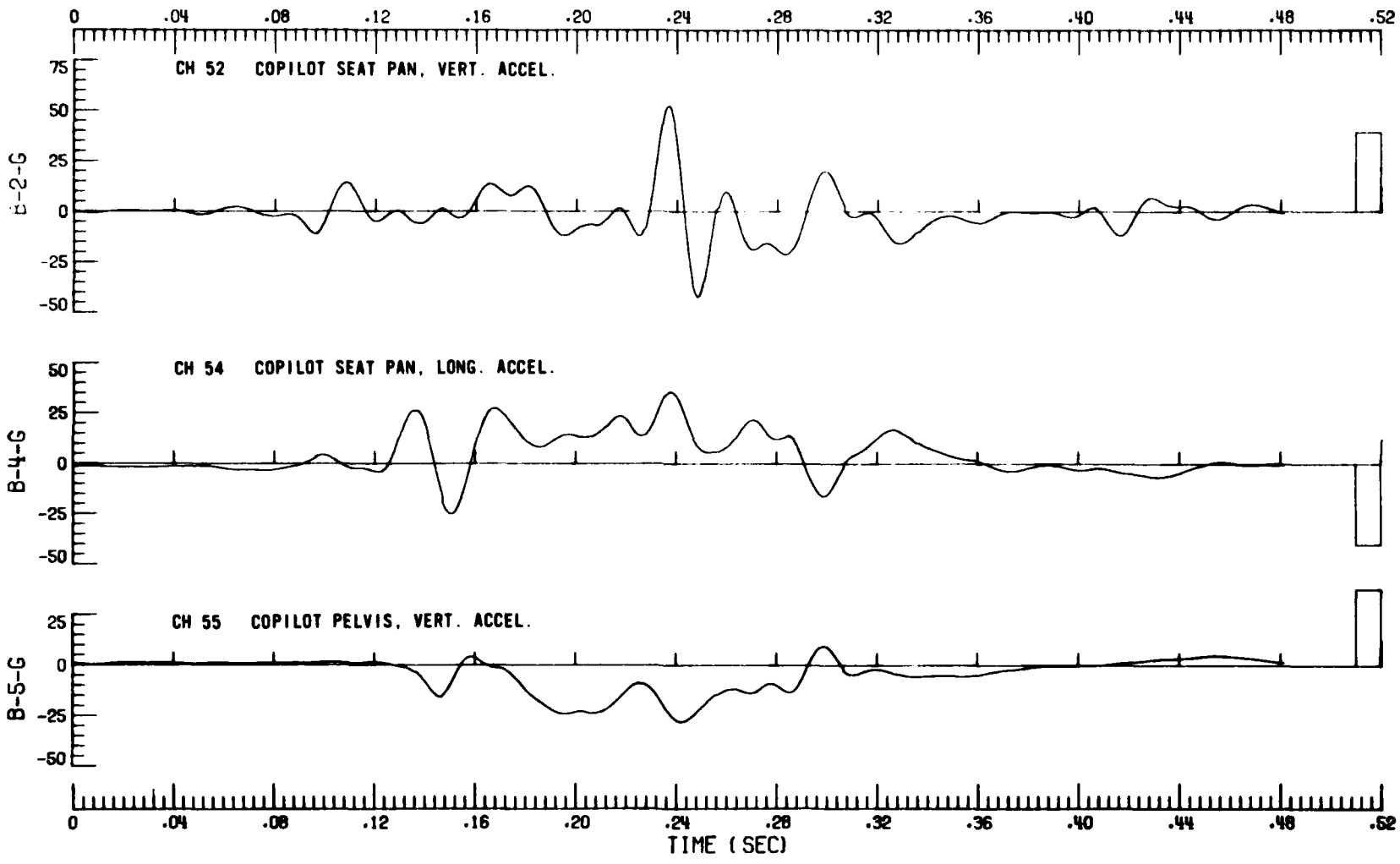
0
.04
.08
.12
.16
.20
.24
.28
.32
.36
.40
.44
.48
.52
CH 52 COPILOT SEAT PAN, VERT. ACCEL.
B-2-G
75
50
25
0
-25
-50
CH 54 COPILOT SEAT PAN, LONG. ACCEL.
B-4-G
50
25
0
-25
-50
CH 55 COPILOT PELVIS, VERT. ACCEL.
B-5-G
25
0
-25
-50
TIME (SEC)

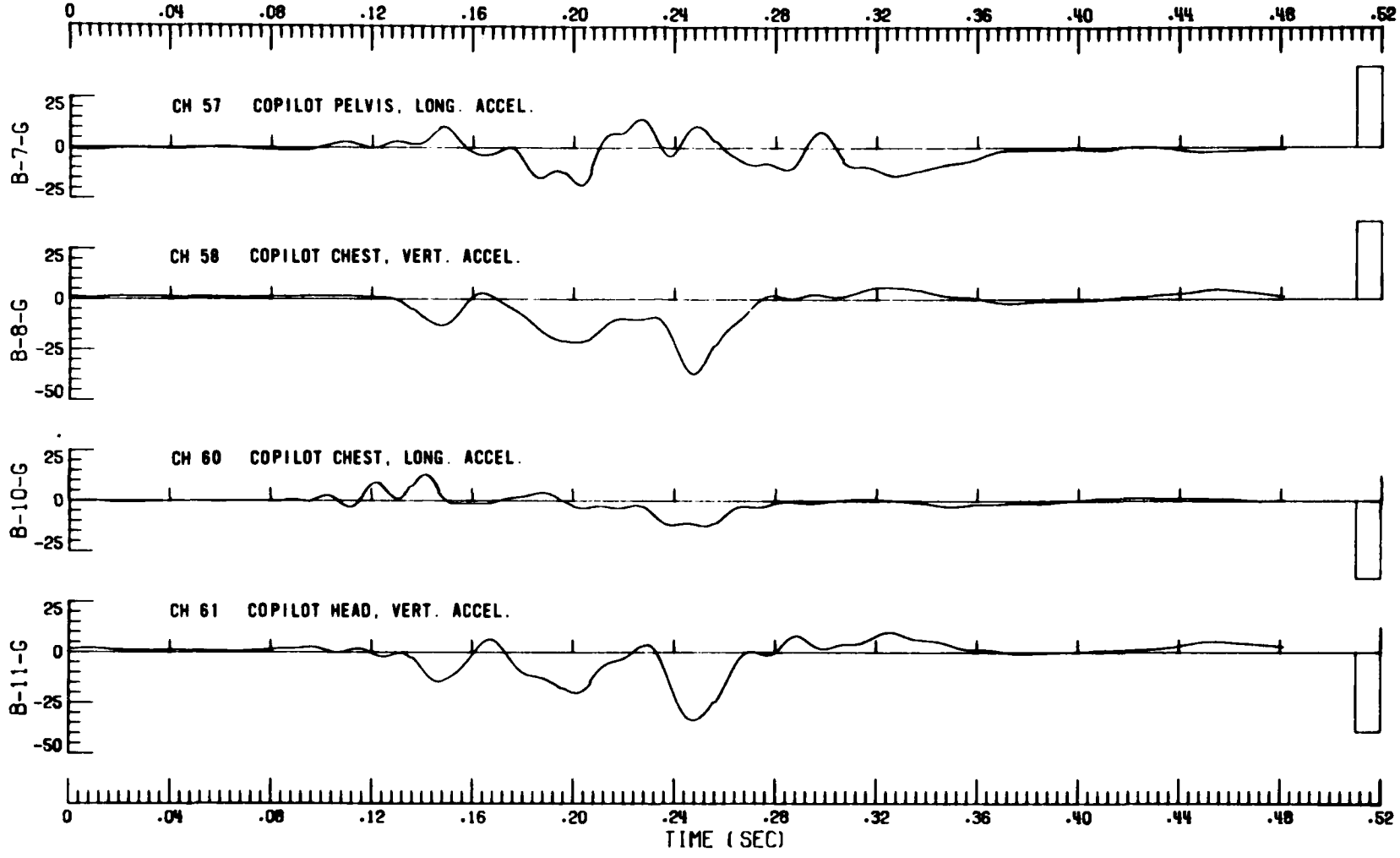
0
.04
.08
.12
.16
.20
.24
.28
.32
.36
.40
.44
.48
.52
CH 57 COPILOT PELVIS, LONG. ACCEL.
B-7-G
25
0
-25
CH 58 COPILOT CHEST, VERT. ACCEL.
B-8-G
25
0
-25
-50
CH 60 COPILOT CHEST, LONG. ACCEL.
B-10-G
25
0
-25
CH 61 COPILOT HEAD, VERT. ACCEL.
B-11-G
25
0
-25
-50
TIME (SEC)

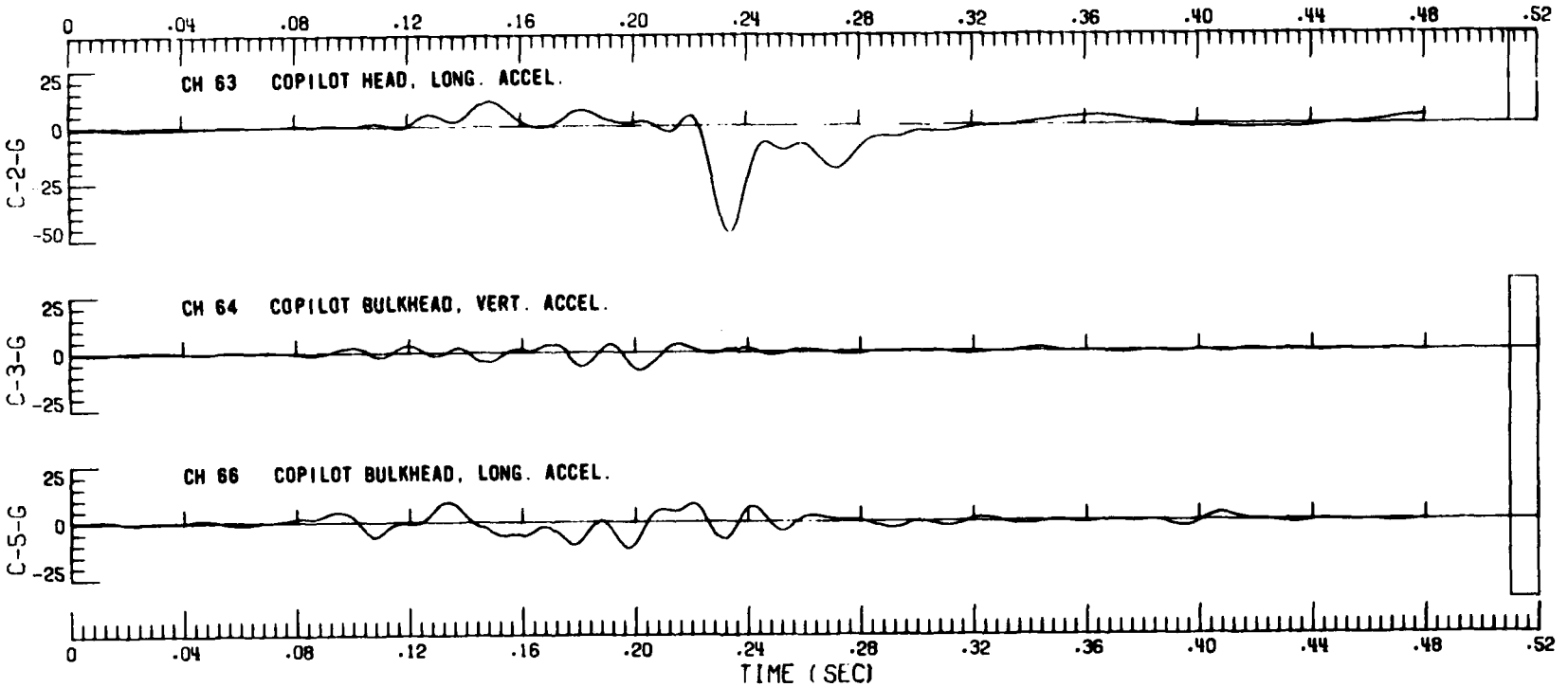
0
.04
.08
.12
.16
.20
.24
.28
.32
.36
.40
.44
.48
.52
CH 63 COPILOT HEAD, LONG. ACCEL.
C-2-G
25
0
25
-50
CH 64 COPILOT BULKHEAD, VERT. ACCEL.
C-3-G
25
0
-25
CH 66 COPILOT BULKHEAD, LONG. ACCEL.
C-5-G
25
0
-25
TIME (SEC)

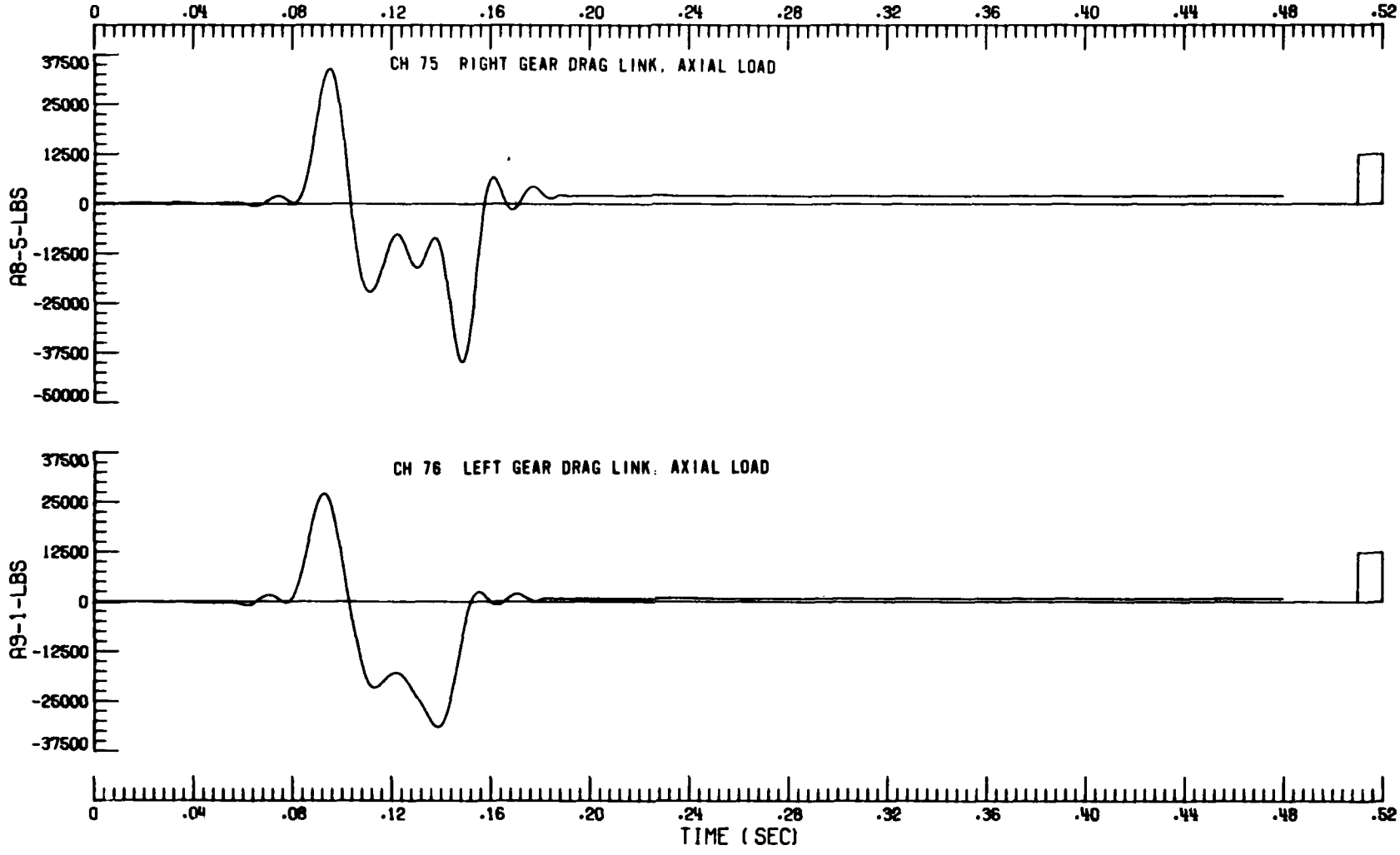
CH 75 RIGHT GEAR DRAG LINK, AXIAL LOAD
A8-5-LBS
37500
25000
12500
0
-12500
-25000
-37500
-50000
CH 76 LEFT GEAR DRAG LINK, AXIAL LOAD
A9-1-LBS
37500
25000
12500
0
-12500
-25000
-37500
0
.04
.08
.12
.16
.20
.24
.28
.32
.36
.40
.44
.48
.52
TIME (SEC)

END

DTIC

6-86